Microscopic Overtaking Model to Simulate Two-lane Highway Traffic Operation and Safety Performance

by

Amir Hosein Ghods

A thesis
presented to the University of Waterloo
in fulfillment of the
thesis requirement for the degree of
Doctor of Philosophy
in
Civil Engineering

Waterloo, Ontario, Canada, 2013

AUTHOR'S DECLARATION

I hereby declare that I am the sole author of this thesis. This is a true copy of the thesis, including any required final revisions, as accepted by my examiners.

I understand that my thesis may be made electronically available to the public.

Abstract

Rural two-lane highways make up a large portion of road networks around the world. The special geometric and traffic attributes of these highways pose special challenges to safety and traffic operation. In recent years, microscopic simulation models have gained increased acceptance as a reliable tool for investigating traffic operations and evaluating safety performance. Despite this trend, the development and application of these models to two-lane highway operations has not kept pace with those of freeways and urban networks, and this is due, in large part, to difficulties in modeling the overtaking process. This process has been rendered complex by the large number of inter-related decision factors that need to be considered by the overtaking driver in a bi-directional driving regime.

In this research, a new overtaking gap-acceptance model is developed to simulate traffic operation and safety performance on two-lane highways. This model considers a wide spectrum of physical and behavioral variables that could affect overtaking. It does so by introducing a new safety-based gap-acceptance decision variable based on the overtaking driver's perception of time-to-collision (TTC) with an opposing vehicle. The decision to overtake was expressed as a function of the perceived TTC in comparison to an established driver risk threshold (critical TTC). The distribution of critical TTC among drivers are determined through a model calibration and validation procedure based on overtaking observational data obtained from a video-recording of a one-kilometer segment of a two-lane highway. Unlike previous models, the proposed gap-acceptance model makes use of only a few calibration parameters. The proposed overtaking models along with other components of a micro-simulation traffic model are implemented in a software framework that can simulate traffic and safety operation for two-lane highways.

The overall simulation results demonstrate that the proposed simulation model can provide reliable measures of traffic and safety for two-lane highway operation. The overtaking model was found to yield both consistent and transferable results. The model is then applied successfully to provide more accurate estimates of traffic measures used in level-of-service analysis for two-lane highways and to compare these results to values reported in the two versions of the Highway Capacity Manual (HCM). In another application, this model is used to investigate the impact of truck mandated speed limiters on safety and traffic operation of two-lane highways and specifically their impact on overtaking. Finally, the potential implications of adaptive cruise control for overtaking and its resultant traffic and safety impacts are studied using the developed simulation model.

Acknowledgements

I express sincere gratitude to my supervisor, Professor Frank Saccomanno, for this research opportunity and his continuous support and guidance during my study. Without his guidance and useful advices this dissertation would not have been possible. I thank my committee members, Professor Liping Fu, Professor Bruce Hellinga, Professor Carl Haas, Professor Ralph Haas, and Professor Jonathan Histon for their time, support and helpful advices and comments. I am also very grateful to my external examiner, Professor Laurence Rilett, for his invaluable time for evaluating my thesis and his helpful comments.

I thank my colleagues Dr. Piero Guido and Giofrè Vincenzo Pasquale at the University of Calabria, Italy for their help in data collection and development of data analysis software for this research. I sincerely thank my good friends and colleagues at the University of Waterloo Ehsan Bagheri, Shahin Karimi, Soroush Salek Moghadam, Reza Noroozi, Shahram Hashemi Vaziri, Akram Nour, Pedram Izadpanah, Usama Shahdah, David Duong, Ramona Mirtorabi, Roshanak Taghipour, and Tae J. Kwon for their help and creating memorable time during the years of my PhD study.

I would like to thank my parents Mohammad Ghods and Parvaneh Shariatpanahi for their unconditional love, support, and motivation to continue my study to higher levels. I am grateful to my older brother Pouria Ghods for his continuing guidance and support and my younger brother Amir Reza Ghods for his help.

Finally and most importantly, I would like to thank my wife Fatemeh for her love, support, encouragement, and patience. My PhD research would have been never possible without her. My warmest thanks and love goes to her for being beside me all the time and for helping me to overcome the study and life difficulties.

Dedication

This thesis is dedicated

To my beloved wife, Fatemeh

And

To my adoring parents.

Table of Contents

List of Figures

List of Tables

Chapter 1
Introduction

1.1 Background

In spite of growth in freeway construction, two-lane highways are still the dominant highway type in most developed and developing countries. In the United States, for example, two-lane highways account for over 65% of total urban and rural route mileage (FHWA, 2008). According to Transportation Association of Canada (TAC), the Canadian highway networks (mostly two-lane highways) summed 879,530 kilometers in 1989 and carried 83% of all domestic travel in 1990 and 84 billion tonne-kilometres of freight travel in 1988 (TAC, 1990). Traffic safety poses special challenges for two-lane highway operations. Lamm et al. (2006) reported that more than 60% of accident fatalities took place on rural two-lane highways. A similar statistic, reported by Transport Canada (2006), shows that rural two-lane highways account for over 62% of road accident fatalities in Canada.

The two-way traffic nature as well as special geometric characteristics of two-lane highways distinguishes it from other type of roads. According to Neuman et al. (2003), 75% of all head-on collisions in the US roads take place on two-lane undivided highways. Persaud et al. (2004) reported that 20% of all fatal accidents on two-lane rural highways (4,500 fatalities per year) were accidents with opposing vehicles. Figure 1-1 presents the percentage of different types of accidents that took place on rural two-lane highways in California between 2004-08 (HSIS, 2012). The data shows that head-on and rear-end accidents account for 5.7% and 19.0% of total accidents, respectively. Hit-Object accidents account for the largest accidents proportion (33.3%).

In two-lane highway traffic operation, overtaking maneuver is desired to improve driving comfort; however, this may create major safety concerns especially head-on accidents. Overtaking can also cause other type of accidents such as sideswipe or rear-end (prior to overtake). Overtaking related accidents on rural two-lane highways tend to be more serious, mainly due to the increased likelihood of high speed head-on collisions. According to the Highway Safety Information System report (FHWA, 1994), based on accident data from three states in U.S., 13.9% of overtaking-related collisions on two-lane rural highways resulted in fatalities or serious injuries, as compared to 9.4% for all accidents on this type of road. In this report, the overtaking related accidents were found to be around 2.01% of total accidents for rural two-lane highways in the three states.

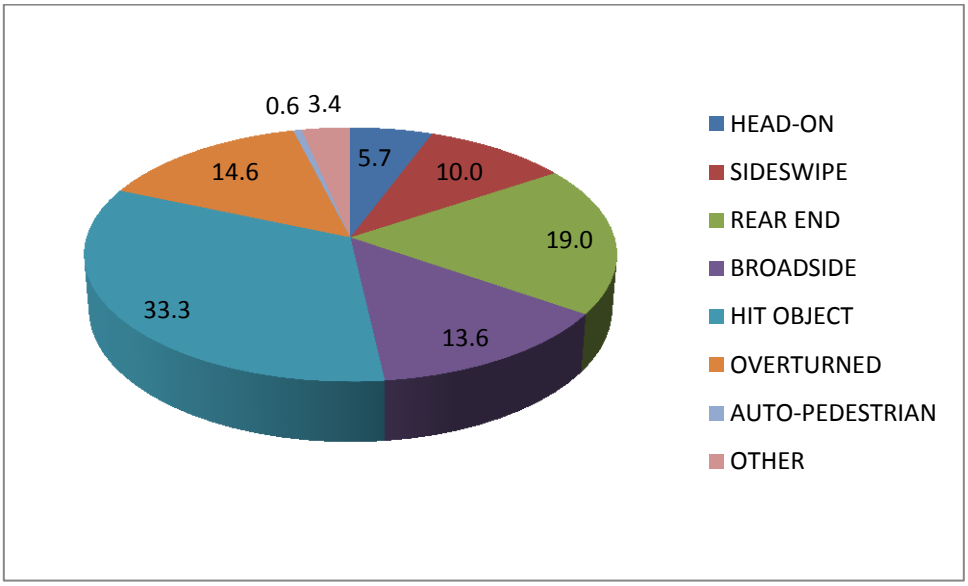

Figure 1-1-Proportion of accident types on two-lane highways in California (HSIS, 2012)

Safety performance and traffic operation efficiency on two-lane highways are highly dependent on providing safe overtaking opportunities for fast vehicles to pass slower moving vehicle in the traffic stream. These opportunities could be limited by geometry or high traffic volume. Road designers try to provide sufficient passing sight distances (PSD) for overtaking along a two-lane highway, where it is cost effective to do so. Koorey (2002) found that drivers are likely to perform unsafe overtakes when they cannot pass slower vehicles due to lack of overtaking opportunities. Morrall and Werner (1990) used overtaking ratio (ratio of accomplished overtakes to the desired number) as an alternative measure for level-of-service for two-lane highways.

1.2 Problem Statement

Microscopic simulation models provide a reliable tool for investigating traffic operations and obtaining various measures of operational traffic performance. In the past few years, micro-simulation models have also been applied to investigate road safety performance. Application of microscopic simulation for safety performance was first undertaken by Darzentas et al. (1980) in their study of conflicts for a typical T-intersection. The main idea underlying this approach is to model the complex behavior of drivers and vehicle interactions that could lead to accident. Vehicle interaction over time serves as an input into establishing surrogate measures of safety performance (Gettman and Head, 2003) and these interactions are a function of time-dependent speeds and spacings for specific pairs of vehicles as they progress along their respective paths.

In spite of advances in traffic simulation models, the application of these models for two-lane undivided highways has not kept pace with the application of simulation for freeway and urban network operations. This is mainly due to difficulty to model overtaking with potential head-on conflict. In order to analyze safety and traffic on two-lane highways we require a full understanding of the overtaking process, when and how it occurs. The modeling of this process is rendered complex by the need to consider a large number of inter-related decision inputs, such as availability of gaps in the opposing traffic stream, instantaneous vehicle speeds, spacing and acceleration profiles, traffic and driver characteristics, as well as road and weather conditions.

The complexity of traffic flow for two-lane highways and the difficulty of collecting reliable field data for validation and calibration are two of the ongoing issues that have hampered progress in modeling two-lane operations. Most of the current commercially available traffic simulation platforms apply only to uninterrupted freeway traffic (Koorey, 2002) and as a result, they fail to adequately consider the overtaking logic. For instance, VISSIM (PTV), AIMSUN (TSS), PARAMICS (Quadstone), and INTEGRATION currently have no specific overtaking logic in their algorithm. TWOPAS (St John and Harwood, 1986; Leiman et al., 1998), TRARR (Troutbeck, 1981; Shepherd, 1994; Hoban et al., 1991), and VTI (Ahman, 1972) are the most well-known two-lane simulation models that were developed during 1970's and 1980's.

The review of current overtaking models indicates that challenges in modeling overtaking maneuver is related to linking the "decision-to-overtake" to available gaps in the traffic stream for different road and traffic conditions. Unlike other driving regimes such as car-following or lane-changing, it has been difficult to specify certain model parameters for overtaking. This is mainly due to involvement of multiple factors influencing gap-acceptance behavior such as size of the available gap, speed, type, and length of vehicles, type of overtaking (flying versus accelerated), and driver's aggression level.

In most of the existing overtaking models the decision to overtake is established as a function of the available gap size (separating overtaking vehicle from the opposing vehicle prior to initiating the overtake), but varies based on other influencing factors that are considered for a limited range of values. For instance, the model determines the probability of gap-acceptance for a given gap size at three speed levels of 80, 90, and 100 km/h. Given the number of these factors and their range of likely values, updating the exiting model or development of a new overtaking model, which considers a wide spectrum of these factors, would require extensive overtaking field data and this is both difficult

and expensive to obtain. This is critical because the data used for calibration of the existing overtaking models are dated now.

These create a motivation to develop a new behavioral overtaking model that considers the overtaking maneuver in a way that it can be calibrated through adjustment of a few parameters with less data collection effort. The structure of the proposed model is such that the influencing overtaking factors are mechanistically encapsulated in a new decision variable that considers the available gap size as well as an estimate of overtaking distance in the overtaking gap-acceptance decision logic.

1.3 Objectives

The purpose of this research is to develop a behavioral overtaking micro-simulation model for two-lane highways and incorporate it in a simulation framework. This model is then applied to simulate traffic and safety performance for two-lane highway operations. The proposed research has the following specific objectives:

1. Develop an enhanced and thorough mechanism for modeling overtaking maneuvers.
2. Propose a mechanistic overtaking gap-acceptance decision logic.
3. Calibrate and validate the gap-acceptance model based on observational overtaking traffic data.
4. Test the validity and transferability of the model against independent field data and the other existing models.
5. Implement different components of two-lane highway operation in a unified micro-simulation platform named OTSIM (OverTaking SIMulation).
6. Apply OTSIM to assess the following specific problems of two-lane highways level-of-service and safety performance.
    a) Analyze traffic operation and level-of-service of two-lane highways and compare the results with the existing findings in the literature.
    b) Evaluate safety and traffic implication of car/truck differential speed limits for two-lane highways.
    c) Evaluate the potential impacts of adaptive cruise control on overtaking for two-way traffic stream.

1.4 Thesis Outline

The remainder of the thesis has been organized into seven chapters. Chapter 2 presents the main structure of the proposed two-lane simulation framework. The basic components of the simulation model including platoon generation model, vehicles performance characteristics, and driving regimes are discussed. In addition, special attention is made to developing and discussing the proposed mechanism and decision logic for overtaking maneuver.

Chapter 3 presents an overview of existing overtaking gap-acceptance models in the literature along with their shortages. A new model for overtaking gap-acceptance logic is subsequently introduced, which is then calibrated, and validated using observational overtaking data collected from video-taping of a two-lane highway segment. The simulation outputs are compared with independent field data and other two other simulation models developed for two-lane highways. In addition, the model outputs' sensitivity to calibration parameters is investigated.

The application of OTSIM in level-of-service analysis for two-lane highways is presented in Chapter 4. Percent time spent following (PTSF) and average travel speed (ATS) are estimated using the simulation model for various ranges of traffic volumes. The results are compared with those reported in two versions of the Highway Capacity Manual (HCM 2000 and HCM 2010).

In Chapter 5, the proposed simulation model is applied to evaluate potential safety and traffic impacts of implementing differential car/truck speed limits for two-lane highways. Traffic, surrogate safety, and overtaking related measures are used in this analysis for a range of traffic volumes, percentage of trucks, and three speed limit scenarios.

Chapter 6 describes the OTSIM application to assess the potential impacts of adaptive cruise control (ACC) on the overtaking process for two-lane highway traffic streams. Traffic, surrogate safety, and overtaking related measures were compared when vehicles are equipped with the system, with different penetration rates, versus the case that no active adaptive cruise control is used.

Chapter 7 summarizes the major contributions of this research along with general conclusions and findings. Several recommendations for future research are proposed.

Chapter 2
Two-lane Traffic Simulation Framework

2.1 Introduction

This chapter discusses the details of the traffic simulation platform developed in this research with a main focus on developing an overtaking simulation logic. Due to unavailability of any appropriate open-source traffic micro-simulation software, it was decided to implement the proposed overtaking model in a new simulation framework. This also provided the flexibility to modify the micro-simulation framework based on the needs proposed by various model applications considered in this research. With the exception of the overtaking component of this framework, the other components are mainly borrowed from the existing models in the literature. The proposed model is cable of simulating two-way traffic for straight road segments and with vertical grades. Horizontal curves are not included in the simulation. In addition, post-processing software was developed to analyze and summarize the simulation output results. The simulation platform developed for this research is called OTSIM (OverTaking SIMulation). In OTSIM, simulation data can be entered through Graphic User Interface (GUI) menus. An optional animation feature is available to show vehicles' movements in the software. OTSIM and its post-processing software were implemented in MATLAB programming environment. The user manual and more details about OTSIM are presented in Appendix A.The proposed traffic micro-simulation framework consists of a number of mathematical and empirical models. In simulation of two-way two-lane traffic, the behavioral components of simulation include car-following and overtaking models. In addition, platoon and headway generation models are used to create realistic initial vehicles flow and headways in the traffic stream.

2.2 Model Structure

OTSIM makes use of a time-based scanning simulation approach such that for every simulated time increment the position and speed of each vehicle in the traffic stream is updated. While a shorter simulation time-step yields smoother and more accurate vehicle trajectories, it can result in a significant increase in simulation run-time. The simulation time-step was selected to be 1 second in OTSIM.

Figure 2-1 illustrates the overall structure of the simulation framework. The OTSIM model inputs consist of road, traffic, and vehicle data, as well as behavioral model calibration parameters. The road

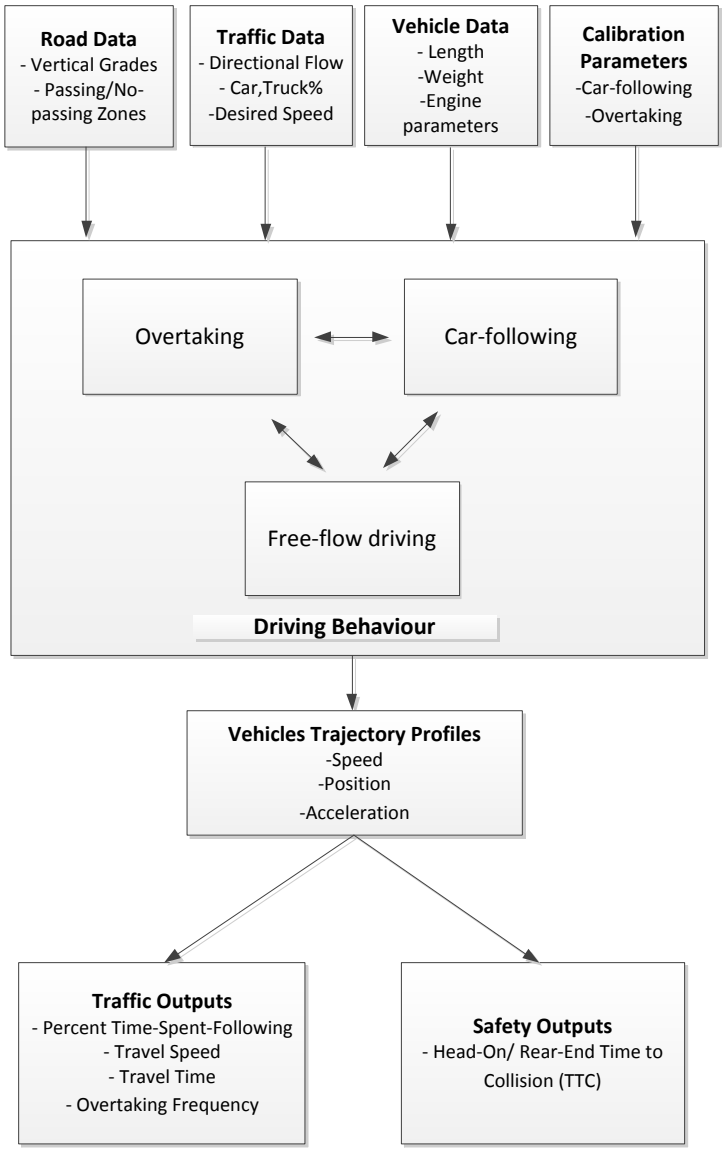

Figure 2-1- OTSIM simulation schematic diagram

data includes geometric design features, such as, segment length and grade as well as location of passing/no-passing zones. The traffic data includes directional flows, proportion of vehicles (passenger-car, truck, RV), and distribution of desired speeds. Vehicle data consists of type, weight, length, and engine power as well as vehicle's acceleration and deceleration parameters. The calibration parameters of the car-following and overtaking models are the other required inputs in OTSIM. The model outputs include both traffic and safety measures which can be calculated from speed, position, and acceleration of individual simulated vehicles. The traffic outputs consist of

percent time spent following, average travel speed, journey time, delay, and overtaking frequency. The safety outputs include head-on and rear-end time-to-collision. However, the traffic measures can potentially be categorized as safety measures too. For instance, percent time spent following and overtaking frequency can also represent the risk of rear-end and head-on collisions, respectively.

2.3 Traffic Flow

The traffic flow (in vehicles per hour) represents the average number of vehicles that want to enter to the road in a given time period. For each direction, volume can be set through the User Interface (UI) menu developed in OTSIM. The actual generated flow is stochastic depending on mean flow and distribution of vehicles headways. Normally for uninterrupted traffic flow, shifted exponential distribution is used to generate vehicles headways. However, the realistic headway pattern in two-lane traffic stream is different from those of freeways in some ways. This is mainly due to formation of platoons in the traffic stream as a result of vehicles' inability to pass. To decrease the simulation equilibrium time, a platoon generation model is employed to create expected initial platoons of vehicles.

2.3.1 Platoon generation model

A two-lane highway segment was considered with a traffic stream for which overtaking is limited by opposing traffic and/or geometry. Faster vehicles tend to catch-up to slower vehicles in the traffic stream and form a queue behind the slower vehicles. The queuing reduces the speed variance of the traffic stream and; consequently, the rate of catch-up is reduced. On the other hand, as more vehicles join the queue, the desire-to-overtake and therefore the overtaking rate (number of overtakes per unit of distance per unit of time) is increased. However, there is an equilibrium point at which the overtaking rate equates the catch-up rate. Figure 2-2 illustrates the overtaking/catch-up rate and the equilibrium point.

The platoon generation model is aimed to determine the *equilibrium* average size of platoons for each traffic direction based on two-directional traffic volumes. This reduces the warm-up time of the simulation to reach the equilibrium point in traffic. In this research, we adopt the platoon generation model proposed by Miller (1967). It is noted that the actual platoon size, as obtained from simulation outputs, depends on traffic composition as well as the underlying simulation models and their parameters (specifically those related to overtaking gap-acceptance), which can be different from the initial generated platoon patterns.

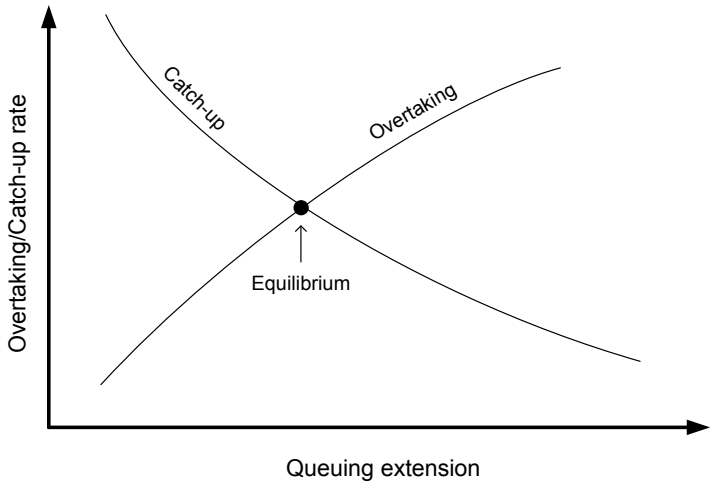

Figure 2-2-Catch-up/overtaking rate versus extension of queue in a two-way traffic stream (reproduced from McLean, 1989)

Based on Miller's model, the average platoon size of r (veh) is given by:

$$r = 0.58 + 1.58z \qquad \text{Eq. 2-1}$$

where, z is a model parameter such that:

$$z = \frac{0.56\sigma k}{\lambda(1-x)} \qquad \text{Eq. 2-2}$$

where,

$k =$ traffic density in the analysis direction (veh/m)

$\lambda =$ overtaking rate (overtakings/h)

$x =$ proportion of the road occupied by vehicles

$\sigma =$ standard deviation of vehicles speed (m/s)

In Miller's model, the overtaking rate was estimated based on the Swedish rural two-lane data for a given opposing direction traffic volume of Q, such that:

$$\lambda = 2750 * Q^{-0.62}$$ Eq. 2-3

The proportion of road occupied is obtained as:

$$x = kd$$ Eq. 2-4

where,

$d =$ average distance between vehicles in the platoon including vehicle length (m)

Each vehicle is assumed to occupy its own length plus a headway distance to the rear of the vehicle ahead. This assumption is consistent regardless whether or not the vehicle is single or a part of the platoon. Therefore, d can be calculated as:

$$d = L + v * \bar{t}_{fo}$$ Eq. 2-5

where,

$L =$ average vehicle length (m)

$v =$ average speed of platoon (m/s)

$\bar{t}_{fo} =$ average time headway between vehicles in the platoon (s)

Substituting Eq. 2-5 in Eq. 2-4 provides:

$$x = k(L + v * \bar{t}_{fo})$$ Eq. 2-6

Substituting Eq. 2-6 and Eq. 2-3 in Eq. 2-2 and then in Eq. 2-1, the average platoon size is given by:

$$r = 0.58 + \frac{\sigma * k}{3108 * Q^{-0.62}\left(1 - k(L + v * \bar{t}_{fo})\right)}$$ Eq. 2-7

The traffic density can alternatively be expressed as:

$$k = \frac{q}{v}$$ Eq. 2-8

where,

q = traffic volume of the analysis direction(veh/s)

Figure 2-3 shows the average size of platoon versus volumes for three opposing traffic volumes (Q) for the variables values presented in Table 2-1.

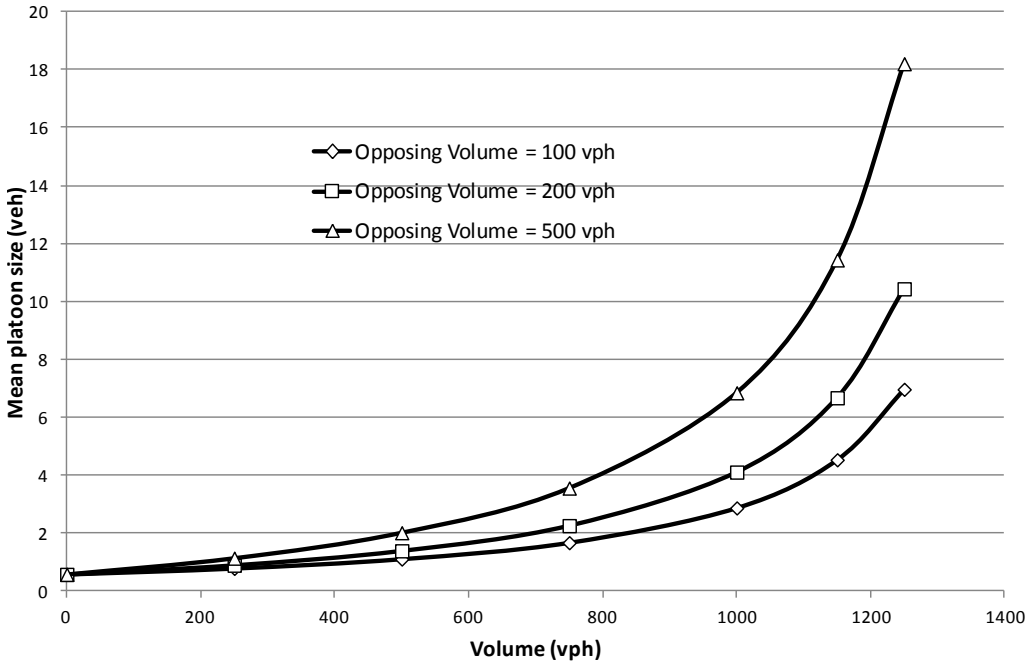

Figure 2-3- Mean platoon size vs. volume for three opposing volumes

Table 2-1-Sample input variables for Miller's platoon generation model

$L(m)$	$\bar{t}_{fo}(s)$	$v(km/h)$	$\sigma(km/h) = 0.12v$
4	2.4	100	12

2.3.2 Headway generation model

Depending on average input volumes, the headway generation model in OTSIM determines the initial time headways between the individual vehicles when they enter the simulation. For a given average platoon size of r, the proportion of free vehicles in the traffic stream would be $1/r$. The initial status of a generated vehicle (free-flow or following in platoon) can be determined using a uniformly distributed random variable $\alpha \sim U[0,1]$ such that:

$$\begin{cases} vehicle\ status = 'free' & if\ \alpha < 1/r \\ vehicle\ status = 'following' & if\ \alpha \geq 1/r \end{cases}$$

In addition, the total time headways must equate the sum of headways of all vehicles such that:

$$\frac{3600}{q} = \bar{t}_{fo}\left(1 - \frac{1}{r}\right) + \bar{t}_{fr}\frac{1}{r} \qquad \text{Eq. 2-9}$$

where,

$\bar{t}_{fr}$ =mean time gap headway of free vehicles

From the above equation, the mean time headway between platoons can be obtained as:

$$\bar{t}_{fr} = \frac{3600}{q}r + (r-1)\bar{t}_{fo} \qquad \text{Eq. 2-10}$$

The time gap between platoons (free vehicles) can be represented by a shifted exponential distribution with mean of $\bar{t}_{fr}$ and minimum value of t_{min}, i.e.:

$$\begin{cases} P(h < t) = 1 - \exp\left(-\dfrac{t - t_{min}}{t_{min} - \bar{t}_{fr}}\right) & if\ t \geq t_{min} \\ P(h < t) = t_{min} & if\ t < t_{min} \end{cases} \qquad \text{Eq. 2-11}$$

Based on the above distribution, a randomly distributed headway variable (h) can be generated as:

$$h = t_{min} - Ln(1-\alpha)\left(\bar{t}_{fr} - t_{min}\right) \qquad \text{Eq. 2-12}$$

where, as previously defined, $\alpha \sim U[0,1]$

2.3.3 Proportion of vehicle types

Three classes of vehicles are included in the OTSIM simulation model: Passenger cars, Recreational Vehicles (RVs), and Trucks. The percentage of each vehicle type in traffic stream needs to be inputted. A uniformly distributed random variable $\alpha \sim U[0,1]$ can be used to determine the type of randomly generated vehicle based on vehicle proportion specified by the user, such that:

$$\begin{cases} vehicle\ type\ 1 & if\ 0 \le \alpha \le P_1 \\ vehicle\ type\ 2 & if\ P_1 \le \alpha \le P_1 + P_2 \\ vehicle\ type\ 3 & if\ P_1 + P_2 \le \alpha \le P_1 + P_2 + P_3 \\ \vdots & \\ vehicle\ type\ N & if\ P_1 + \ldots + P_{N-1} \le \alpha \le 1 \end{cases}$$

where, $0 < P_i < 1$ is the proportion of vehicle type i.

2.4 Vehicle Characteristics and Performance

The physical characteristics of the vehicles in OTSIM include vehicle length, vehicle mass, and engine power parameters. Figure 2-4 illustrates a vehicle (here truck) ascending an up-grade with the corresponding forces applied to it. The equation of motion for this vehicle is given by:

$$M\frac{dv}{dt} = F_t - F_a - F_r - Mg\sin\theta \qquad \text{Eq. 2-13}$$

where,

F_t = tractive force (N)

F_a = air resistance (N)

F_r = rolling resitance (N)

M = vehicle mass (kg)

g = acceleration due to gravity (9.8 m/s^2)

v = vehicle speed (m/s)

θ= grade angle(degree)

The pulling force is given by:

$$F_t = \frac{P}{v} \qquad \text{Eq. 2-14}$$

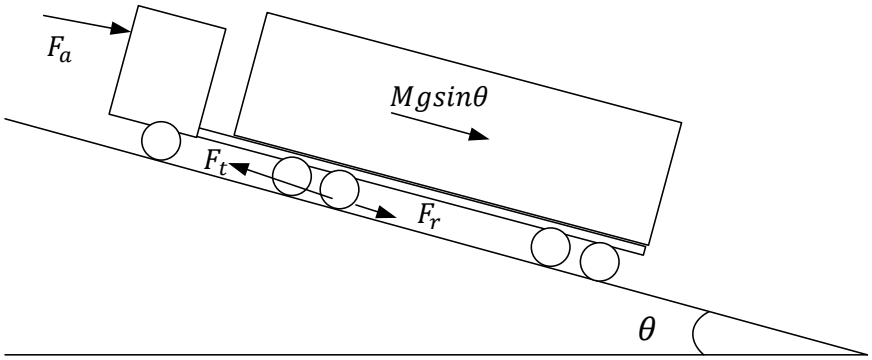

Figure 2-4- Forces on a vehicle ascending an upgrade (reproduced from McLean, 1989)

where, P is the utilized power in Watt. Drivers usually use the maximum power for a performance-limited vehicle, e.g. trucks, on an up-grade (McLean, 1989).

The air resistance can be expressed as (McLean, 1989):

$$F_a = 0.5 C_d A \rho v^2 \qquad \text{Eq. 2-15}$$

where,

C_d = drag coefficient (dimensionless)

A = projected frontal area (m^2)

ρ = air density (kg/m^3)

The drag coefficient (C_d) is a dimensionless quantity that is used as a measure of vehicles resistance against air. The more aerodynamic vehicle, the less drag coefficient it takes.

The rolling resistance can be approximated as:

$$F_r = C_R M g \qquad \text{Eq. 2-16}$$

where,

C_R = rolling resistance coefficient (dimensionless)

The rolling resistance coefficient is a function of tire wear and pavement conditions.

Substituting Eq. 2-14, Eq. 2-15, and Eq. 2-16 in Eq. 2-13 provides:

$$\frac{dv}{dt} = \frac{P}{M}\frac{1}{v} - \underbrace{\frac{0.5C_d A\rho}{M}}_{K_A} v^2 - gC_R - g\sin\theta \qquad \text{Eq. 2-17}$$

The value of $\frac{P}{M}$ is known as power to mass ratio. When the forces are in equilibrium$\left(\frac{dv}{dt} = 0\right)$, the vehicle gets an equilibrium speed of v_e which is also known as *crawl speed*.

In simulation of vehicles dynamics, Eq. 2-17 can be used to calculate the instant vehicle acceleration for a given speed of v and a grade angle of θ. For passenger cars and RVs, Eq. 2-17 can be approximated with a linear relation between acceleration and the vehicle speed:

$$\frac{dv}{dt} = a_m\left(1 - \frac{v}{v_m}\right) - gsin(\theta) \qquad \text{Eq. 2-18}$$

where,

$\boldsymbol{a_m}$ = maximum acceleration at zero speed (m/s^2)

$\boldsymbol{v_m}$ = maximum speed attainable (m/s)

Table 2-2 presents a list of physical characteristic of four types of passenger-car vehicles with their corresponding specifications used in OTSIM. For each set of parameters listed in Table 2-2, Eq. 2-17 was solved numerically to estimate passenger-cars speed profiles. Then, the best estimates of a_m and v_m parameters was determined by fitting Eq. 2-18 to the speed curves (Figure 2-5). The list of the parameters obtained for the regression analysis for four passenger-cars is presented in Table 2-3.

Table 2-2- Updated passenger-car physical specifications used in the simulation model (Source: www.carfolio.com)

Vehicle type	Engine size (cc)	Power (watt)	Mass (kg)	Frontal Area (m^2)	Drag Coef.	Rolling Coef.	Length (m)
1	3000	177000	1706	2.12	0.3	0.14	5.5
2	2000	114000	1400	2.19	0.27	0.14	5.2
3	1800	88000	1370	2.19	0.27	0.14	4.9
4	1600	77200	1255	2.22	0.3	0.14	4.3

Table 2-3- Passenger-car parameters for Eq. 2-18 as obtained from the regression analysis

Vehicle Type	$a_m(m/s^2)$	$v_m(m/s)$
1	6.4	55.5
2	5.6	47.6
3	4.7	42.5
4	4.6	40.1

The list of physical parameters for the four types of recreational vehicles is presented in Table 2-4.

Table 2-4- Recreational vehicle (RV) performance parameters used in OTSIM (Allen et al., 2000)

Vehicle Type	$a_m(m/s^2)$	$v_m(m/s)$	Length (m)
1	4.3	38.1	11
2	3.8	36.6	8.5
3	3.4	35.1	6.4
4	2.7	33.5	9.8

Table 2-5 provides the list of physical parameters used for four truck types in OTSIM.

Table 2-5- Truck physical parameters used in OTSIM (Allen et al., 2000)

Truck Type	Power/Mass (W/kg)	Mass/Frontal Area (kg/m^2)	Rolling Coef. (m/s^2)	Length(m)
1	7.2	3329.9	0.08	19.8
2	9.3	2255.7	0.08	19.8
3	11.7	1660.1	0.08	19.8
4	21.6	849.6	0.08	9.1

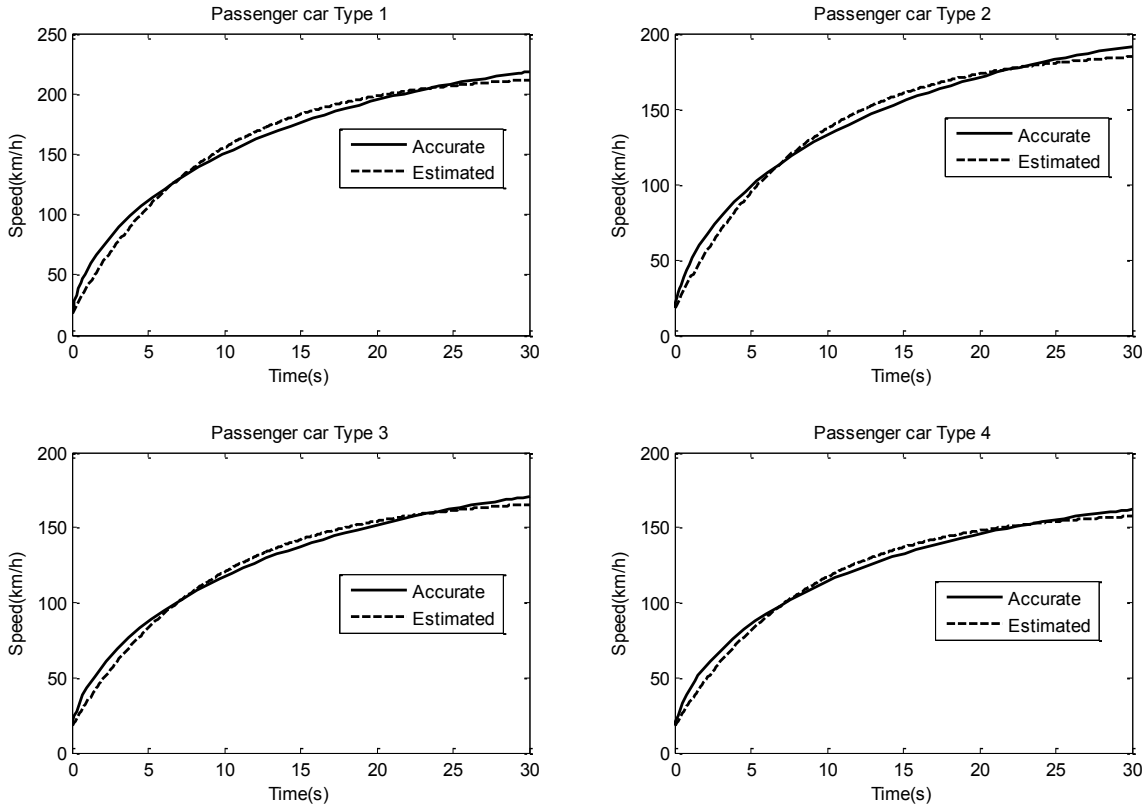

Figure 2-5-Passenger-car speed curves

2.5 Desired Speed

In micro-simulation models, for highway traffic, the desired speeds are usually obtained from a truncated normal distribution. Users can specify the mean and standard deviation of the distribution plus a minimum and maximum value set to avoid generating very low and very high speeds. In OTSIM, the mean desired speed can be set by users based on field data or the speed limit for each class of vehicles. McLean (1989) found that a normal distribution with mean speed between 90 and 100 km/h and coefficient of variation between 0.11 and 0.14 can represent the distribution of desired speeds of vehicles on two-lane highways. In OTSIM, the default coefficient of variation of speed is set to be 0.12; however, users can specify any value for the standard deviation of desired speed based on field observations.

In generating random desired speed from the assumed distribution, the following criteria must be checked to ensure that the desired speed is attainable according to the vehicle engine performance; i.e., (Tapani, 2005):

$$\frac{P}{M} \geq K_A {v_d}^3 + C_R v_d \qquad \text{Eq. 2-19}$$

where,

v_d= generated free-flow (desired) speed

Figure 2-6 shows the distribution of free flow speeds for passenger cars obtained from a two-lane highway in Italy (SS18 highway near Amantea CS). The distribution of passenger cars appears to be normal with a mean value of around 89.7 km/h and standard deviation of 17.6 km/h. A similar distribution can be assumed for trucks; however, the distribution of trucks free-flow speeds under a mandated speed limiter does not follow the normal distribution. This is further discussed in Chapter 5.

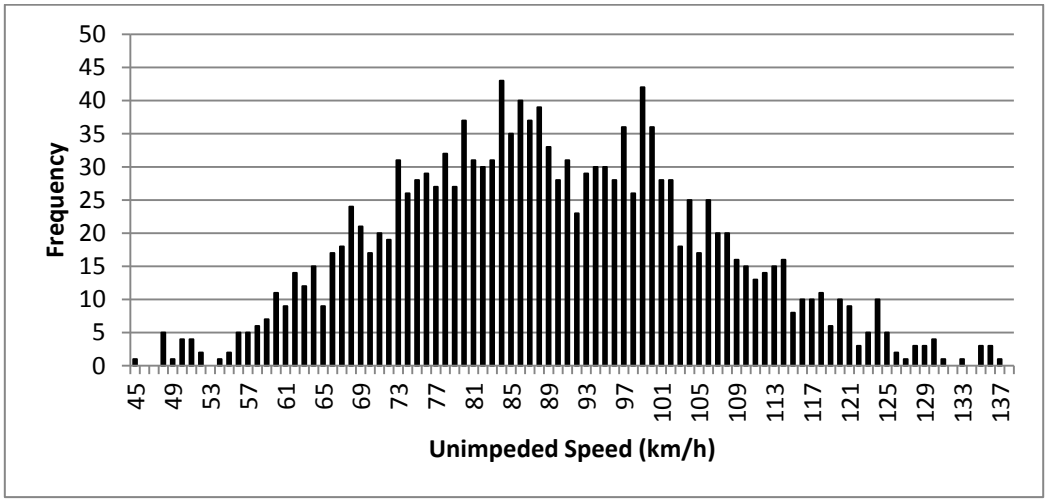

Figure 2-6– Distribution of passenger car speeds for a two-lane highway in Italy

2.6 Road Data

The road data consist of geometric information such as road length, width, elevation, grade percentage and location of passing/no-passing zones. Horizontal curvatures are not included in OTSIM. The percentage grade is convertible to angle unit as:

$$\theta = \tan^{-1}\left(\frac{Slope\%}{100}\right) \qquad \text{Eq. 2-20}$$

where,

$Slope$ = road slope in percentage

θ = road slope in angle

It is known that truck performance is highly dependent on the road segment grade. Figure 2-7 illustrates how truck speed declines from 110 km/h to the crawl speed on a 3% and 6% upgrade for four types of trucks used in OTSIM.

In the road data entry menu, users can specify the no-passing zone segments. In the real world the no-passing zones are marked by solid lines on the pavement. In the model, the vehicles do not overtake if they are located in the no-passing zones of the highway. The no-passing zone marking is normally determined according to available passing sight distance based on criteria provided in Manual on Uniform Traffic Control Devices (MUTCD, 2006).

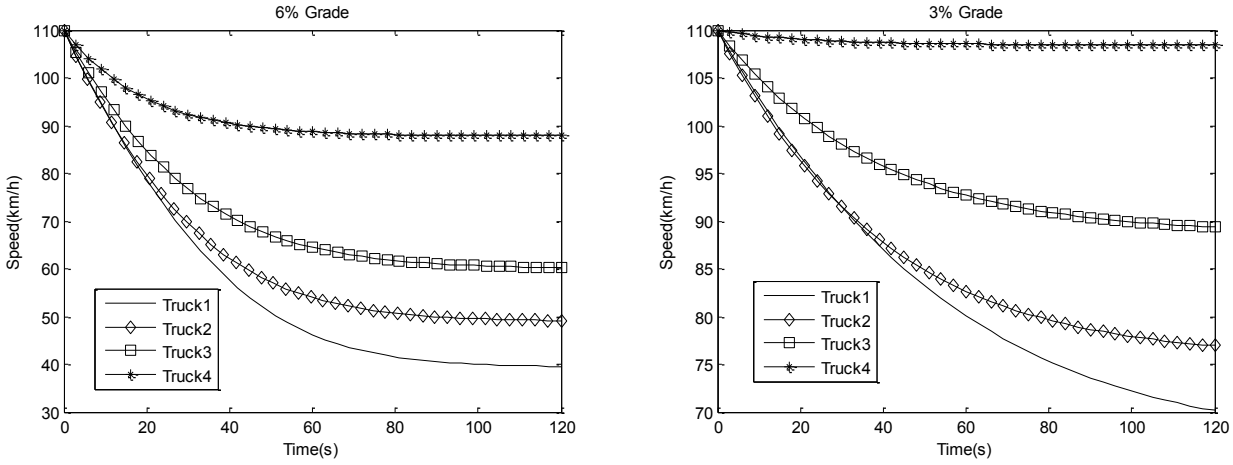

Figure 2-7- Truck speed decline on 6% and 3% upgrade segments

2.7 Driving Regimes

Three driving regimes consisting of free-flow, car-following, and overtaking are considered for simulating vehicle movement on two-lane highways in OTSIM. Depending on the position and speed of the simulated vehicle and its surrounding vehicles, the driving regime for each simulation time step

is determined and the corresponding acceleration/deceleration is calculated. In the following sections, the description of each driving regime and the underlying simulation models are presented.

2.7.1 Free-flow

In this mode of driving, drivers accelerate/decelerate to achieve their desired speed. In this situation, no interaction occurs between the simulated vehicle and the other surrounding vehicles. The amount of acceleration employed is a function of speed differential between the target desired speed and the current speed of the vehicle such that:

$$V_{diff}(t) = v_d - v(t) \quad \text{Eq. 2-21}$$

where,

v_d = desired speed of vehicle

$v(t)$ = current speed of vehicle

The actual acceleration employed is given by:

$$a_{act}(t) = min(a_{max}(t), kV_{diff}(t)) \quad \text{Eq. 2-22}$$

where,

a_{max} = maximum acceleration available at speed $v(t)$

k = calibration parameter

For passenger cars and trucks, the maximum available acceleration at time t and instant speed of $v(t)$ can be determined from the following equations:

$$a_{max}^{car}(t) = a_m\left(1 - \frac{v(t)}{v_m}\right) \quad \text{Eq. 2-23}$$

$$a_{max}^{truck}(t) = \frac{P}{M}\frac{1}{v(t)} - K_A v(t)^2 - C_R - g\sin\theta \quad \text{Eq. 2-24}$$

Figure 2-8 presents speed and acceleration profiles of a simulated vehicle starting from stop position accelerating up to 90 km/h for $k = 0.3$.

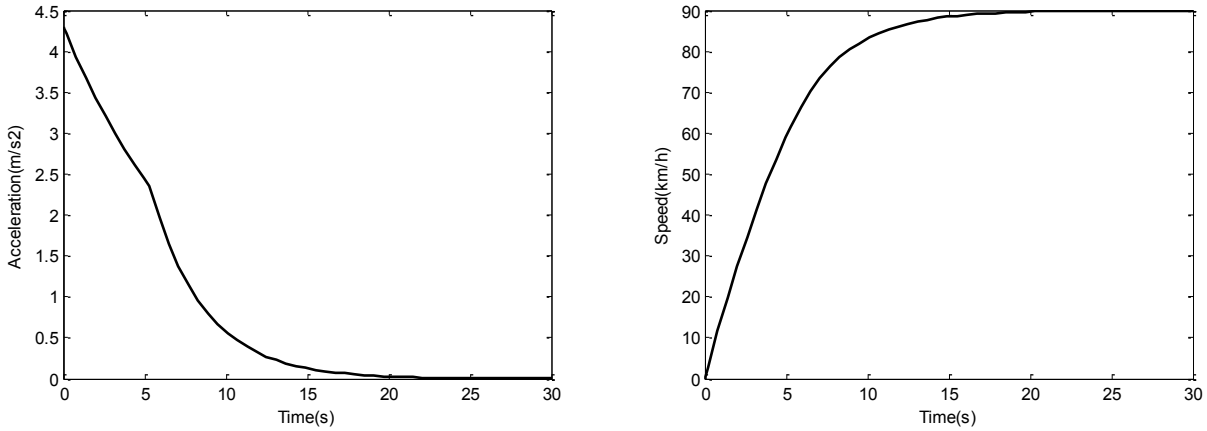

Figure 2-8- Acceleration to desired speed of 90 km/h for k=0.3 (free-flow regime)

2.7.2 Car-following

Two types of car-following models are used in OTSIM. The car-following model adopted for normal driving is borrowed from the Gipps model (Gipps, 1981). The second car-following model embedded in OTSIM is used for simulation of adaptive cruise control (ACC) system. This model is discussed and used in the investigation of ACC effect on overtaking in Chapter 6. The Gipps model is a safety distance (collision avoidance) model. The model is based on the logic that drivers always keep a safe headway such that they can stop without colliding if the preceding vehicle comes to a sudden stop. Table 2-6 presents the notations used in this model. The speed of the following vehicle (v_n) during time $[t, t+T]$ can be determined as:

$$v_n(t+T) = \min\{v_n^a(t+T), v_n^b(t+T)\} \quad \text{Eq. 2-25}$$

where,

$$v_n^a(t+T) = v_n(t) + 2.5a_n^{max}T\left(1 - \frac{v_n(t)}{V_n}\right)\sqrt{0.025 + \frac{v_n(t)}{V_n}} \quad \text{Eq. 2-26}$$

and

$$v_n^b(t+T) = d_n^{max}T + \sqrt{(d_n^{max}T)^2 - d_n^{max}\left[2\{x_{n-1}(t) - s - L_{n-1} - x_n(t)\} - v_n(t)T - \frac{v_{n-1}(t)^2}{\hat{d}_{n-1}}\right]} \quad \text{Eq. 2-27}$$

Table 2-6- Gipps car-following model parameters definition and notations

x_n	Position of the following vehicle(m)
v_n	Speed of the following vehicle(m/s)
x_{n-1}	Position of the lead vehicle(m)
v_{n-1}	Speed of the lead vehicle(m/s)
a_n^{max}	Maximum desired acceleration of the following vehicle (m/s^2)
d_n^{max}<0	Maximum desired deceleration of the following vehicle, (m/s^2)
$\hat{d}_{n-1}$	Estimation of max. desired deceleration rate of the lead vehicle (m/s^2)
s	desired distance to the lead vehicle while standing (front to end)
L_{n-1}	length of the lead vehicle, (m)
V_n	Desired speed of the following vehicle (m/s)
T	Reaction time of the following vehicle, (s)

One of the advantages of the Gipps model is that the model parameters are associated with physical characteristics of vehicles and behavioral characteristics of drivers. As long as reasonable values are assigned to these parameters the model can be an acceptable reflection of real car-following behavior (Panwai and Dia, 2005). The calibration results for the car-following model are reported in Chapter 3.

2.7.3 Overtaking

The overtaking maneuver refers to the situation when the following vehicle driver in the traffic stream decides to pass the lead vehicle using the opposing lane. Figure 2-9a provides an overtaking situation snapshot. The overtaking vehicle (also referred to as the following vehicle or FV) overtakes the lead vehicle (or LV). The third vehicle of interest in this process is the on-coming or opposing vehicle (OP). Based on the current available gap (D), the FV driver checks whether initiating an overtaking is safe or not. This means whether it is possible to pass the slower moving vehicle(s) and return back before the OP reaches some critical spacing or the geometric sight distance ends. Figure 2-9b illustrates the overtaking maneuver in a time-space diagram. In this demonstration, there are five operational stages for overtaking namely catch-up, desire-to-overtake, acceptance or rejection of the

gap, passing, and return to travel lane. Next, we elaborate on these five operational stages and introduce their underlying modeling relationships. In the remaining of this thesis, the "following vehicle" (FV) and the "lead vehicle" (LV) terms will be used interchangeably as the "overtaking vehicle" and the "overtaken vehicle", respectively.

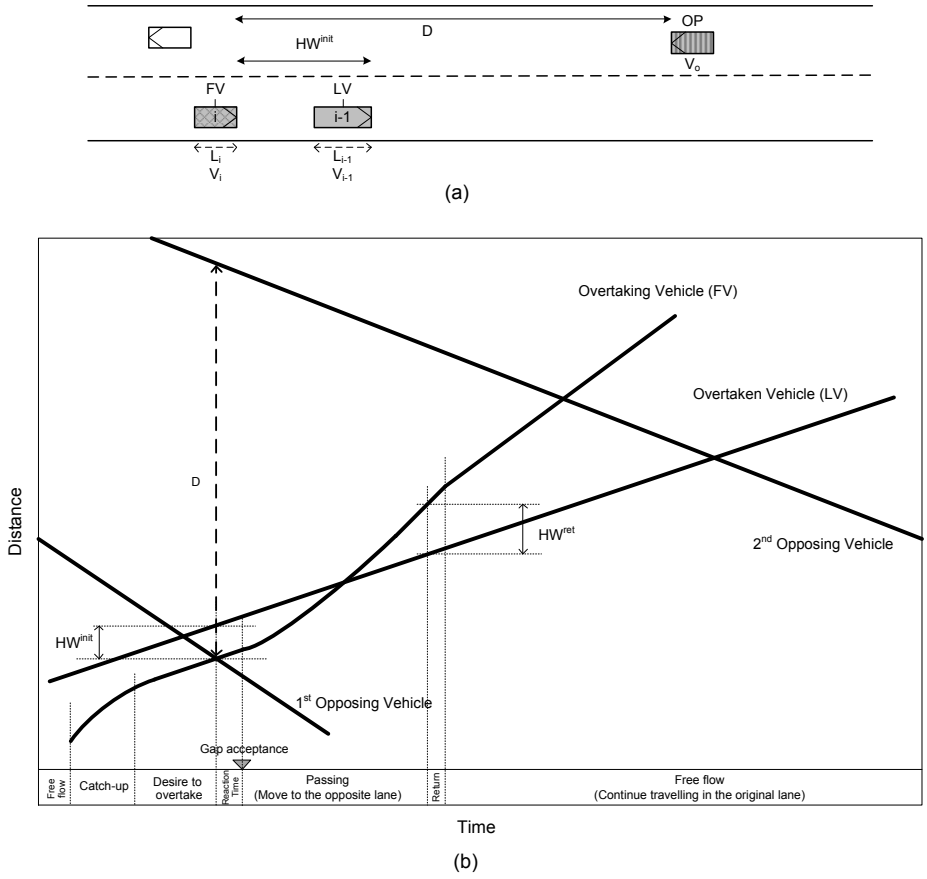

Figure 2-9- a) An snapshot of vehicles involved in an overtaking decision process b) Time-space diagram of an overtaking maneuver consisting of five sequential stages

The following rules are used in OTSIM overtaking logic:

1- The drivers cannot overtake if the vehicle is in an overtaking restriction zone (solid single or double lines).

2- A vehicle cannot overtake if it is being overtaken.

3- A vehicle cannot overtake if the vehicle in front is overtaking.

4- The travel speed of vehicles before and during the overtake can exceed the speed limit.

2.7.3.1 Catch-up, desire-to-overtake, gap-acceptance

The catch-up stage refers to the time interval during which the FV approaches the slower moving LV and matches its speed in a car-following state. The catch-up stage normally takes place prior to initiating the overtaking. However, in flying overtakes this stage can be partially or fully skipped; i.e., the FV does not slow down to the speed of LV and passes the LV with its initial speed. The distance to the LV, from which the speed of FV begins to be impeded by the lower speed of LV and deceleration is required, can be estimated using a simple motion equation as (Tapani, 2005):

$$C_i = T_i^d . v_{i-1}(\mathrm{t}) + \frac{(v_i(\mathrm{t}) - v_{i-1}(\mathrm{t}))^2}{2d_i^{desire}}, v_i > v_{i-1} \qquad \text{Eq. 2-28}$$

where:

C_i = catch-up distance (m)

d_i^{desire} = desired deceleration rate of the FV (m/s^2)

T_i^d = desired following time headway of the FV (s)

v_i, v_{i-1} = operating speed of the FV and LV respectively at a given point in time (m/s)

After this stage the FV keeps desired time headway of T_i^d to the LV. Following catch-up, a "desire-to-overtake" can be triggered by comparing LV operating speed to FV driver's desired speed, and estimating:

$$SD = v_i^{des} - v_{i-1} \qquad \text{Eq. 2-29}$$

where, v_i^{des} is the desired speed of the FV (a function of driver attributes) and v_{i-1} is the "actual" operating speed of the LV. We assume that FV driver will consider overtaking if SD exceeds a pre-set speed differential or threshold (SD_{thre}). In OTSIM a default value of 8 km/h is used for SD_{thre} as reported by Kim and Elefteriadou (2010).

After this stage the driver considers overtaking the slower vehicle in the traffic stream if suitable gaps become available. This decision is central in modeling the overtaking maneuver and will be discussed in detail in the next chapter. Based on the position of the vehicle in the platoon, the initial decision can be overtaking of a single or multiple vehicles in the traffic stream. Once the gap is accepted the overtaking vehicle moves to the opposing lane and accelerates to pass.

2.7.3.2 Passing and return

When the gap in the opposing direction is accepted, the driver pulls out to the opposite lane and accelerates to his/her desired overtaking speed (usually higher than normal desired speed) to pass the slower vehicle ahead. The overtaking vehicle continues its path in the opposing lane until a safe time gap between the rear bumper of overtaking vehicle (FV) and the front bumper of overtaken vehicle (LV2) is available to return back. At this point (whether or not the initial gap-acceptance decision was to overtake single or multiple vehicles) the driver checks the gap between the overtaken vehicle (already passed) and any other possible vehicle in front (second potential overtaken vehicle, LV1). This gap is named as the return or *pull-back-gap* (G_{ret}). Depending on G_{ret} size, overtaking vehicle may react differently (return back, continue, abort overtake). Figure 2-10 illustrates the overtaking vehicle in four situations of return back and the corresponding possible decisions as discussed below.

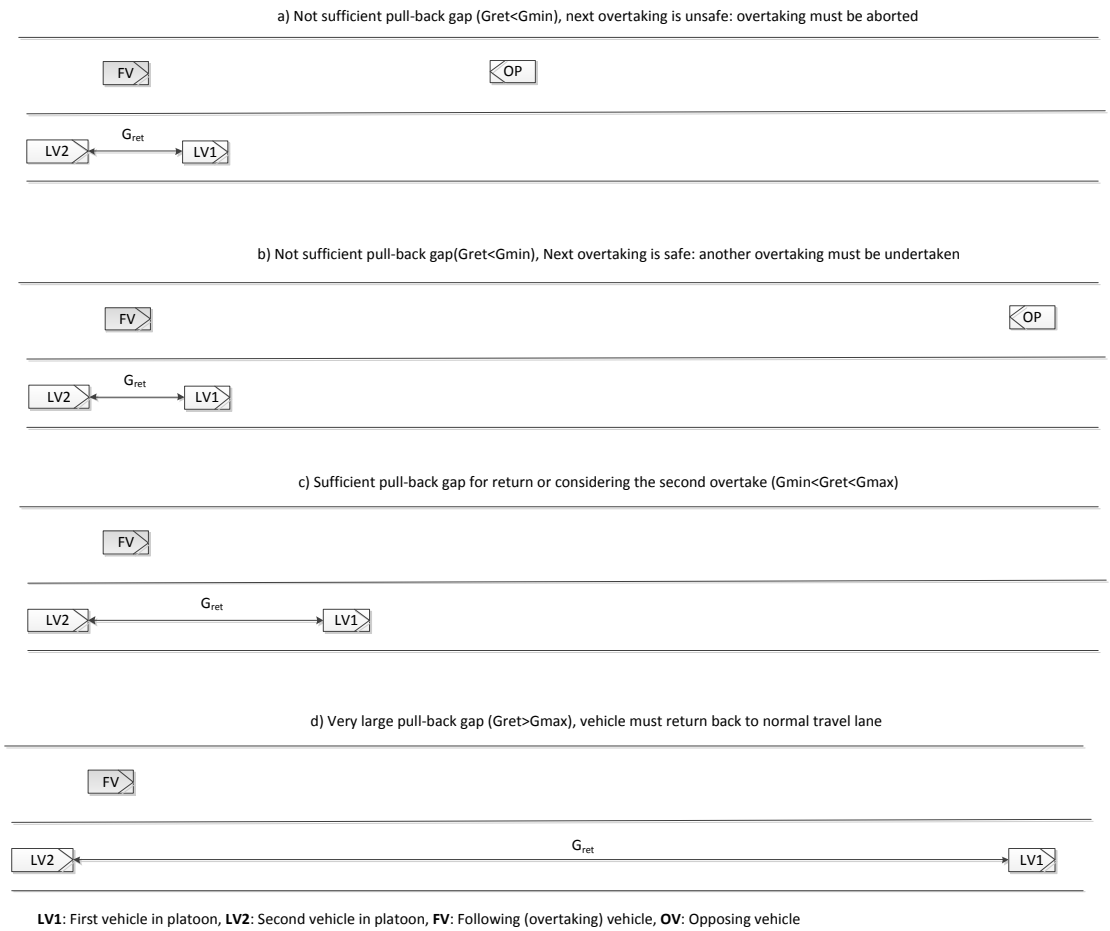

LV1: First vehicle in platoon, **LV2**: Second vehicle in platoon, **FV**: Following (overtaking) vehicle, **OV**: Opposing vehicle

Figure 2-10- Possible decision situations at the return back position

If G_{ret} is shorter than a minimum safe return gap (G_{min}) then the driver must either overtake the next vehicle if it is safe to do so (situation "a") or abort overtake because there is not enough safe space to return and second overtake is unsafe (situation "b"). However, if G_{ret} is larger than G_{min} and shorter than a max value (G_{max}), the overtaking vehicle may return back or consider the second overtaking (situation "c"). In this situation, if the overtaking driver has desire-to-overtake the second vehicle (refer to desire-to-overtake condition) and the gap-acceptance decision is to pass, the next overtake occurs. In this case, the second overtake can be treated as a flying overtake since the overtaking vehicle is already in the opposing lane and the catch-up stage is skipped. However, if there is no further desire-to-overtake or the next available gap is rejected, the vehicle returns back to its normal travel lane. If the distance to the next slow moving vehicle is larger than G_{max} (situation "d"), the overtaking vehicle returns back to the normal travel lane and any future overtake will be considered later down the road.

Figure 2-11 illustrates the decision flowchart that is discussed in above. When the driver returns back to the normal travel lane he/she slows downs to the normal desired travel speed.

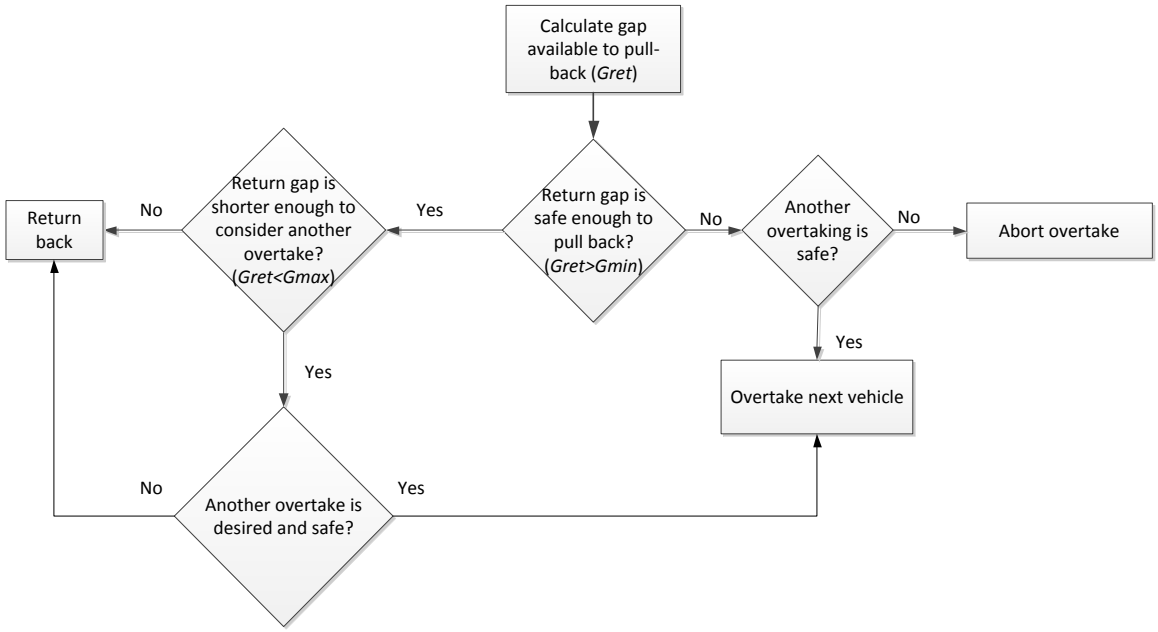

Figure 2-11- Passing process decision flowchart

2.7.3.3 Abort

In situations where continuing overtake is not safe, the overtaking vehicle will abort the maneuver by using appropriate deceleration. The overtaking vehicle continues to decelerate until a safe headway between its front bumper and the rear bumper of the overtaken vehicle is available. The employed deceleration rate and the return headway are calibration parameters associated with this process. One of the abort situations was discussed in the above section. In addition, during the passing phase if continuing overtaking becomes unsafe the logic considers to abort the overtake. This check is done up to the abreast position.

2.8 Simulation Platform

OTSIM was implemented in MATLAB programming environment. The software makes use of Graphic User Interface (GUI) for entering the simulation input data, animation of micro-simulation, and presenting the simulation outputs. Separate post-processing software is developed to analyze the simulation log data and provide detailed specific output results. OTSIM makes use of maximum 20 simulation random seeds. Each random seed consists of series of random generation numbers that create stream of pseudo random numbers for generating traffic and driver attributes including traffic flow, desired speeds, vehicle composition, and drivers' aggression level. The evaluation of traffic and safety outputs are normally based on an average of 10 to 20 runs depending on the variance of the output variable, the desired confidence level, and an acceptable error value.

Figure 2-12 proposes the overall simulation flowchart used in OTSIM. The following steps are executed during the simulation run:

1) Generate random traffic and vehicle/driver attributes ($t = 0$).
2) For every time increment (1s) the following steps are carried out until the simulation stop time is reached ($t = Tend$):
   a) Load a vehicle to the road if it is time to do so.
   b) For each vehicle i currently on the road ($i = 1\ to\ N$) update the acceleration, speed, and position of the vehicles based on the vehicle status j (j:*Free*, *Following*, *Overtaking*, *Aborting*).
   c) Remove the vehicle from the road if it has reached end of the road.
   d) Update the graphical animation.
3) Log the output results if requested.

The following pseudo code represents the sequence of algorithm execution:

For $t = 1$ **to** $t = Tend$

For $i = 1$ **to** $i = N$

Case j

"Free"

Acceleration to desired speed

Switch to "Following" or "Overtaking" if conditions are met

"Following"

Acceleration/Deceleration based on GHR car-following formula

Switch to "Overtaking" or "Free" if conditions are met

"Overtaking"

Acceleration to desired overtaking speed

Switch to "Free" or "Abort" if conditions are met

"Aborting"

Deceleration using abort deceleration rate

Switch to "Free" if conditions are met

End

End

End

At each simulation time step, depending on the vehicle's status (free-flow, following, overtaking, or aborting), an appropriate acceleration/deceleration is calculated for the corresponding driving regimes, and the position of the vehicle is then updated. In addition, at every time step, conditions are checked as whether switching from a driving regime to another regime is necessary. Figure 2-13 illustrates this process using a state flow diagram. Conditions for transition between different states are indicated on the links connecting two states. The triangular bubbles present the corresponding actions (e.g. acceleration/deceleration) associated with each driving regime.

The diagram illustrates that free-flow state can change to car-following or overtaking states. For the first case the following vehicle slows down to catch-up to the speed of the lead vehicle while for the latter case the following vehicle fly-overtakes the lead vehicle without reducing its speed. The overtaking state may lead to free-flow state when the maneuver is successfully finished or to abort state when continuing overtaking is unsafe. Car-following can be switched to overtaking if the gap is accepted or to free-flow state if the lead vehicle departs the road or changes lane (overtake).

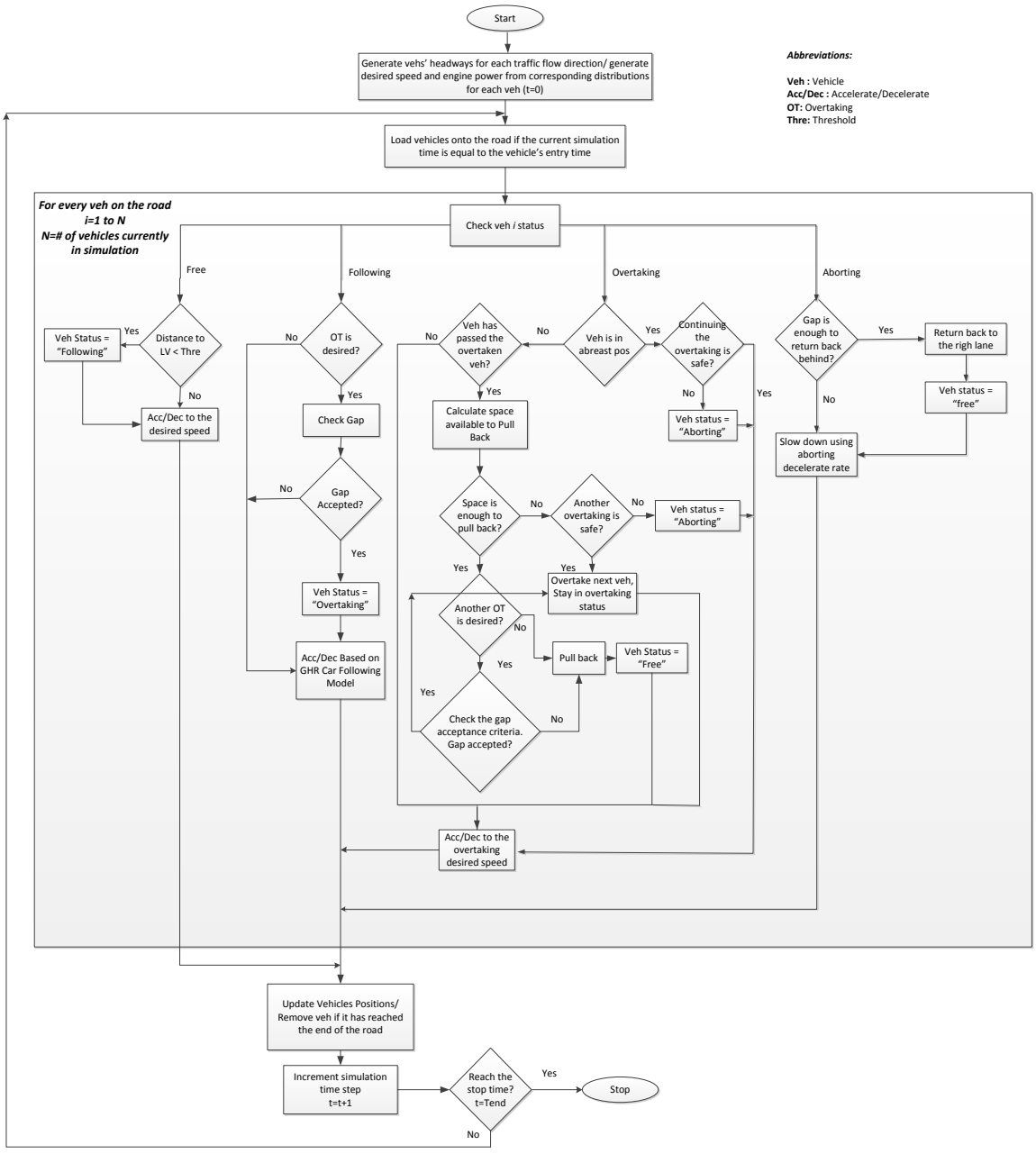

Figure 2-12- OTSIM simulation flowchart

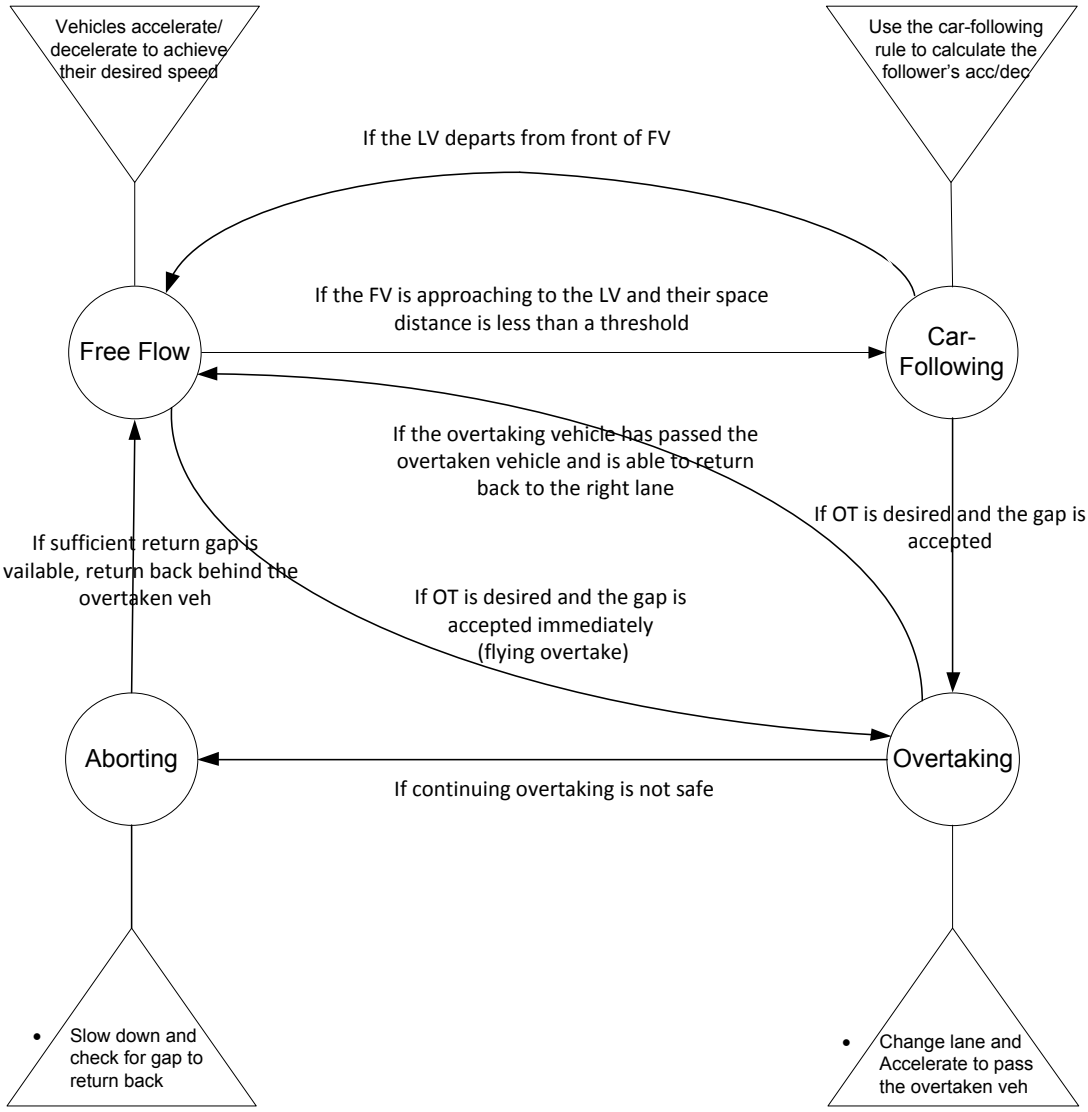

Figure 2-13- The transition process between the driving regimes

2.9 Conclusion

In this chapter, the overall structure of the proposed two-lane simulation model (OTSIM) was discussed in detail. The traffic generation model including platoon and headway models were presented and the corresponding model parameters were introduced. Vehicle performance parameters for passenger-cars, recreational vehicles and trucks were determined and the underlying motion

equations were presented. In OTSIM, a normal distribution was assumed to generate vehicles desired speeds. The road data in OTSIM presents the segment grade as well as passing and no-passing zones. The truck performance on upgrade was simulated for a sample truck and segment grade. As shown, OTSIM consists of three behavioral driving models listed as free-flow, car-following and overtaking. The overtaking process was broken down to a number of phases and the underlying relationships and mathematical formulations were presented. Finally, a large view of the simulation algorithm and its flowchart were illustrated and switching conditions between driving regimes were discussed. In the next chapter, the discussions will mainly focus on the development and the calibration of the overtaking gap-acceptance model introduced as part of the overtaking process in this chapter.

Chapter 3
Overtaking Gap-acceptance Model

3.1 Introduction

As discussed in the previous chapter, the gap-acceptance decision is a part of the overtaking process, where the following vehicle finds a sufficient gap in the opposing traffic and decides to pass the slower lead vehicle in the traffic stream. The purpose of this chapter is to develop and calibrate a new mechanistic (physical) overtaking gap-acceptance model for application to two-lane highways. The structure of this model is such that it can more easily be calibrated and validated than the existing models from observational overtaking data. Unlike previous models, the proposed gap-acceptance is based on the driver's perception of safe separation between overtaking and opposing vehicles after the overtaking maneuver has been completed. This includes the perception of overtaking distance into the decision logic. Because the gap-acceptance decision is made at the beginning of the maneuver, this separation needs to be perceived by the overtaking driver at the beginning of the maneuver, based on incomplete traffic information. Hence this unknown perceived overtaking gap is subject to estimation error that needs to be taken into account in the model. The content of this chapter is published in Ghods and Saccomanno (2013a).

3.2 Overtaking Gap-acceptance Behavior

An appreciation of how overtaking drivers respond to the size of available gaps in the opposing traffic stream is central to modeling the overtaking process. The overtaking gap is defined as the separation distance of the overtaking vehicle from the first opposing vehicle (if any) at the moment the gap becomes available given the driver has desire-to-overtake.

McLean (1989) noted that the gap-acceptance logic for overtaking (similar to street crossing gap-acceptance) can be categorized into two basic behavioral assumptions: consistent and inconsistent gap-acceptance. In the case of consistent behavior, it is assumed that each driver has a critical minimum acceptable gap (critical gap). These critical gaps are ascribed to individual drivers based on an assumed probability distribution (e.g. normal or log-normal). More aggressive drivers have shorter critical gaps. In this assumption, the decision to accept or reject a gap is assumed to be deterministic, based on gaps shorter or longer than critical. The consistent behavior refers to "between-driver" variability.

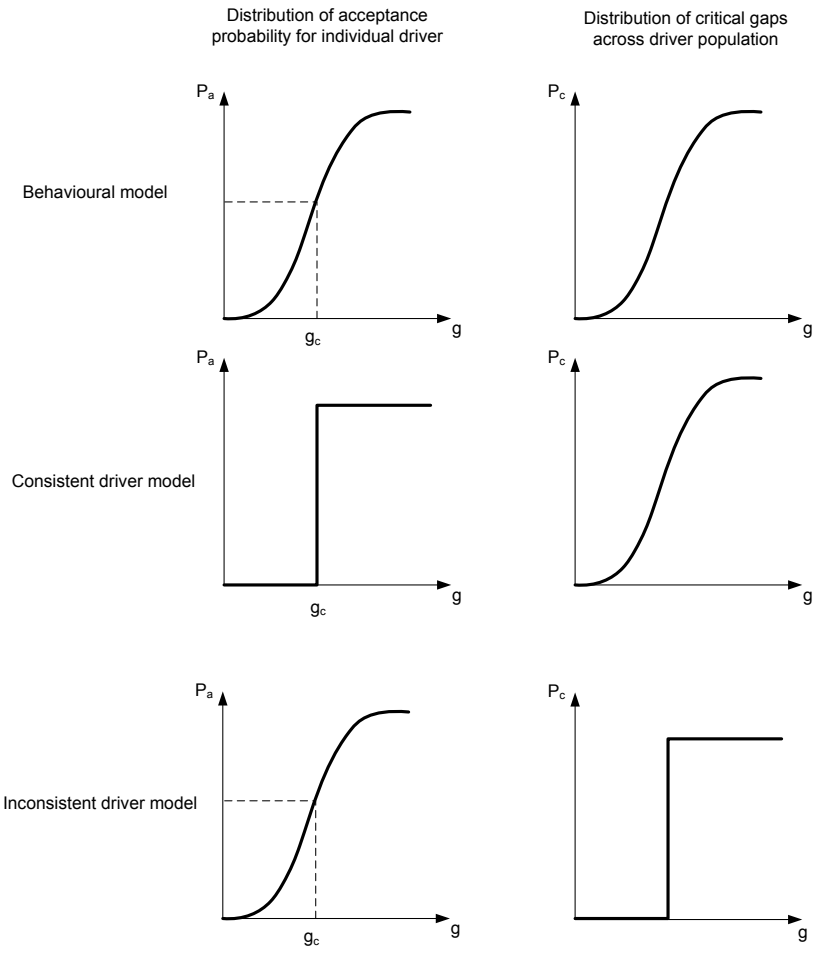

Figure 3-1- Three models of overtaking gap-acceptance behavior (reproduced from McLean 1989)

For inconsistent behavior, however, drivers will accept or reject gaps within some level of "behavioral" variability or uncertainty, such that, a particular driver responds to an available gap stochastically. This can be modeled through an assumed gap-acceptance probability such that the longer the gap, the greater the probability of acceptance. The inconsistent behavior refers to "within-driver" variability. Figure 3-1 illustrates the concept of overtaking gap-acceptance behavior. The nature of parameters underlying these models will need to be established from observational gap-acceptance data. In practice, the drivers' gap-acceptance overtaking logic lies somewhere between inconsistent and consistent behavioral assumptions (Figure 3-1-behavioural model). However, unlike stream crossing gap-acceptance behavior, the consistent behavior appears to be more dominant in overtaking mainly due to the larger impact of vehicles' performance in the overtaking maneuver,

which reduces the tendency of drivers to change their aggression level very frequently (McLean 1989). In addition, unlike stream crossing, there is less social pressure from other vehicles in the platoon to encourage the driver to overtake aggressively because overtaking gap-acceptance is an optional choice for drivers (McLean 1989). Although these statements are valid, drivers usually tend to become more aggressive in accepting shorter gaps as their following time behind a slow moving vehicle is increased (Koorey, 2007). However, considering both between and within drivers' variability, in a more complex model structure, requires more extensive field data for calibration and validation. This has been a challenge since overtaking can occur anywhere on a road section, where information regarding the past gap-acceptance and following time circumstances are unknown.

3.3 Previous Models

Various methods have been investigated for modeling the overtaking gap-acceptance logic and its application in traffic simulation. As compared to car-following or lane-changing models, however, it has been difficult to provide specific calibration parameters for overtaking gap-acceptance due to complexity of the process and lack of suitable vehicle tracking and overtaking data for two-lane highways for model validation. In this section of the chapter we briefly review several major microscopic traffic simulation models that have been developed for application to two-lane highway operations including: TWOPAS (St John and Harwood, 1986; Leiman et al., 1998), TRARR (Troutbeck, 1981; Shepherd, 1994; Hoban et al., 1991), and VTI (Ahman, 1972).

TWOPAS was developed by MRI (Midwest Research Institute) in the early seventies and was modified by Leiman et al. (1998) under the name of UCBRURAL. This model was applied to estimate two-lane highway capacity and level-of-service in the Highway Capacity Manual (HCM) (TRB 2000). TWOPAS has also been applied in the Interactive Highway Safety Design Model (IHSDM) (Paniati and True, 1996) as a Traffic Analysis Module (TAM). The overtaking logic in TWOPAS is probabilistic in nature and is based on gap-acceptance probability functions for a number of overtaken vehicle speeds and available sight distance types limited by opposing vehicle or geometry (Figure 3-2). The probability functions in TWOPAS were determined from empirical overtaking data collected in the early seventies (Harwood et al., 1999). In this chapter the output results of the proposed overtaking gap-acceptance logic will be compared to those of TWOPAS.

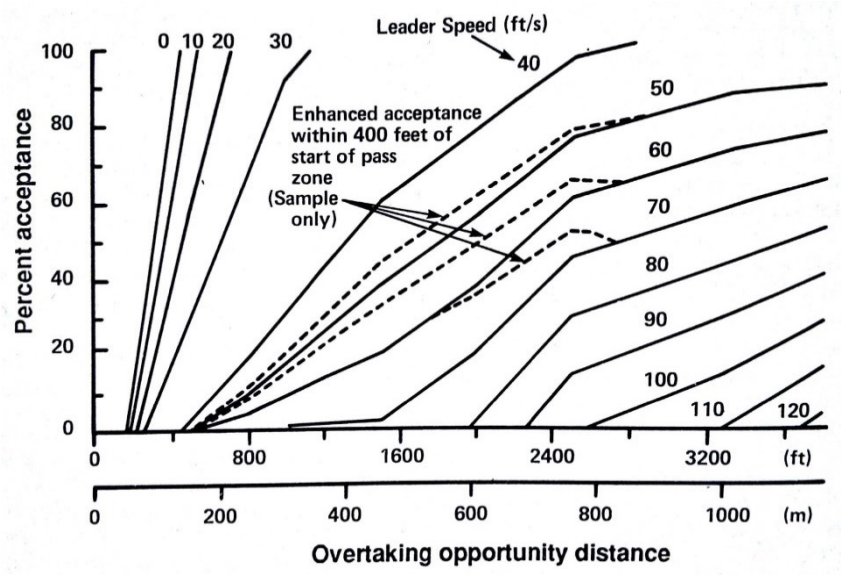

(a)

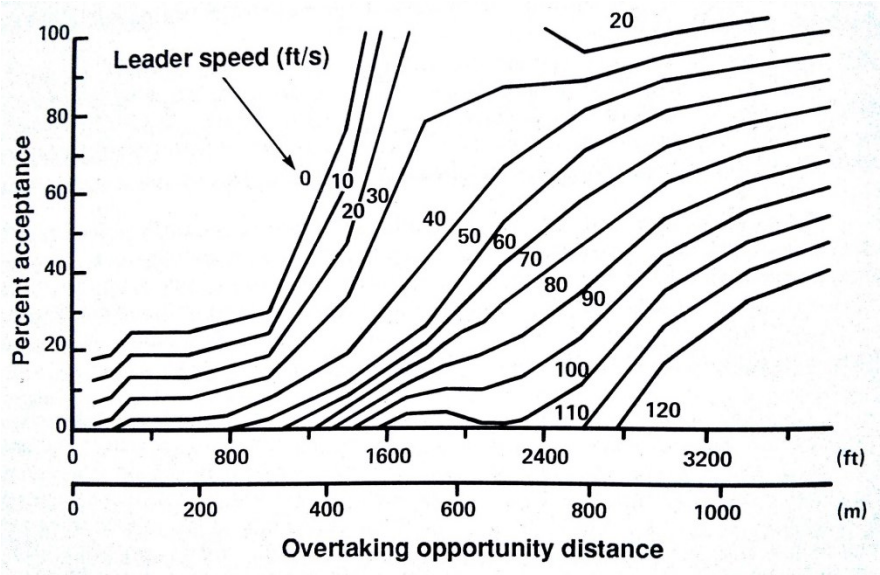

(b)

Figure 3-2- Gap-acceptance probability function used in TWOPAS: (a) Sight-distance-limited (b) Opposing-vehicle-limited (Source: St John and Kobett, 1978 from McLean, 1989)

TRARR was developed by the Australian Road Research Board (ARRB) as a research tool for the design of passing lanes in level highway segments (Hoban et al., 1991; Lovell et al., 1993). The overtaking logic in TRARR is deterministic and the decision to overtake is based on the available overtaking time gap multiplied by a vehicle-specific safety factor. A driver aggressiveness factor is

assigned to each vehicle such that drivers do not overtake when their aggression level is lower than that for any driver vehicle(s) in the lead position(s). Hegeman (2004) reported that the application of TRARR in the Netherlands resulted in higher overtaking frequencies or rate when compared to field observations. In this chapter, the application of the proposed overtaking gap-acceptance logic will be compared to results from the Netherlands data.

The VTI model was developed to analyze traffic behavior for rural two-lane highways in Sweden. The stochastic overtaking logic of VTI is generally more advanced than either TWOPAS or TRARR. It accounts formally for a large number of factors affecting overtaking, such as, type of overtaking (flying or accelerated), available gap with opposing vehicles, type of overtaken vehicle (car or truck), road cross-sectional width and grade, etc. A total of 32 combinations of these factors are considered by VTI for which a separate gap-acceptance versus gap size function was developed. Figure 3-3 illustrates some of the gaps acceptance curves originally developed for the VTI model. As can be expected, given the large number of factors that could affect overtaking, the VTI model requires a significant amount of field data for calibration that accounts for the full spectrum of overtaking situations (combination of factors). A modified version of VTI known as RuTSim is proposed in Tapani (2005) for two-lane highways by adding intersection control logic to the simulation framework; however, the same VTI overtaking model was used. The application of RuTSim for overtaking assistance systems is used in Hegeman et al. (2009).

Among other models, Farah et al. (2009a) used a critical gap-acceptance concept and a binary choice Logit model in their proposed gap-acceptance logic. The critical gap for an overtaking vehicle was determined based on traffic variables, road geometry, and driver characteristics as obtained from a driving simulator. In this work, limited traffic and road conditions were evaluated and the validity of simulator data may have introduced some bias into the model results. In Farah et al. (2009b) a regression model was developed to link overtaking time-to-collision (TTC) with respect to opposing vehicles for different assumed road, traffic, and driver characteristics, as obtained from a driving simulator.

Recently, Li and Washburn (2011) implemented a two-lane highway simulation algorithm into CORSIM model (Halati et al., 1997). The overtaking decision in this model is based on comparing available gaps with estimates of safe passing sight distances (PSD) as proposed by the AASHTO

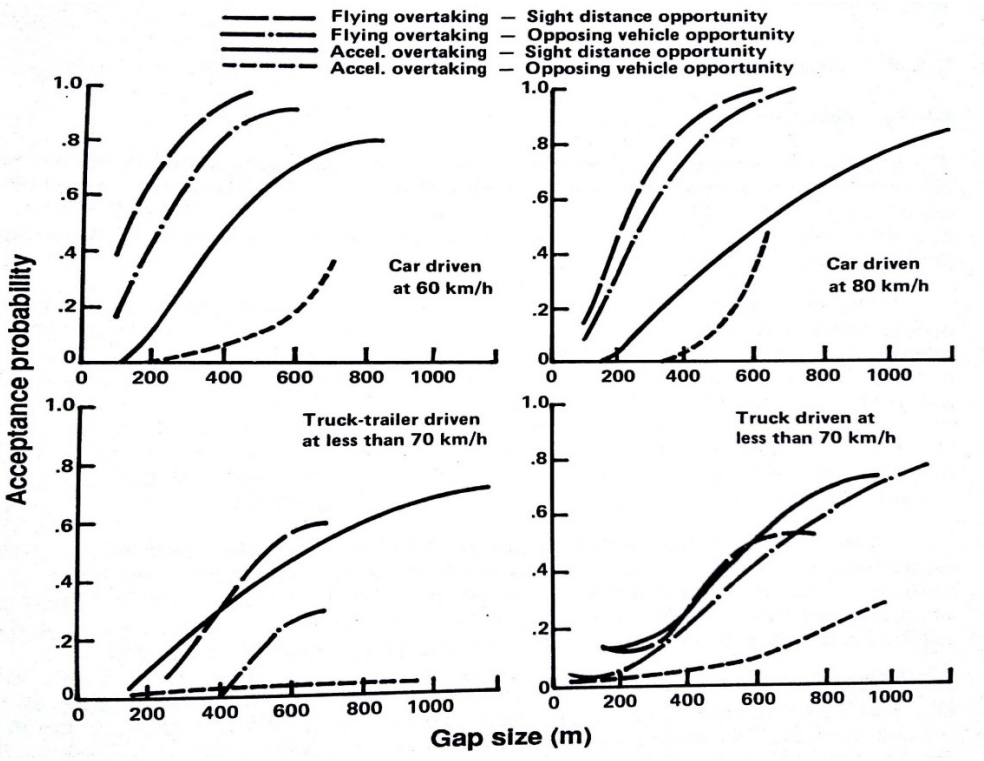

Figure 3-3- Gap-acceptance probability function for accelerative and flying overtake for two overtaking gap types originally developed for the VTI model (Source: Ahman, 1972 from McLean, 1989)

Green Book (AASHTO, 2004). This approach, although simple to implement, does not make use of any overtaking field data for calibration nor does it propose a new behavioral overtaking logic. In addition, a number of studies have reported that PSD values in AASHTO are very conservative for application to overtaking behavior (Harwood et al., 2008). Although the proposed model is also able to use the Manual of Uniform Traffic Control Devices (MUTCD) PSD values, there has not been any attempt to show which one may yield more realistic results. Similarly, Kim and Elefteriadou (2010) used AASHTO Green Book guidelines to develop an overtaking simulation model known as TWOSIM for application to two-lane highway capacity analysis.

The review of current overtaking gap-acceptance models indicates that challenges in modeling overtaking maneuver is related to linking decision to overtake to available gaps in different road, traffic, vehicles, and driving conditions. Unlike other driving regimes such as car-following or lane-changing, it has been difficult to specify model parameters for the overtaking gap-acceptance model. This is mainly due to separate involvement of factors influencing gap-acceptance behavior, in the

simulation logic. Given the number of these factors and their range of likely values, any updates to these models would require extensive overtaking field data that is difficult and expensive to obtain.

3.4 OTSIM Overtaking Gap-acceptance Model

The gap-acceptance logic in OTSIM takes a mechanistic view of the overtaking process (established on motion physical laws). In principle we would expect that the overtaking decision depends on the overtaking driver's perception of the residual gap separating the overtaking vehicle from the opposing vehicle after the maneuver has been completed as perceived by the overtaking driver *prior to initiating the overtaking maneuver*. It is reasonable to assume therefore, that the overtaking driver needs to be cognizant of this "safe separation" in order to avoid a potential head-on crash with the on-coming vehicle.

Unlike previous models that use the available gap to the opposing vehicle or maximum sight distance at the beginning of maneuver in the decision logic, in OTSIM the decision to overtake is also dependent on a prediction (perception) of the driver's overtaking distance prior to initiating the maneuver and estimate of distance travelled by the opposing vehicle during the overtaking time. The inclusion of overtaking distance in the decision logic can systematically take into account a number of overtaking conditions that may occur at different speeds and composition of vehicles (with different physical attributes) involved in overtaking. This logic is established based on estimate of the perception of the residual gap separating the overtaking vehicle from the opposing vehicle after the maneuver is completed. This estimate is based on: 1-vehicle dynamics information available prior to the maneuver (e.g. speed of overtaking and overtaken vehicles and the distance headway between them), 2- estimates of variables that determine overtaking distance (e.g. overtaking acceleration and speed profiles), and 3-estimate of distance travelled by the opposing vehicle during the overtaking. The difference between the available gap and the distances by overtaking and opposing vehicle during the overtaking provide the estimation of the residual gap.

In this chapter, this separation gap is referred to as the overtaking vehicle's "time-to-collision" or TTC, a measure that encapsulates a full spectrum of physical variables influencing the gap-acceptance process. In other words, the perceived TTC is assumed to combine all physical (vehicle, traffic, and driver) attributes that play a role in the overtaking process because it takes into account an estimate of overtaking distance in initiating gap-acceptance decision. Finally the perception of TTC

will need to exceed some driver specific critical value (threshold) before the gap is accepted and overtaking is initiated.

In the proposed overtaking gap-acceptance logic two measures of TTC need to be considered: 1) that which is perceived by the overtaking driver prior to initiating the maneuver (TTC^p) and 2) the actual value that can be calculated after the maneuver is completed (TTC). Because it is not possible to obtain an estimate of TTC^p, we assume that TTC^p can be expressed as a random variable with the mean of TTC (the actual overtaking-opposing vehicles separation time) plus a random error term, such that:

$$TTC^p = TTC + \varepsilon \qquad \text{Eq. 3-1}$$

where, ε is randomly distributed; i.e., $\varepsilon \sim N(0, z^2)$

The assumption of normality and variance of the error term will need to be verified empirically based on observed traffic data.

As noted previously TTC is a function of the overtaking distance. As a result, the adoption of TTC and TTC^p in the overtaking gap-acceptance model can systematically account for physical length of vehicles, and type of overtaking behavior, i.e., flying or accelerated as well as single or multiple vehicles overtakes.

3.4.1 Estimation of TTC

In this section, the "following vehicle" (FV) and the "lead vehicle" (LV) terms will be used interchangeably as the "overtaking vehicle" and the "overtaken vehicle", respectively.

As illustrated in Figure 3-4, the estimation of TTC involves three sequential overtaking distances (or decision phases):

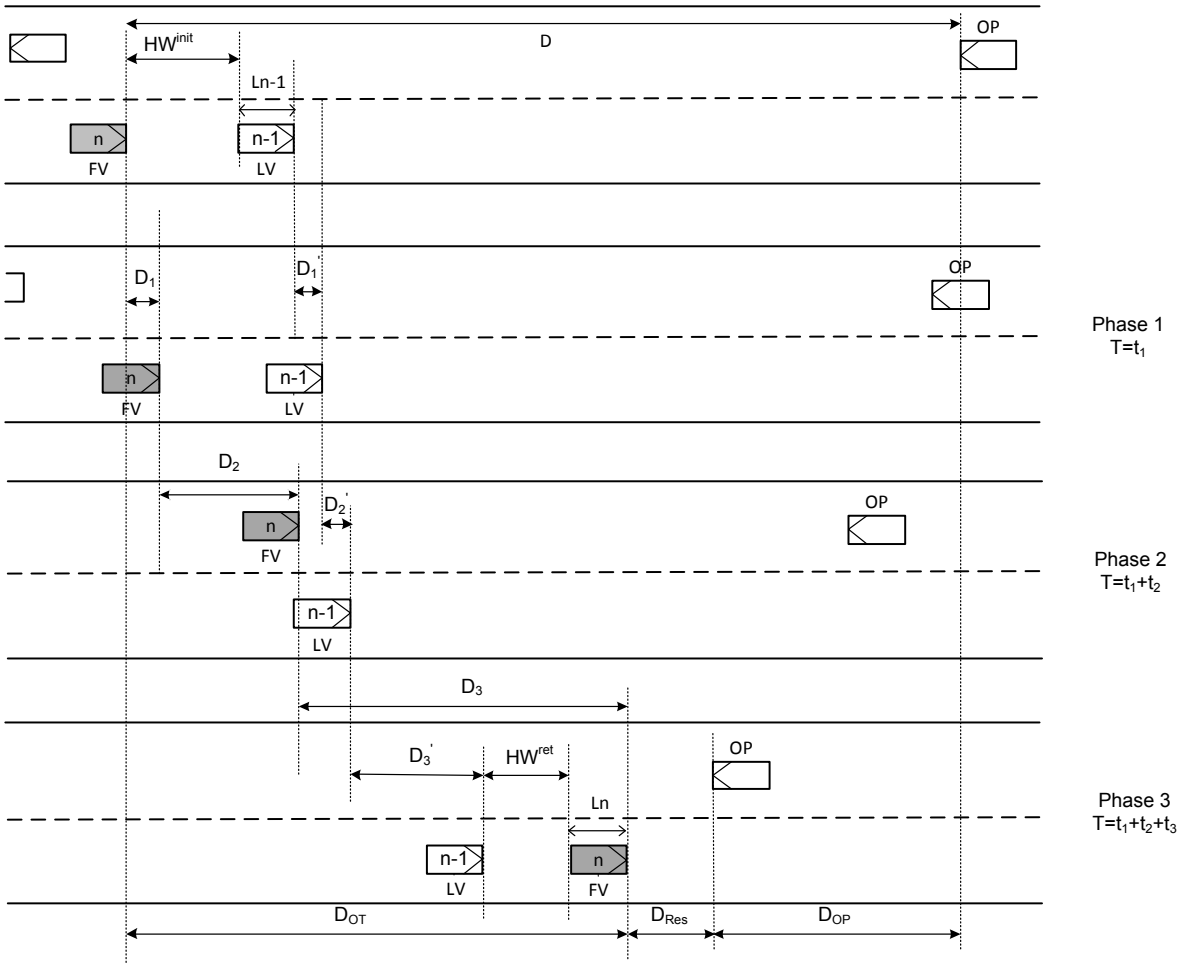

Figure 3-4- Snapshots of overtaking maneuver phases for TTC estimation.

D_1: Distance travelled by the FV from the initial decision-to-overtake point to pull out (beginning of the OT maneuver)

D_2: Distance travelled by the FV from pull-out to the point where desired overtaking speed is achieved, and

D_3: Distance travelled by the FV to achieve safe separation with the overtaken vehicle while returning to its normal travel lane.

To estimate D_1, we assume a perception/reaction time of $t_1 = T_{react}$ and a constant initial FV speed of v_n^{ini} such that this vehicle will cover a distance of:

$$D_1 = v_n^{ini} \times t_1 \quad \text{Eq. 3-2}$$

During this time, the LV is assumed to cover a distance of D_1' assuming a constant speed of v_{n-1}, such that:

$$D_1^{'} = v_{n-1} \times t_1 \quad \text{Eq. 3-3}$$

To estimate D_2, the time for FV to pull out and attain its desired overtaking speed (v_n^{des-ov}) is estimated to be t_2 (derivation in Appendix A):

$$t_2 = -\frac{v^{max}}{ka^{max}} \times ln\left(\frac{v^{max} - v_n^{des-ov}}{v^{max} - v_n^{ini}}\right) \quad \text{Eq. 3-4}$$

where,

v_n^{des-ov} = desired overtaking speed of the FV

v^{max} = maximum achievable speed of the FV (vehicle specific)

a^{max} = maximum achievable acceleration of the FV from stopped position (vehicle specific)

k = proportion of maximum acceleration employed by the driver for overtaking

The distance covered in the interval t_2 is estimated as:

$$D_2 = v^{max} t_2 + \frac{v^{max}}{ka^{max}}\left(v^{max} - v_n^{ini}\right)\left(e^{-\frac{ka^{max}}{v^{max}}t_2} - 1\right) \quad \text{Eq. 3-5}$$

and the corresponding distance traversed by the LV during this t_2 time interval is:

$$D_2^{'} = v_{n-1} \times t_2 \quad \text{Eq. 3-6}$$

To estimate D_3, the distance covered by the FV in passing the LV and completing the maneuver during the interval t_3 is estimated as:

$$D_3 = t_3 \times v_n^{des-ov} \quad \text{Eq. 3-7}$$

where, t_3 is obtained from the expression involving headways, length of vehicles, speeds and distances, such that:

$$t_3 = \frac{HW^{ret} + L_{n-1} + HW^{init} + L_n - (D_1 + D_2 - D_1^{'} - D_2^{'})}{v_n^{des-ov} - v_{n-1}} \quad \text{Eq. 3-8}$$

where,

HW^{init} = initial distance headway between front bumper of the FV and rear bumper of LV

HW^{ret} = distance headway for pull back (rear bumper of FV and front bumper of LV).

L_{n-1} = length of overtaken vehicle

L_n = length of overtaking vehicle

The total overtaking distance and time interval for FV is calculated as:

$$D_{OT} = D_1 + D_2 + D_3$$
$$T_{OT} = t_1 + t_2 + t_3 \quad \text{Eq. 3-9}$$

The opposing vehicle (OP) is also assumed to maintain a constant speed of v_{OP} during the FV overtaking maneuver. During the T_{OT} time interval, the distance covered by the OP can be calculated as:

$$D_{OP} = T_{OT} \times v_{OP} \quad \text{Eq. 3-10}$$

The difference between the initial separation between FV and OP prior to pull out (main gap, D) and the "closing" distance covered by these vehicles during the overtaking is the *residual distance gap* (D_{Res}). This gap reflects a "safe" separation distance remaining between the FV and OP after overtaking maneuver such that a head-on crash is avoided. D_{Res} can be estimated as:

$$D_{Res} = D - (D_{OT} + D_{OP})$$ Eq. 3-11

TTC is basically D_{Res} in units of time such that:

$$TTC = \frac{D_{Res}}{v_{OP} + v_n^{des-ov}}$$ Eq. 3-12

In those instances where the desired overtaking speed (v_n^{des-ov}) is not achieved prior to the FV pull back or return point, we set the end point for distance D_2 to the return point and distance D_3 to zero. We note that in the case of multiple overtaking, a contiguous platoon of vehicles (separated by short time headway of less than 3s and up to three vehicles) is considered such that all vehicles in the platoon are assumed to travel at the same speed of $v_{n-1}(t)$ and act as a single "undivided" decision unit. Hence the FV driver's initial decision is to overtake all or none of the LV vehicles in the platoon. However, this decision may alter during the passing process as discussed in section 2.7.3.2. In order to generalize the TTC for multiple-vehicle overtakes, the term L_{n-1} in Eq. 3-8 is replaced with the estimated length of the platoon. This acts to reduce the estimated TTC resulting in a lower overtaking gap-acceptance probability.

In case of flying overtaking, v_n^{ini} takes the initial non-reduced operating speed of FV, which is normally higher than that of LV. In this case D_2 will be close to zero since the driver has skipped the catch-up process and the overtaking desired speed is already achieved. This results in reduced overtaking distance and increased TTC.

As shown, TTC encapsulated the traffic and physical factors that might influence overtaking, in a single decision variable.

3.4.2 Procedure for calibration

In this overtaking model we assume that each driver (n) has a critical minimum acceptable gap (TTC_n^{crit}) for overtaking, which is normally distributed with a mean of $\overline{TTC}^{crit}$ and a given variance of σ^2, such that:

$$TTC_n^{crit} = \overline{TTC}^{crit} + e_n$$ Eq. 3-13

where, the error term is assumed to be normally distributed; i.e., $e_n \sim N(0, \sigma^2)$.

The parameters of the distribution for TTC_n^{crit} in Eq. 3-13 can be determined empirically from observed overtaking gap-acceptance data. For accepting a gap, the available TTC^p must exceed the critical value for the n^{th} overtaking driver (TTC_n^{crit}).

We define the probability that perceived time-to-collision (TTC^p) is accepted/rejected as series of FV binary decisions, such that for the n^{th} FV in the traffic stream:

$$y_n = \begin{cases} 1 & \text{if } TTC^p \text{ is accepted} \\ 0 & \text{if } TTC^p \text{ is rejected} \end{cases} \qquad \text{Eq. 3-14}$$

The probability that the n^{th} overtaking driver accepts an available perceived gap of size TTC^p can be expressed as:

$$\begin{aligned} P_n\left(Accept\ TTC^p \middle| \overline{TTC}^{crit}, \sigma^2\right) &= \mathrm{P}\left(TTC^p > TTC_n^{crit}\right) \\ &= \mathrm{P}(TTC^p > \overline{TTC}^{crit} + e_n) \\ &= \emptyset\left(\frac{TTC^p - \overline{TTC}^{crit}}{\sigma}\right) \end{aligned} \qquad \text{Eq. 3-15}$$

where, $\emptyset(.)$ in the above expression denotes the standard cumulative normal curve of the Probit function. This type of relationship has been applied in the literature to a gap-acceptance problem for stream crossing by Mahmassani and Sheffi (1981) and Daganzo (1981).

The overtaking gap-acceptance parameters can be estimated using maximum likelihood method such that:

$$\underset{\overline{TTC}^{crit}, \sigma}{\arg max}\ L = \prod_{n=1}^{N} P_n^{y_n} (1 - P_n)^{1 - y_n} \qquad \text{Eq. 3-16}$$

where, N corresponds to the number of vehicles in the traffic stream being considered in "desire-to-overtake" mode. For a given distribution of TTC^{crit}, the gap-acceptance function is defined as the probability that a randomly selected driver will accept an available "perceived" TTC^p.

3.5 Calibration of Gap-acceptance Model

In this section, details of field data collected for calibration of the gap-acceptance model are discussed, and then the results of the model calibration are presented.

3.5.1 Calibration data

The overtaking data used to calibrate and validate the gap-acceptance model were obtained from a traffic videotaping survey of a 1-km stretch of two-lane highway in Southern Italy (the SS18 near Amantea CS). The videotaping was carried out over a three-hour period on two consecutive weekdays. The posted speed limit on this segment of highway was 80 km/h. The segment was selected such that overtaking was permitted and geometry did not significantly restrict maximum sight distances within the studied segment. The videotaped segment was situated between two short tunnels or overpasses. As illustrated in Figure 3-5, two cameras were located approximately 50 meters above the highway at an offset distance of about 200 meters from the centerline. Placement of cameras was such that driving behavior was not influenced. An average two-way volume of 533 vph was observed for the first day and 436 vph for the second day.

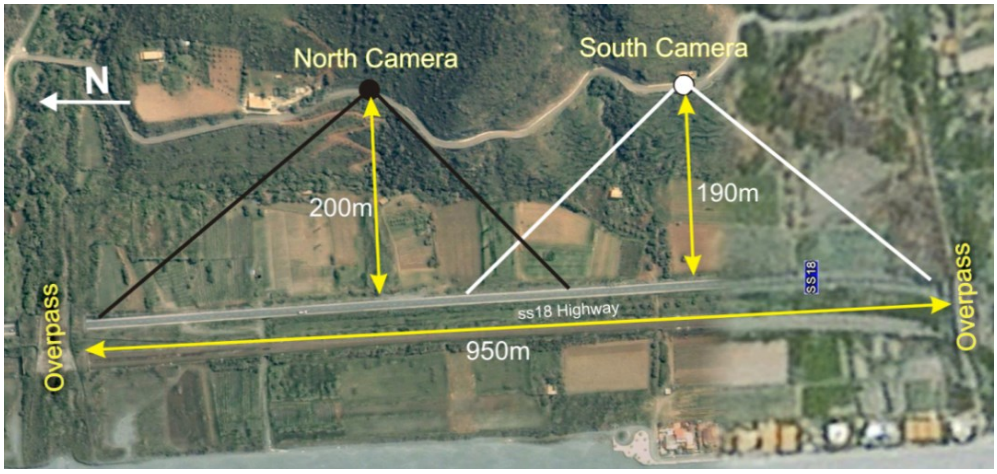

Figure 3-5- Site characteristics for video recording

A program was developed by Guido et al. (2013) to extract frame-by-frame video images of the trajectory and speed of individual vehicles in 0.1s intervals as they progressed along their travel path. The accuracy of the video extraction program was tested based on a sample of GPS equipped vehicles. The GPS tracking system which yielded the benchmark vehicle profiles for this test was a Trimble® GPS Pathfinder® ProXRT considered accurate within a tolerance of 10 cm.

In order to compare the accuracy of the video extraction measures to those obtained from GPS, three measures were considered: X and Y-coordinates for longitudinal and lateral offsets and speed. The Root Mean Square Error (RMSE) was estimated using an expression of the form:

$$RMSE = \sqrt{\frac{\sum(X_{GPS} - X_{video})^2}{N}} \quad \text{Eq. 3-17}$$

where,

X_{GPS} = measure obtained from GPS

X_{video} = measure obtained from video image processing algorithm

N = number of evaluation time intervals

The RMSE errors are summarized in Table 3-1 for nine test runs. The average RMSE values were found to be 1.22 meters for the X position, 1.10 meters for the Y position, and 1.09 km/h for the speed. These results indicate a close match between the GPS measures and the video extraction for the nine trajectories, and suggest that the extracted video-taped trajectories obtained for the 1km test road segment can be used to calibrate the overtaking model in this study.

Table 3-1- Analysis of errors between vehicle position and speed obtained from video image processing software and GPS

Trajectories	RMSE		
	X (m)	Y (m)	Speed (km/h)
1	2.12	1.05	0.96
2	0.63	0.81	0.77
3	1.28	0.87	1.04
4	0.75	0.91	1.14
5	1.09	0.99	1.34
6	0.93	1.31	1.30
7	1.30	1.39	1.31
8	0.99	1.22	0.87
9	1.85	1.34	1.16
Average	1.22	1.10	1.09

For the overtaking model calibration, a total of 97 vehicles trajectories were extracted from the three-hour videotaping in which the potential overtaking vehicle (referred to FV) was assumed to be

in "desire-to-overtake" mode although not necessarily in the process of overtaking. To be in desire-to-overtake at least one of the following two conditions was required:

- FV accepts an eventual gap within the observed segment after one or more gaps were rejected
- FV is observed to veer toward the centerline, presumably searching for an overtaking opportunity and the headway between the lead and following vehicles is less than 30 meters.

The latter assumption agrees with findings reported in Hegeman et al. (2005), that the distance between overtaking and overtaken vehicles at the beginning of maneuver was distributed with mean of 17.8 m and standard deviation of 9.8 m and about 92% of these headways were found to be less than 30 m. The 97 sample trajectories yielded a total of 171 gaps of which 81 were accepted and 90 were rejected.

Using Eq. 3-2 to Eq. 3-12, the corresponding perceived time-to-collision was estimated at the moment the overtaking gap is available. To estimate TTC^p we assumed the following *perceived* parameters to estimate overtaking distance and distance travelled by the opposing vehicle:

- v_n^{des-ov} is assumed to be *m* (km/h) higher than the speed of overtaken vehicle (v_{n-1})

According to Harwood and Sun 2008, the overtaking speed differential (m) between the FV and LV vehicles can be obtained based on the speed of the LV (v_{n-1}), such that:

$$m = 44.1 - 0.25v_{n-1}$$
$$v_n^{des-ov} = v_{n-1} + m \qquad \text{Eq. 3-18}$$

- Return headway HW^{ret} is assumed to be 1 second as specified by Glennon (1988)
- Speed of the opposing vehicle v_{OP} is assumed to be the average speed of the traffic stream as observed from the survey (90 km/h).
- v^{max} is 160 km/h for all the vehicles. ka^{max} was assumed to be 1.82 (m/s^2). This value is calculated from results of a recent overtaking acceleration study conducted by Brooks (2012)

The other parameters involved in calculation of TTC^p such as D, HW^{init}, v_{n-1}, and v_n^{ini} are assumed to be perfectly known by the driver at the beginning of the maneuver.

After TTC^p is estimated, FV driver's gap-acceptance decision with respect to the perceived time-to-collision was recorded as a binary decision variable (0 for Rejected, 1 for Accepted). The results of this procedure are presented for a sample of trajectories in Table 3-2.

Table 3-2- A sample of processed disaggregate overtaking data from video cameras

Vehicle #	Gap size (m)	Decision (0:Reject) (1:Accept)	Overtaking veh speed (km/h)	Overtaken veh speed (km/h)	Oppossing veh speed (km/h)	HWinit (m)	HWret (m)	Max speed (km/h)	k*MaxAcc (m/s2)	OT desired speed (km/h)	T_{OT} (s)	D_{OT} (m)	D_{OP} (m)	Actual ResGap (m)	Perceived ResGap (m)	Actual TTC (s)	Perceived TTC (s)
1	328	0	105.5	105.5	90.0	15	25	160	1.82	123.2	9.2	300.9	231.7	NA	-204.6	NA	-3.4
	600	1	105.5	105.5	90.0	15	25	160	1.82	123.2	8.9	292.1	197.3	110.6	167.3	2.0	3.2
2	462	0	90.1	90.1	90.0	22	25	160	1.82	111.7	9.3	271.0	228.4	NA	-37.4	NA	-0.7
	93	0	90.1	90.1	90.0	22	25	160	1.82	111.7	9.3	271.0	228.4	NA	-406.4	NA	-7.3
	211	0	90.1	90.1	90.0	22	25	160	1.82	111.7	9.3	271.0	228.4	NA	-288.4	NA	-5.2
4	383	0	117.6	77.9	90.0	20	25	160	1.82	117.6	4.2	125.6	95.0	NA	162.4	NA	2.9
	800	1	77.9	77.9	90.0	20	25	160	1.82	102.5	8.0	207.2	199.0	592.8	483.9	20.8	18.5
5	800	1	85.5	85.5	90.0	21	25	160	1.82	108.2	8.8	246.4	219.7	553.6	561.0	18.4	18.6
6	800	1	78.4	78.4	90.0	20	25	160	1.82	102.9	9.4	239.7	234.7	560.3	607.8	19.6	20.6
8	800	1	81.0	81.0	90.0	20	25	160	1.82	104.9	7.5	205.4	188.0	594.6	704.9	20.4	22.7
9	80	0	79.2	79.2	90.0	20	25	160	1.82	103.5	8.0	211.4	182.3	NA	-313.8	NA	-6.1
	42	0	79.2	79.2	90.0	20	25	160	1.82	103.5	8.0	211.4	182.3	NA	-351.8	NA	-6.8
	165	0	79.2	79.2	90.0	20	25	160	1.82	103.5	8.0	211.4	182.3	NA	-228.8	NA	-4.4
	620	1	79.2	79.2	90.0	20	25	160	1.82	103.5	8.5	222.0	211.9	398.0	447.9	13.8	14.9
10	476	0	82.3	82.3	90.0	21	25	160	1.82	105.8	8.3	226.9	241.4	NA	7.7	NA	0.1
...	...	...	...	...	...	...	...	...		...		...	...	...	...	...	...

In this study, it is assumed that gap decisions are independent events, such that for a single driver the decision to accept a gap is independent of previous rejected gaps. In reality, the decision to accept a gap and overtake is very likely influenced by the number of gaps rejected previously, such that overtaking drivers are subject to an impatience factor in the process that builds with the number of gaps that have been rejected. Hence, the higher the number of gaps rejected, the shorter the gap that is eventually accepted to initiate the overtaking. In this case, the impatience factor can be represented by an addition adjustment term in the critical gap formulation so that Eq. 3-13 and can be revised as:

$$TTC_n^{crit} = \overline{TTC}_{crit} + f\left(\sum_{i=1}^{k} t_i\right) + e_n \qquad \text{Eq. 3-19}$$

where,

$t_i =$ time duration of the i_{th} gap in the opposing traffic stream given the overtaking desire is triggered

$k =$ number of gaps rejected before the one accepted

The impatience term $f\left(\sum_{i=1}^{k} t_i\right)$ in Eq. 3-19 could be obtained by observing a sequence of rejected gaps for a longer highway segment observed over a more extensive period of time. However, such data were not available for this study and hence, this term has not been used in this analysis.

The error term associated with TTC^p, as defined in Eq. 3-1, can be estimated from observations of accepted overtaking gaps for which we can calculate TTC from the traffic data at the end of each overtaking maneuver. For the 81 accepted gaps, the difference between the measured valued for the k^{th} accepted gap at the end of the maneuver (TTC_k) and its perceived value (TTC_k^p) at the beginning of the maneuver established the error term. For the k^{th} overtaking driver this time difference or error in gap perception is estimated as:

$$\varepsilon_k = TTC_k - TTC_k^p \qquad \text{Eq. 3-20}$$

Figure 3-6 illustrates the distribution of perception errors for a sample of overtaking accepted gaps in the videotaped data. The mean of the perceived distance and time distributions was found to be around zero with corresponding standard deviations of 52 meters and 1.2 seconds, respectively. We note that, this is consistent with our assumptions that the error terms for TTC are approximately normally distributed.

In simulation, however, the complete information about speed of individual vehicles, physical variables and overtaking process are known; hence, TTC can be estimated (from Eq. 3-2 to Eq. 3-12 using accurate parameters), but the decision to overtake is based on the value of TTC^p obtained by adding the random error term (as determined above) to the calculated TTC value.

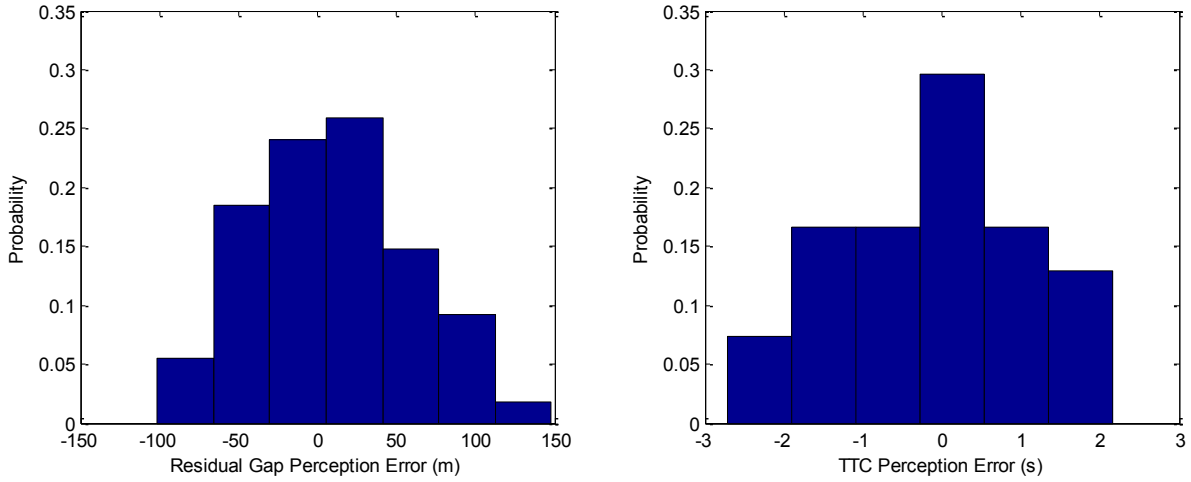

Figure 3-6- Perception error distribution estimated from observed accepted gaps

3.5.2 Calibration results

For the 171 overtaking gap decisions in the sample, 70% were randomly selected for calibration and 30% for validation. A generalized linear Probit model based on Eq. 3-15 and Eq. 3-16 was fitted to the calibration data with the results summarized in Table 3-3. The mean and variance of TTC^{crit} was estimated from the traffic data to be 3.0 seconds and 0.7s, respectivly. These parameters were found to be statistically significant at 95% confidence level ($p < 0.05$). The log likelihood value for this expression was found to be -16.35.

Table 3-3- Parameter estimates for the critical residual gaps based on the Probit model

Model: $TTC^{crit} \sim N(\overline{TTC}_{crit}, \sigma^2)$			
Parameter	Estimated Value	Standard Error	P-value
$\overline{TTC}_{crit}(s)$	3.0	0.80	0.010
$\sigma(s)$	0.7	0.51	0.003
Log likelihood = - 16.35			

Figure 3-7 illustrates the distribution of critical TTC superimposed on the Probit cumulative distribution function. The dot points on "1" and "0" lines represent accepted and rejected overtaking gaps, respectively. The negative values for the TTC perceived variable corresponds to unsafe available gaps which would have led to head-on collision if the gap had been accepted.

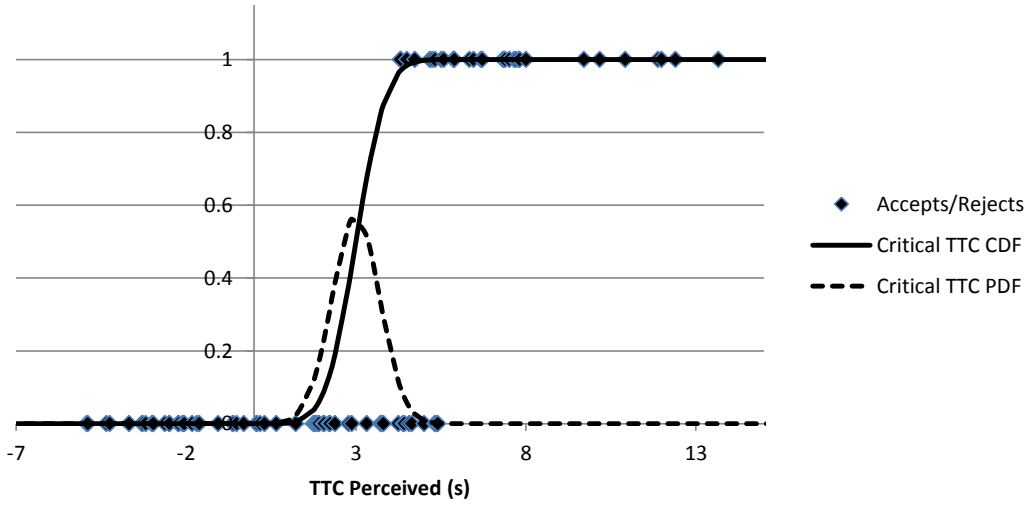

Figure 3-7- Probit regression and distribution of TTC critical gaps for the population of drivers

3.5.3 Model validation

In order to determine predictive ability of the overtaking gap-acceptance model, the Probit model was applied to an "independent" sample of gaps comprising 30% of the total data. The percent correct prediction rate for the validation sample was found to be 89%, confirming that the calibrated model predicts overtaking gap-acceptance for a different dataset with good transferability.

To further validate the gap-acceptance relationship, simulated overtaking frequency from OTSIM and observed frequencies from the data collection study as discussed above can be compared. For this purpose, the proposed gap-acceptance model was implemented in OTSIM with overtaking gap acceptance parameters obtained as obtained above. To simulate the studied location, the input volumes composition of vehicles, and distribution of desired speeds were selected in accordance with the observed traffic data (mean unimpeded speeds = 90 km/h, standard deviation of unimpeded speeds = 17 km/h). In addition, the car-following calibration parameters must be determined such that the observed vehicle headways match the simulated headways. From the video recording study, the average following time headways for vehicles in desired-to-overtake mode was found to be 0.8 second while this value for other drivers in the car-following mode, but without overtaking desire, was 1.3 s. This shows that overtaking vehicles tend to keep shorter headways possibly to minimize their overtaking time and distance. This finding is relatively consistent with those reported by Hegeman et al. (2005). The Gipps model parameters presented in Table 3-4 were found to generate the average headways as observed in field data for normal following and following with desire-to-overtake.

As shown in Table 3-4, two parameters of the car-following model are changed to address changes in the two car-following situations. In general lower d_n^{max}(maximum desired deceleration of the following vehicle) and higher $\hat{d}_{n-1}$ (estimation of maximum desired deceleration rate of the lead vehicle) results in less conservative following behavior. This leads to shorter time headway between the lead and following vehicles when overtaking is desired. The coefficient variation of 0.15 is assumed for the all car-following parameters which are randomly assigned to the drivers.

From 20 simulation runs, the simulated overtaking rate was found to be 27.2±5 maneuvers/km/h versus an observed rate of 24.6 maneuvers/km/h from the video-taped data. This suggests a good measure of consistency for overtaking frequency between the simulation and field data.

Table 3-4- Gipps car-following model calibration parameters

Gipps Car-following Parameters	$a_n^{max}(m/s^2)$	$d_n^{max}(m/s^2)$	$\hat{d}_{n-1}(m/s^2)$	$L_{n-1}(m)$	$T(s)$	$s(m)$
Normal Following	1.7	-3.4	-3	4.9	1	2
Following With Overtaking Desire	1.7	-3.7	-2.7	4.9	1	2

To check whether the overtaking dynamics simulated in OTSIM properly represent actual overtaking attributes, another simulation case study was carried out for a six-kilometer straight segment of a two-lane highway with overtaking permitted in both directions. Overtaking attributes including overtaking time and distance as well as speed differential between overtaking and overtaken vehicles were compared with estimates obtained from three sources of: 1) calibration video-recorded segment, 2) observations reported by Harwood and Sun 2008 from their video-recording exercise, and 3) observations reported by Carlson et al. (2006) from a set of instrumented vehicle experiments.

Table 3-5 provides a summary of the average, standard deviation, minimum, and maximum estimates of the overtaking attributes for three posted speed limits (80 km/h, 90km/h, and 110 km/h). The first speed limit reflects maximum posted speed for the video-recorded segment used in the calibration and validation of the model. The second and third limits reflect the average posted speeds for highways reported in Harwood and Sun (2008) and Carlson et al. (2006) studies respectively. As can be seen, the results suggest a close match between the simulated values and field observations. The three posted limits yield the expected results; i.e., overtaking time and distance increase with speed limit.

3.6 Model Transferability and Comparison

In this section, we test the transferability of the proposed gap-acceptance model to independent field data and to simulated results as obtained from TRARR and TWOPAS models. The field data and TRARR results were obtained for a five kilometers segment of a two-lane highway in Netherlands, as reported by Hegeman (2004). The posted speed for the Netherland highway is 100 km/h for cars and 80 km/h for trucks with volumes for all vehicle types of 1026 vph and 471 vph in direction 1 and 2, respectively. A few basic features of Netherlands highway traffic data are given in Table 3-6.

Since the primary focus of this research is overtaking, the performance measures used in comparing model results are: average overtaking rate (OR) and average travel speed (ATS). For this exercise, we

have assumed that the average desired speed of vehicles is equal to the posted differential speed limits of 100 km/h and 80 km/h for cars and trucks, respectively. The coefficient of variation for the desired speed is assumed to be 0.1 (details about these assumptions are provided in Fitzpatrick, 2003).

Table 3-5- Comparison of simulated and field overtaking attribute measures

Posted Speed (km/h)	Study	# of Observations	Mean	Standard Deviation	Minimum	Maximum
		Travel Time in Opposing Lane (s)				
80	OTSIM	250	9.1	1.4	5	13
	Video recording	74	8.5	1.8	4	13
100	OTSIM	250	9.4	1.6	5	16
	Harwood et al. (2008)	60	10	2.8	5	19
110	OTSIM	250	9.7	1.7	7	17
	Carlson et al. (2006)	105	9.9	2.5	5.3	18.2
		Travel Distance in Opposing Lane (m)				
80	OTSIM	250	229	46	110	382
	Video recording	74	208	43	106	330
100	OTSIM	250	255	56	116	509
	Harwood et al. (2008)	60	282	75	123	491
110	OTSIM	250	285	60	205	472
	Carlson et al. (2006)	105	313	62	195	533
		Speed Differential Between Overtaking and Overtaken Vehicle (km/h)				
80	OTSIM	250	25.2	4.4	8.5	28.4
	Video recording	74	24.6	7.7	6.6	46
100	OTSIM	250	23.1	19	1.6	26
	Harwood et al. (2008)	60	24.8	11.3	0.2	53.3
110	OTSIM	250	20.9	2.5	16	30
	Carlson et al. (2006)	105	19.8	5.1	8.2	32.2

Table 3-6- Traffic data information reported in Hegeman (2004) study

	Direction 1	Direction 2
Volume (vph)	1026	471
Truck Percentage (%)	7.2	5.2
Average speed (km/h)	85.9	91.8
Standard deviation of speed (km/h)	5.8	7.2
Minimum speed (km/h)	61	71.6
Maximum speed (km/h)	115.7	114.5

Table 3-7 provides comparison of OR and ATS between OTSIM and TWOPAS with respect to the field data and TRARR, as reported by Hegeman for the Netherlands data. As reported by by

Hegeman (2004) , TRARR was found to significantly overestimate the overtaking rate in comparison to the field data. However, the OTSIM overtaking rate yielded the lowest error with respect to these data for direction 1. TWOPAS, on the other hand, generated a significantly higher error (lower overtaking rate) compared to OTSIM for this direction. For direction 2, the lowest error was obtained for TWOPAS, although the difference between the two simulations (TWOPAS and OTSIM) is not high. For ATS, the absolute difference between simulation and the field data was found to be lowest for OTSIM as compared to TWOPAS. It appears that OTSIM was able to yield closer overtaking rates and average travel speed with respect to field data than were obtained from the TRARR and TWOPAS model simulations.

Table 3-7- Observed versus simulated overtaking rate for the three simulation model of TRARR, OTSIM, and TWOPAS

Data source		Field Data*	TRARR*	OTSIM	TWOPAS (IHSDM)	Absolute Difference		
						TRARR vs. Field	OTSIM vs. Field	TWOPAS vs. Field
Overtaking rate (OT/km/h)	Direction 1	52.1	109	49.8	30.5	56.9	2.3	21.6
	Direction 2	3.7	66	7.5	2.5	62.3	3	1.2
Average travel speed (km/h)	Direction 1	85.9	NA**	81.6	77.2	NA	4.3	8.7
	Direction 2	91.8	NA	87.2	84.5	NA	4.6	7.3

* Reported in Hegeman (2004)

** Not Available (reported to be lower than field data)

A further comparison was made between OTSIM, TWOPAS and values reported in HCM 2010 (TRB, 2010) based on the percent time spent following (PTSF). The PTSF is an indicator of the inability of the FV to overtake so as to attain the desired speed in two-lane traffic operations. As PTSF increases, we would expect the number of vehicles successfully overtaking to decrease. For this test, simulation results were obtained for a range of analysis volumes (100 pc/h to 1700 pc/h) and opposing volume (100 pc/h to 1600 pc/h) as illustrated in Figure 3-8.

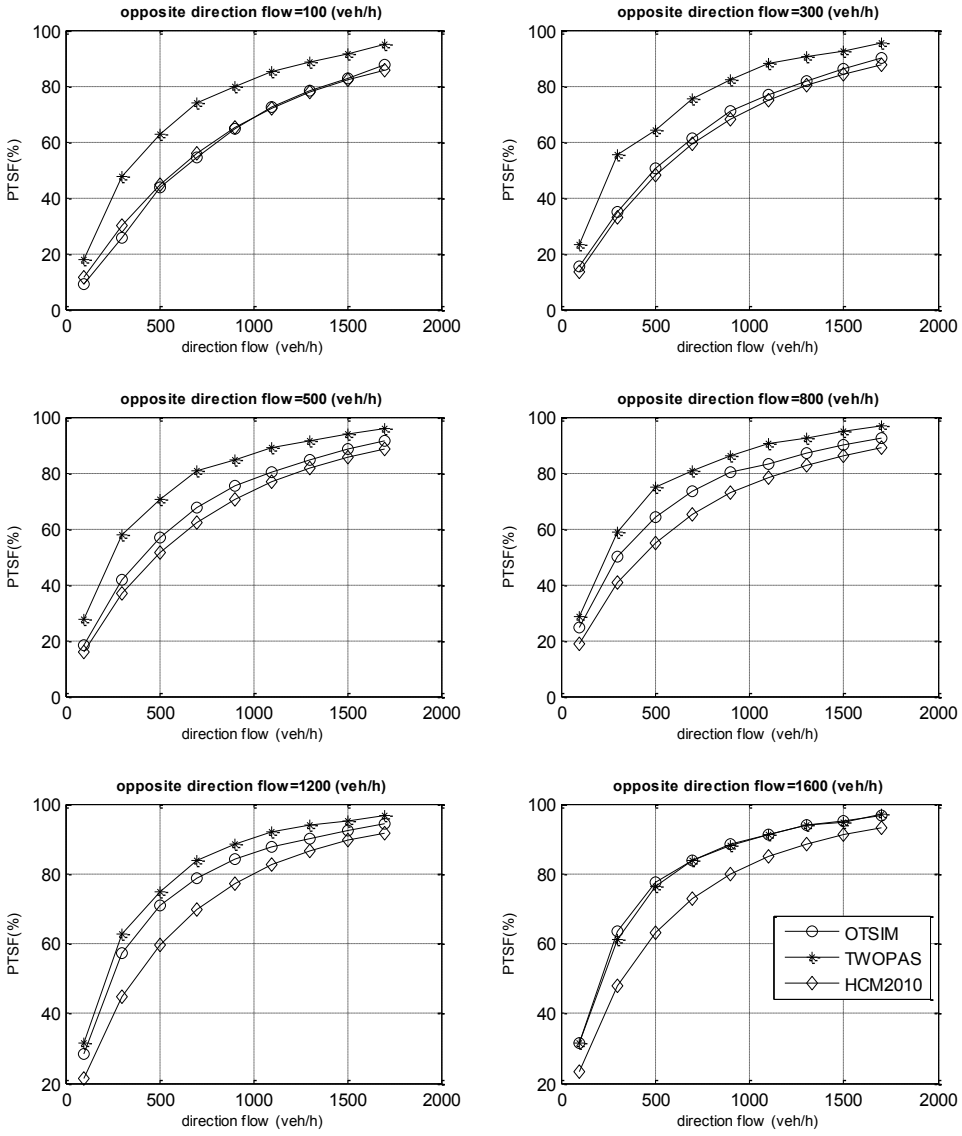

Figure 3-8- Comparing PTSF between OTSIM, TWOPAS, and HCM2010

We note that, at low opposing volumes, where we would expect higher passing opportunities, there is a closer match in PTSF between OTSIM and HCM 2010. The TWOPAS results suggest higher values of PTSF and presumably fewer overtaking maneuvers. This is consistent with the findings from application of OTSIM and TWOPAS to the Netherlands data, as discussed above. As opposing volume increases and passing opportunity are reduced, there is a shift in OTSIM estimates away from the HCM values towards those suggested by TWOPAS. For example, at 1600 pc/h opposing volume, PTSF obtained from OTSIM matches that from TWOPAS. These results are encouraging in that they

suggest an acceptable level of transferability in OTSIM simulation results. These results also indicate that the adjustments made to PTSF values in HCM 2000 and reported in HCM 2010 may have been exaggerated. This is discussed in more details in the next chapter of the thesis.

3.7 Model Sensitivity to Calibration Parameters

In this section, we conduct a sensitivity analysis of simulated traffic and safety measures to the OTSIM calibration parameters including mean critical TTC ($\overline{TTC}^{crit}$) as introduced in this chapter and the speed differential threshold (SD_{thre}) between overtaking and overtaken vehicle used to trigger desire-to-overtake, as introduced in section 2.7.3.1 of this thesis. Four measures of average travel speed (ATS), percent time spent following (PTSF), overtaking rate (OTrate), and average overtaking head-on time-to-collision (TTC) are considered in this analysis.

3.7.1 Sensitivity analysis for mean critical TTC

For this purpose, simulations are conducted with four levels of volumes with 50/50 directional split. For each simulation case, four levels of $\overline{TTC}^{crit}$ with the same standard deviation of 0.7 s (as obtained from the calibration study in the previous section) and a no-passing-allowed scenario are considered and the corresponding measures are compared. The speed differential threshold (SD_{thre}) is set at 8km/h. Figure 3-9 illustrates the simulation results for the four model outputs with critical TTC ranges from 1.5 s to 6 s. As shown, speed drops when volume increases. Lower critical TTC resulted in statistically significantly higher speeds (based on t-stat test). This was the case for the whole range of volume considered based on paired comparison of simulation seeds ($p<0.05$), although the difference is very marginal. The ultimate case (highest speed drop) corresponds to the no-passing scenario when critical TTC becomes close to infinity. At 500 vph volume, the maximum speed drop, from lowest critical TTC (1.5 s) to the no-passing scenario, was close to 5% (from 89 km/h down to 85 km/h).

The PTSF increases with volume. The impact of critical TTC to increase PTSF is statistically significant, although very marginal for the range of critical TTC values considered. The highest critical TTC, the highest PTSF will be. PTSF shows maximum increase at 500 vph volume from 56% (1.5 s critical TTC) to 70% (no-passing scenario). The impact of critical TTC on PTSF (similar to ATS) at high volumes is the lowest.

The overtaking rate increases initially with volume then reaches a maximum and then drops with further increase in volume. This shows how overtaking demand and supply changes. At low volumes the gaps in the opposing traffic are quite large and drivers can overtake easily. With volume increased the overtaking demand increases and there are still quite large gaps in the opposing traffic. This will increase the number of overtakes up to a certain point. Then, with further two-directional volume increase, the gaps become shorter and the overtaking becomes more limited and overtaking frequency drops. At 500 vph volume overtaking rate increases 16 OT/km/h when mean TTC critical decreases from 6 seconds to 1.5 seconds.

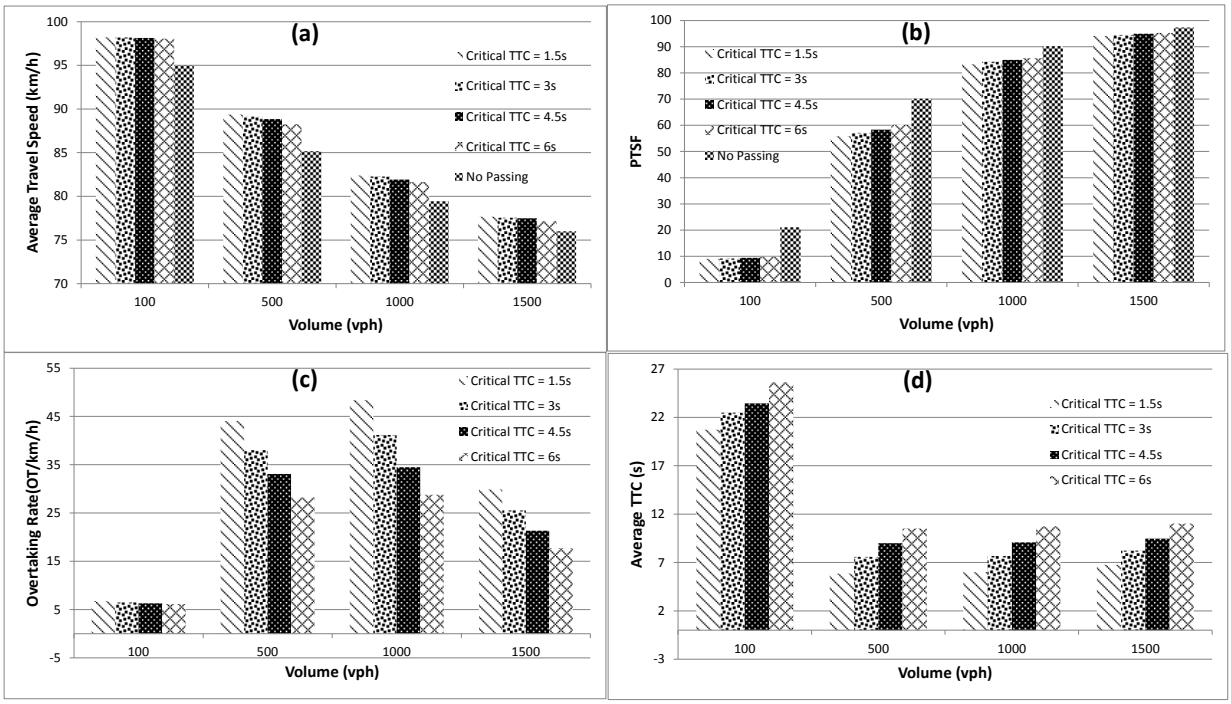

Figure 3-9- Model output sensitivity to mean critical TTC (50/50 split): a) Average travel speed, b) Percent time spent following, c) Overtaking rate, d) Time-to-collision

Average TTC sharply drops with initial increase in volume then it increases slightly. Lower values for critical TTC caused lower average TTC. This is an indication of increased head-on risk associated with lower critical TTC. The effect of critical TTC on average TTC was statistically significant ($p<0.05$) and substantial. At 500 vph volume, the average TTC associated with 6 seconds threshold is 5.8 seconds lower than that of 1.5 seconds. It can be concluded that, for the range of parameter values considered, average TTC and overtaking rate showed higher sensitivity to the mean critical TTC than ATS and PTSF.

Another simulation was conducted to investigate the distribution of available and accepted gaps in the traffic stream. Figure 3-10 illustrates histograms of ”available” and “accepted” residual gaps for this simulation case with volumes set at 500 and 1000 vph for direction 1 and 2, respectively. In this analysis, “available gaps” means calculated TTC or residual gaps values greater than zero, which potentially provide non-crashing overtaking opportunities. The corresponding calibration parameters for this simulation were 3 seconds and 0.7 second for mean and standard deviation of critical TTC, respectively. Comparing available and accepted residual gaps, one can determine the proportion of gaps that were not accepted. The shortest accepted residual gap is around 150 meters. The available gaps look to have an exponential distribution form. This figure also illustrates that the average residual gaps available for overtaking, when the opposing volume is 1000 vph, is much lower than that of the case when the opposing volume is 500 vph. Figure 3-11 shows a similar histogram for available and accepted TTC values obtained from the simulation. The observed minimum accepted TTC was 1 second. This corresponds to residual gap of around 50 meters.

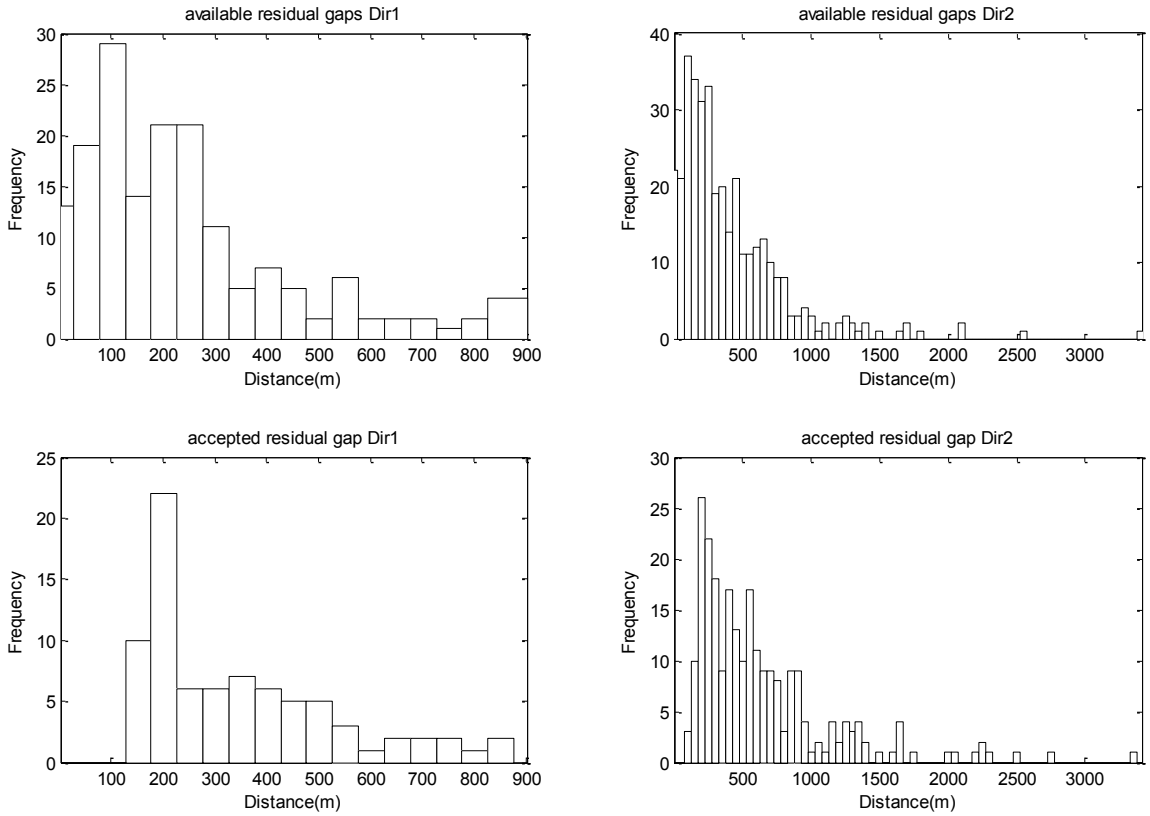

Figure 3-10- Histograms of available and accepted residual gaps (Simulation of the case with direction1=500vph, direction2=1000vph volumes)

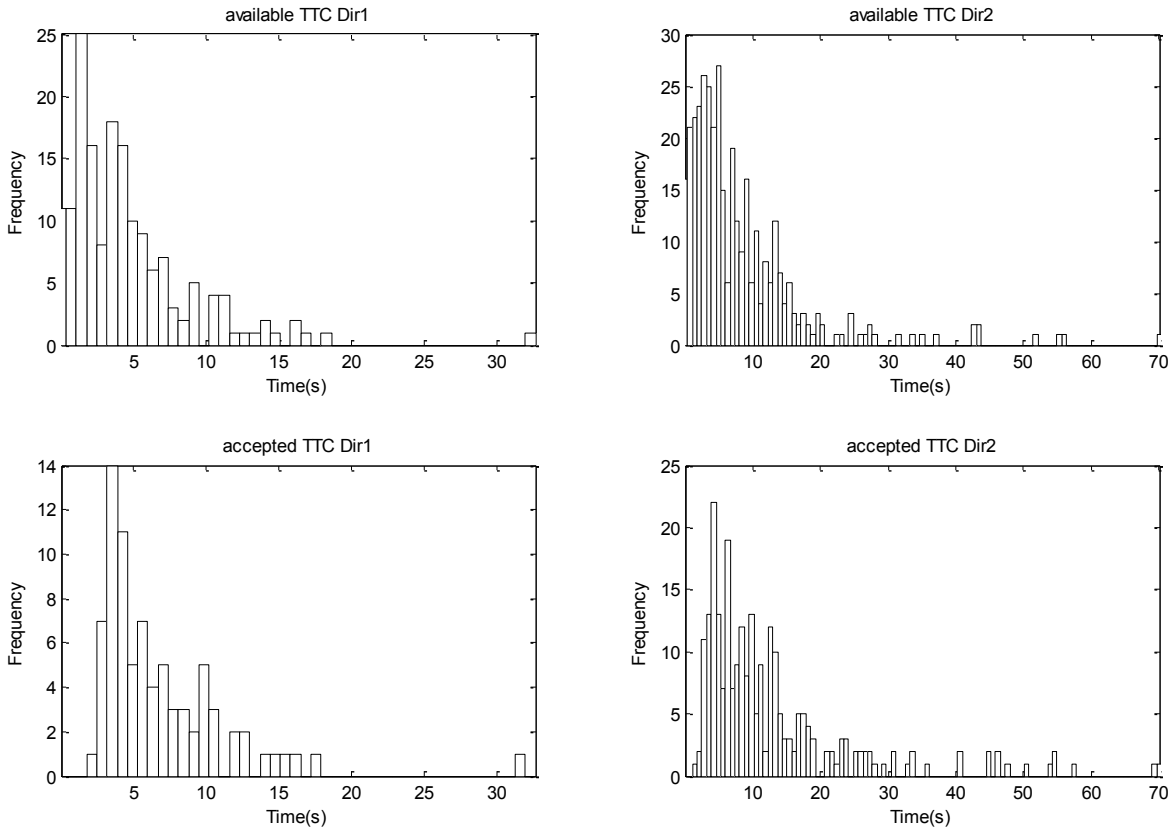

Figure 3-11- Histograms of available and accepted TTC gaps (Simulation of the case with direction1=500vph, direction2=1000vph volumes)

3.7.2 Sensitivity analysis for speed differential threshold

The overtaking speed differential was defined as the difference between desired speed of overtaking vehicle and actual speed of the overtaken vehicle. If this exceeds a predetermined threshold the desired-to-overtake is triggered. To investigate how simulation outputs change with this parameter, four levels of SD_{thre} including 4, 6, 8, and 10 km/h were test in simulation with 500 vph volumes with 50/50 directional split. Figure 3-12 illustrates the simulation results of this analysis. As seen, average speed drops with increased threshold. However, the maximum speed drop from 4 km/h to 10 km/h thresholds is only 0.5 km/h which is not very significant. PTSF increases with the threshold. For the range of thresholds tested, the maximum observed increase in PTSF from lowest to highest threshold is around 4%. As expected, overtaking rate decreases with the speed differential threshold. The highest drop is around 10 OT/km/h. TTC does not appear to be sensitive to speed differential threshold for the range of parameter values considered in this study.

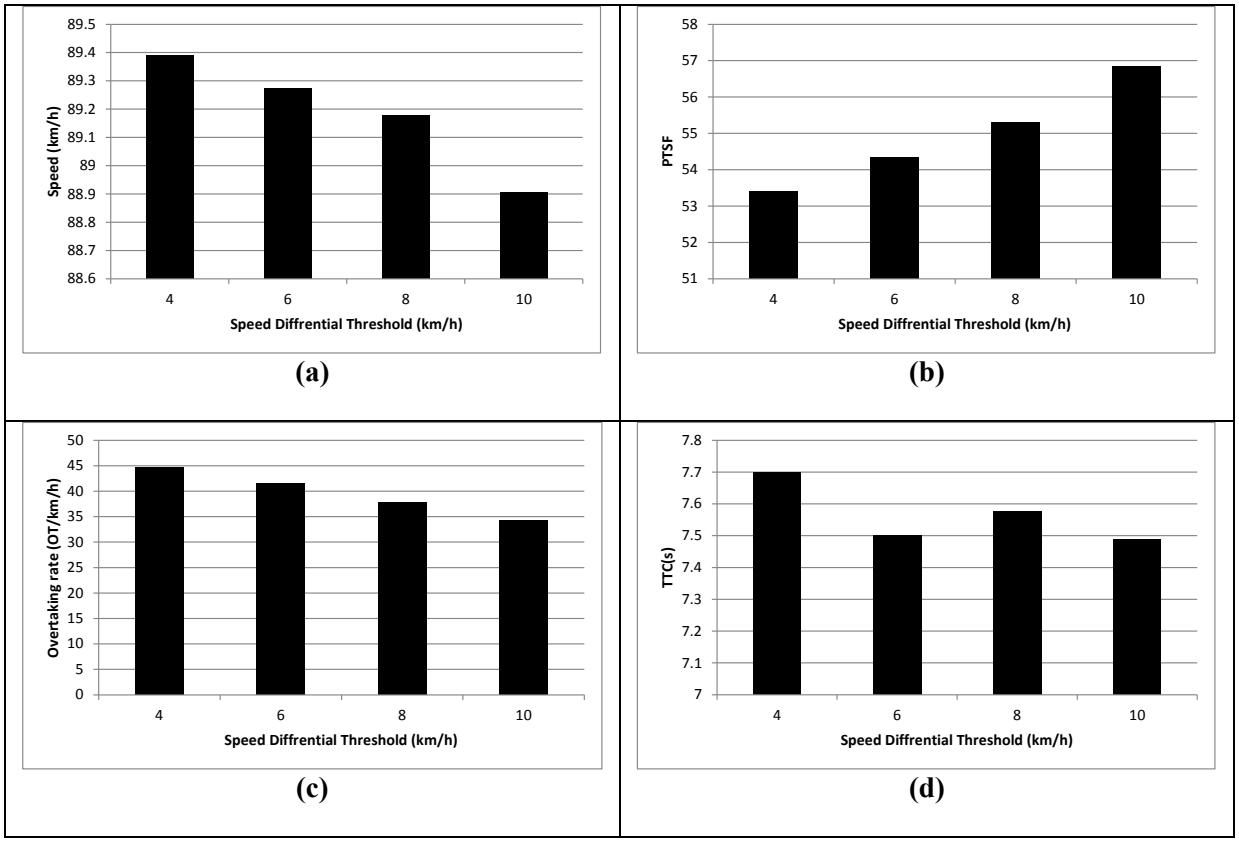

Figure 3-12- Model output sensitivity to speed differential threshold (50/50 split): a) Average travel speed, b) Percent time spent following, c) Overtaking rate, d) Time-to-collision

3.8 Conclusion

An in-depth analytical and behavioral formulation of the overtaking gap-acceptance process for two-lane highway operations was discussed in this chapter. The decision to overtake was expressed as a function of the perceived time-to-collision (TTC) and established driver gap-acceptance thresholds. The gap-acceptance logic adopted in this research is assumed to encapsulate the full spectrum of physical variables influencing the gap-acceptance decision, resulting in reduced numbers of parameters requiring calibration. The model was calibrated using observed overtaking data obtained by video-taping a two-lane highway segment. The distribution of critical TTC gaps for a population of drivers was found to be normally distributed with a mean of 3.0 seconds and standard deviation of 0.7s. The model was then compared with independent aggregate field data as well as simulated results based on TRARR, TWOPAS and HCM models. The overtaking model was found to yield both consistent and transferable results for PTSF, ATS, and overtaking rate when compared to field data

and other simulation model values. The sensitivity of model outputs to the proposed calibration parameters was analyzed. For the range of values considered, critical TTC showed marginal impact on the traffic measures including average travel speed and percent time spent following. However, this impact is quite significant for safety measures including overtaking rates and averageTTC. In this chapter we could demonstrate that in spite of complexity of overtaking maneuver and challenges posed by data collection, it is possible to develop and calibrate a logical overtaking gap-acceptance model that yields both consistent and transferable results in two-lane highway operations.

Chapter 4
Level-of-service Measures for Two-lane Highways using OTSIM (Model Application 1)

4.1 Introduction

Level-of-service (LOS) has been widely used by traffic engineers to measure the operational efficiency of transportation facilities, such as, freeways, highways, intersections, transit systems, etc. The Highway Capacity Manual (HCM) proposes guidelines and procedures for estimating the capacity and quality of service for various highway facilities. Along with empirical models, established on field data, simulation models have been a viable alternative tool for the purpose of highway capacity analysis (Courage et al., 2010).

The purposed of this chapter is to discuss the application of OTSIM in level-of-service analysis for two-lane highways. In this analysis the proposed overtaking component of the simulation model plays a central role in the estimation of traffic measures used in determination of two-lane highways level-of- LOS. The Highway Capacity Manual (HCM) makes use of two main traffic attributes in determination of LOS for two-lane highway operations: average travel speed (ATS) and percent time spent following (PTSF). ATS is the average travel time taken by vehicles to traverse a given length of highway and this serves as a mobility indicator for LOS for the traffic stream. PTSF is the average percentage of time spent by vehicles behind slower moving vehicle as a result of an inability to overtake. PTSF reflects a kind of freedom to maneuver in the traffic stream as an indicator of LOS at the highway location. In LOS analysis for two-lane traffic, an accurate estimation of ATS and PTSF are very important. Once a simulation model is used for this purpose, these measures are dependent on reliability and accuracy of the underlying simulation model especially those related to overtaking such that underestimation of number of overtakes results in higher PTSF and lower ATS and vice versa. The link between these scalar measures and LOS for two-lane highways has been expressed in the HCM using five distinctive categories that range from “high” for level-of-service (A) to “poor or inadequate” for level-of-service (E).

The two most recent versions of HCM use linear and exponential empirical expressions to model the relationship between traffic volume and the ATS and PTSF, respectively. In preparation of HCM 2010 version, there have been attempts to improve the accuracy and reliability of the traffic measures over the previous HCM 2000 version (Zegeer et al., 2008). Although the nature of the expressions

adopted in HCM 2010 is similar to those used in HCM 2000, for directional PTSF, the model coefficients were modified. User feedback concerning the HCM 2000 suggested that estimation of directional PTSF resulted in lower LOS than expected. Harwood et al. (2003) reported that based on this feedback, the PTSF indicators given in HCM 2000 tended to overestimate PTSF. The overestimation of PTSF was found to be especially problematic at low traffic volumes. The HCM 2010 expressions attempted to correct this bias by adjusting the model coefficients of the HCM 2000 version for PTSF. Because two-way analysis curve of PTSF was found to be properly estimated, Harwood et al. (2003) used this curve to generate additional data points for low volume conditions and to correct the directional segment analysis curves in HCM 2000. These adjustments were subsequently published in the HCM 2010 version for two-lane highways. It was further stated that ATS was estimated properly in HCM2000 and no change was applied to ATS equation except unit change from "km/h" (HCM 2000) to "mile/h" (HCM 2010).

As seen, in order to take into account the difference between the HCM 2000 values and the suggested feedback estimates, the modification to directional PTSF was applied externally. In the earlier HCM 2000 version, TWOPAS was used to establish model some of the relationships for PTSF and ATS. However, in the updating procedure for HCM 2010 neither new field data was used nor any simulation model was employed. In other word, the revisions that were made tended to be aggregate in nature. The purpose of this chapter is to use OTSIM to provide estimates for ATS and PTSF for two-lane highway operation and compare them with those reported in HCM 2000 and 2010. In addition, standard deviation of desired speeds is suggested to add as an adjustment factor in estimation of ATS and PTSF.

4.2 HCM Level-of-Service Measures for Two-lane Highways

The expressions used in HCM 2000 and HCM 2010 to estimate ATS for two-lane highway operations are given as (TRB, 2000; TRB, 2010):

$$ATS_d = FFS_d - 0.0125(v_d + v_o) \quad \text{Eq. 4-1}$$

where,

ATS_d = is average travel speed in the analysis direction (km/h)

FFS_d= free flow speed in the analysis direction (km/h)

v_d = passenger-car equivalent flow rate for the peak 15-min period in the analysis direction (pc/h)
v_o = passenger-car equivalent flow rate for the peak 15-min period in the opposing direction (pc/h)

ATS is expressed as a function of Free Flow Speed (FFS) and traffic volume in the travel and the opposing directions. In this expression the effect of each direction volume on ATS of the analysis direction is assumed to be the same since a single coefficient is used for v_d and v_o.

The relationship between PTSF and volume in both HCM 2000 and HCM 2010 is based on an underlying expression of the form:

$$PTSF_d = 100(1 - \exp(a{v_d}^b)) \quad \text{Eq. 4-2}$$

where,

v_d = passenger-car equivalent flow rate for the peak 15-min period in the analysis direction (pc/h)
a, b = coefficients determined from the volume in the opposing direction.

The parameters a and b in Eq. 4-2 are a function of the volume in the opposing direction. The parameter values used in HCM 2000 and HCM 2010 for estimating PTSF are given in Table 4-1 for a range of volumes from 200 to greater than 1600 vph. The differences between the 2000 and 2010 parameters in this table reflect adjustments applied to the "overestimated" HCM 2000 values in accordance with observation-based feedback concerning the previous estimates.

The other difference between the 2000 and 2010 HCM versions concerns the introduction of an additional indicator called Percent Free Flow Speed (PFFS) for class III highway in the HCM 2010. A Class III refers to highways that serve moderately developed areas while Class I and Class II refer to major intercity routes and access routes, respectively (refer to TRB 2010 for more information on two-lane highway classes). PFFS reflects an ability of vehicles in the traffic stream to travel at or near the posted speed limit for a given highway location, such that:

$$PFFS = \frac{ATS}{FFS} \quad \text{Eq. 4-3}$$

where,
FFS= Free flow speed

The application of these measures in determination of LOS for distinctive types of highways is indicated in Table 4-2.

Table 4-1- Coefficients used in estimating PTSF in HCM 2000 and HCM 2010 (TRB, 2000; TRB, 2010)

	HCM 2000		HCM 2010	
v_o Opposing volume (pc/h)	a	b	a	b
≤ 200	-0.013	0.668	-0.0014	0.973
400	-0.057	0.479	-0.0022	0.923
600	-0.100	0.413	-0.0033	0.870
800	-0.173	0.349	-0.0045	0.833
1000	-0.320	0.276	-0.0049	0.829
1200	-0.430	0.242	-0.0054	0.825
1400	-0.522	0.225	-0.0058	0.821
≥ 1600	-0.665	0.199	-0.0062	0.817

Table 4-2- HCM 2000 and HCM 2010 LOS criteria for two-lane highways (TRB, 2000; TRB, 2010)

	HCM 2000			HCM 2010			
Highway Class	Class I		Class II	Class I		Class II	Class III
LOS	PTSF(%)	ATS(km/h)	PTSF(%)	PTSF(%)	ATS(mi/h)	PTSF(%)	PFFS(%)
A	≤35	>90	≤40	≤35	>55	≤40	>91.7
B	>35-50	>80-90	>40-55	>35-50	>50-55	>40-55	>83.3-91.7
C	>50-65	>70-80	>55-70	>50-65	>45-50	>55-70	>75.0-83.3
D	>65-80	>60-70	>70-85	>65-80	>40-45	>70-85	>66.7-75.0
E	>80	≤60	>85	>80	≤40	>85	≤66.7

The ATS and PTSF values in HCM, as presented in above expressions, are for the "base" traffic and road conditions. The base conditions for two-lane highways include:

- Lane widths greater than or equal to 12 ft
- Clear shoulders wider than or equal to 6 ft
- No no-passing zones
- All passenger cars in the traffic stream
- Level terrain, and
- No impediments to through traffic (e.g., traffic signals, turning vehicles)

Adjustment factors are normally used to correct the estimates if any of the above conditions are violated.

4.3 OTSIM Two-Lane Highway Level-of-Service Measures

In this section, the result of a case study simulation, carried out in OTSIM, for a six-kilometer segment of a two-lane highway with overtaking permitted in both directions is reported. The purpose is to compare ATS and PTSF as obtained from the simulation with those reported in HCM manuals. The basic geometric attributes of the simulated highway segment are illustrated in Figure 4-1. The first one kilometer on each end are considered as the warm-up zones and will not be included in the simulation results. The simulation period is 70 minutes in duration, including a 10 minutes warm-up interval. An average of 20 simulation runs was carried out for each simulation case, with directional traffic flows input varying from 100 vph to 1700 vph. Mean and standard deviation of desired speed for the traffic stream were set at 100 km/h and 12 km/h, respectively. Average ATS and PTSF values were estimated for each direction.

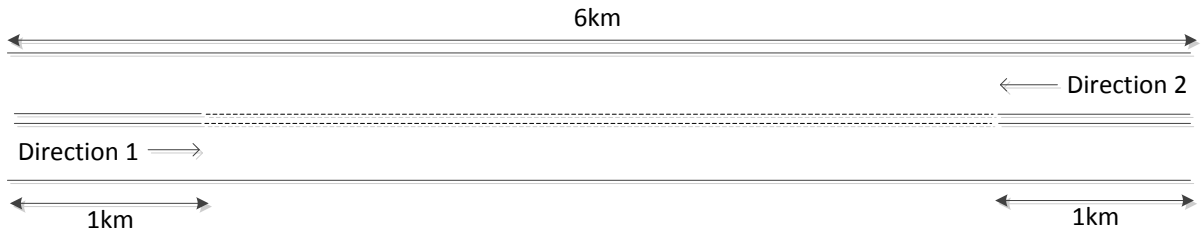

Figure 4-1- Case study highway segment

Figure 4-2 illustrates ATS versus the travel volume (in the analysis direction), for different opposing volumes, as obtained from simulation (with the corresponding error bars) and those from HCM expressions (ATS is the same for both versions so only one curve is shown). From this figure, we note that ATS decreases gradually with increasing travel volumes. When compared to the OTSIM results, the estimates given in HCM appear to be significantly lower especially at high volumes. At low volumes simulated results tend to approximate the free flow speed of 100 km/h for the different opposing volumes. This makes sense because regardless of opposing volume, at low travel volumes vehicles in the traffic stream are generally well-spaced with minimal interactions, such that drivers can attain their desired speeds without being impeded by the speed of any slower moving vehicle. Therefore, the speed drop at low volumes should not be very significant. This was captured in the simulation results more clearly than using the expression used in the HCM. Unlike the HCM assumption, ATS decreases nonlinearly with volume.

In this thesis, we suggest considering the following exponential expression to estimate ATS more accurately.

$$ATS_d = FFS * \exp(a{v_d}^b) \quad \text{Eq. 4-4}$$

where,

ATS_d = average travel speed for analysis direction of traffic (km/h)

FFS= free flow speed (km/h)

v_d= traffic flow of the analysis direction (veh/h)

a, b= coefficients determined from the volume in the opposing direction

In this new expression, as opposed to HCM, the effects of directional volumes on ATS are not the same for the analysis and opposing directions.

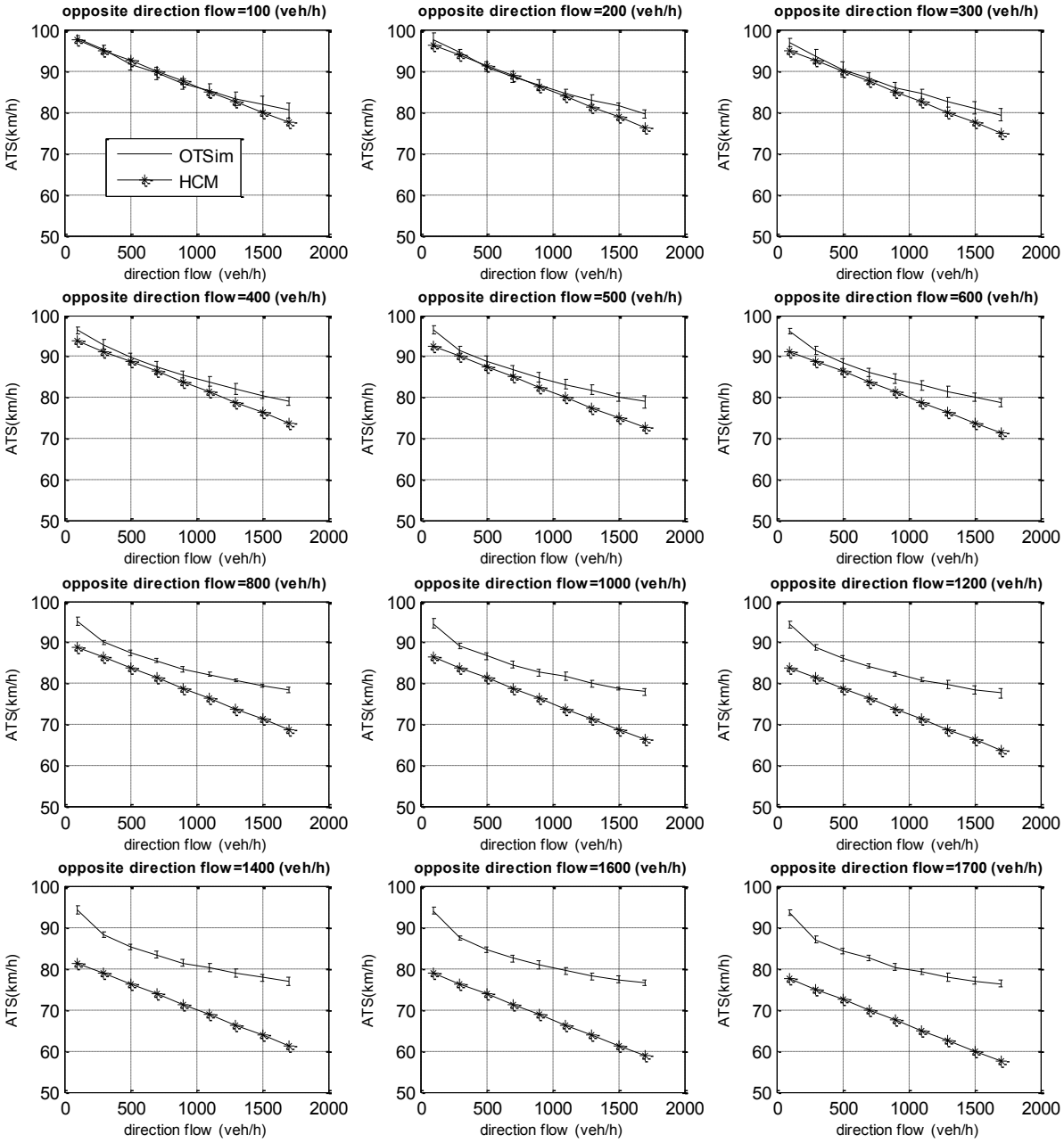

Figure 4-2- Average travel speed (ATS) versus travel volume for different opposing volume obtained from OTSIM simulation, HCM 2000, and HCM 2010

Table 4-3 presents the coefficients values of a and b obtained from the regression analysis. For this regression, all coefficients were found to be statically significant, and the expression exhibited an excellent goodness of fit (Average R-squared ≈ 0.98).

Figure 4-3 illustrates the relationship between PTSF and travel volume for different opposing volumes from the simulation (with the corresponding error bars) and the HCM expressions. As shown in this figure, PTSF obtained from HCM 2010 closely matches simulated results at low opposing volume. Simulated PTSF is estimated to be higher than HCM 2010 values as opposing volume increases. As can be seen PTSF obtained from HCM 2000 is significantly overestimated.

Table 4-4 provides a summary of model coefficients relating PTSF to travel volume for different volumes in the opposing direction. These coefficients are obtained by applying a nonlinear expression relating simulated PTSF to the volumes obtained by regression. For this regression, all coefficients were found to be statically significant (t-test), and the expression exhibited an excellent goodness of fit (Average R-squared ≈ 0.99).

Table 4-3- Coefficients for new ATS expression obtained from regression and OTSIM data

	Simulated ATS coefficients $ATS_d = FFS\exp(av_d{}^b)$	
v_o Opposing volume (pc/h)	a	b
100	-0.00064	0.786
200	-0.00091	0.744
300	-0.00141	0.714
400	-0.00191	0.648
500	-0.00289	0.593
600	-0.00345	0.571
800	-0.00527	0.517
1000	-0.00720	0.479
1200	-0.00766	0.474
1400	-0.00897	0.458
1600	-0.0104	0.441
1700	-0.0113	0.432

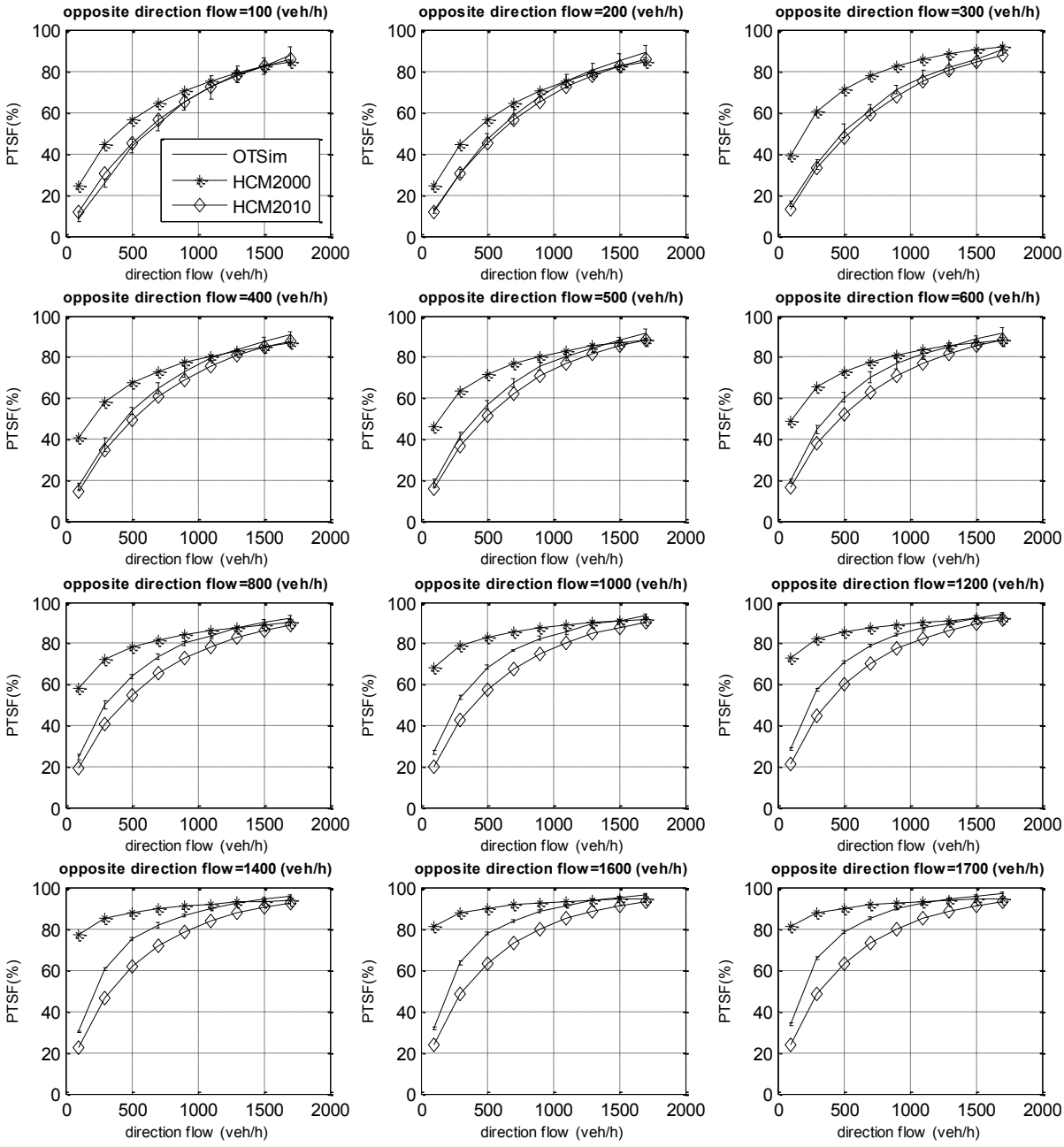

Figure 4-3- Percent time spent following (PTSF) versus travel volume for different opposing volume obtained from OTSIM, HCM2000, and HCM2010

Table 4-4- Updated coefficients for estimating PTSF as obtained from OTSIM

	Simulated PTSF coefficients $PTSF = 100(1 - \exp(a{v_d}^b))$	
v_o, Opposing volume (pc/h)	a	b
100	-0.000655	1.083
200	-0.001157	1.012
300	-0.002085	0.936
400	-0.00268	0.909
500	-0.00391	0.863
600	-0.00521	0.828
800	-0.00877	0.764
1000	-0.01078	0.746
1200	-0.01225	0.737
1400	-0.01225	0.751
1600	-0.01227	0.764
1700	-0.01365	0.754

4.1 Effect of Standard Deviation of Speeds on ATS and PTSF

As mentioned previously, the HCM adjustment factors are aimed to provide correction to ATS and PTSF measures if the conditions deviate from those assumed for the base case. One factor that can be considered as an adjustment factor is the effect of standard deviation of speeds. This factor can play an important role in efficiency of two-way traffic flow operation and is easy to obtain using conventional speed measurement devices such as dual loop detectors or radars. Wardrop (1953) proposed an overtaking demand formula (catch-up rate) that can be mathematically described as:

$$P = \frac{0.56\sigma Q^2}{V^2} \qquad \text{Eq. 4-5}$$

where,

P = overtaking demand (overtaking/km/h)

Q = stream flow (veh/km)

V = mean of unimpeded speed (km/h), and

σ = standard deviation of the unimpeded speed distribution (km/h)

Eq. 4-5 expresses the upper bound of the overtaking demand. The actual overtaking rate in real traffic conditions are less than this value. Based on this expression, the catch-up rate between vehicles increases with standard deviation of unimpeded (desired) speeds. Presumably, higher variation in unimpeded speeds result in higher catch-up rate and because overtaking opportunity is always limited by opposing volume or geometry, this leads to increased PTSF, and decreased ATS.

To address the effect of standard deviation of speeds as an adjustment factor in calculation of ATS and PTSF, simulations for four levels of directional traffic volumes of 100, 500, 1000, and 1500 vph and three levels of 0.10, 0.12, 0.14 for Coefficient of Variation (CV) of free-flow speed were conducted. For average free flow speed of 100 km/h, this results in standard deviation (SD) for desired speed of 10, 12, 14 km/h. The base condition corresponds to CV=0.10 and correction factors are provided for CV=0.12 and CV=0.14. The updated form of Eq. 4-4, which includes the CV correction factor, has the following form:

$$ATS_d = FFS \exp\left(a v_d{}^b\right) - f_{ATS-CV} \qquad \text{Eq. 4-6}$$

where, f_{ATS-CV} = ATS adjustment factor for the coefficient variation of free-flow speeds

Figure 4-4 illustrates the simulation results for ATS for three levels of coefficient of variation and four flow rates. As shown, the effect of standard deviation of speeds is to decrease the average travel speed. This effect is more significant at higher volumes when the average speed gets closer to the speed of slowest vehicle in the traffic stream and passing opportunity is very limited. The lowest speed in the traffic steam is lower when standard deviation of speed is higher.

Table 4-5 provides the list of coefficients for ATS base condition (CV=0.10) as obtained from regression. The corresponding adjustment factors for CV=0.12 and CV=0.14 are listed in Table 4-6.

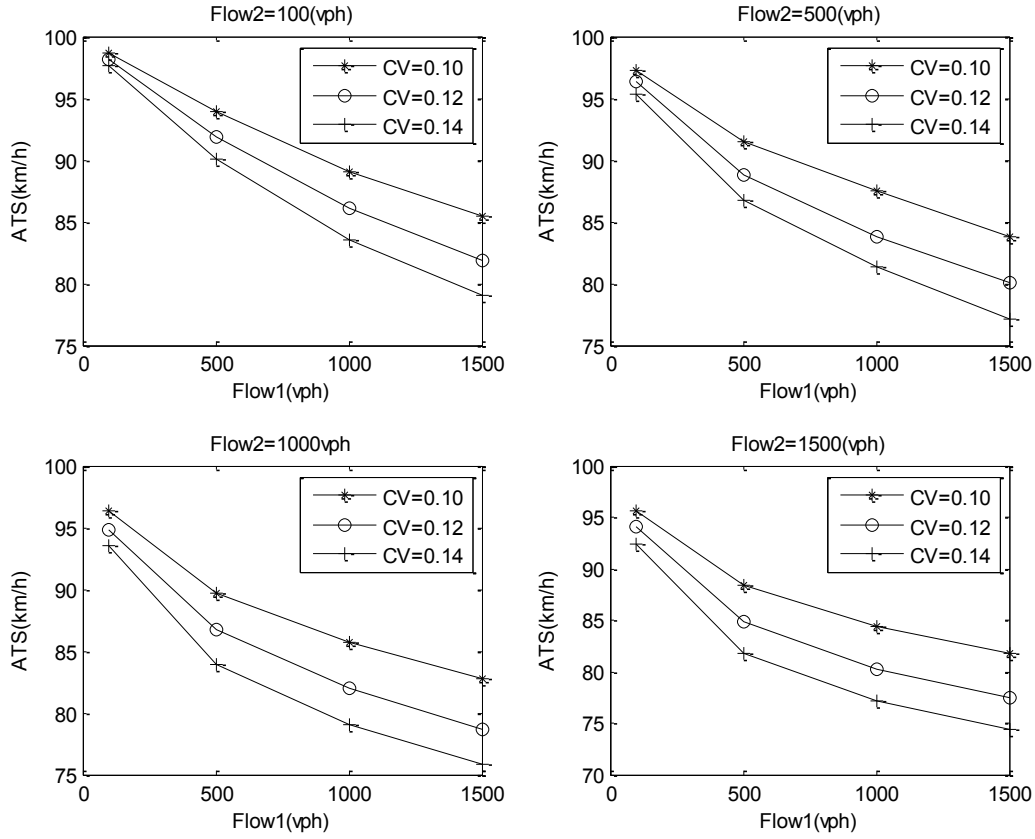

Figure 4-4-Average travel speed versus volume for three standard deviation of speeds

Table 4-5- ATS coefficients for base condition

	ATS coefficients (CV = 0.10) $ATS_d = FFS \exp(av_d{}^b)$	
v_o Opposing volume (pc/h)	a	b
100	-0.00031	0.853
500	-0.00146	0.655
1000	-0.00324	0.558
1500	-0.00483	0.513

Table 4-6- ATS adjustment factors for coefficient of variation of free-flow speed

v_o Opposing direction volume (pc/h)	v_d Analysis direction volume (pc/h)	f_{ATS-CV} (CV=0.12)	f_{ATS-CV} (CV=0.14)
100	100	0.5	1.1
	500	2.1	3.9
	1000	3.0	5.6
	1500	3.6	6.4
500	100	0.8	1.9
	500	2.7	4.8
	1000	3.7	6.2
	1500	3.8	6.7
1000	100	1.6	2.8
	500	2.9	5.8
	1000	3.7	6.6
	1500	4.1	6.9
1500	100	1.5	3.2
	500	3.5	6.6
	1000	4.2	7.2
	1500	4.3	7.3

A similar analysis is conducted for PTSF. For this measure, the updated form of Eq. 4-2 with CV correction factor has the following form:

$$PTSF_d = 100(1 - \exp(a{v_d}^b)) + f_{PTSD-CV} \quad \text{Eq. 4-7}$$

where, $f_{PTSF-CV}$ = PTSF adjustment factor for the standard deviation of free-flow speeds

Figure 4-5 illustrates the simulation results for PTSF for three standard deviations of speeds. As shown, the effect of standard deviation of speeds is to increase PTSF. This effect is less significant at higher volumes, where the overtaking opportunities are scarce and regardless of speed deviations vehicles must follow slower moving vehicles in the traffic stream.

Table 4-7 provides the list of coefficients for PTSF base condition (CV=0.10) as obtained from non-linear regression. The corresponding adjustment factors for CV=0.12 and CV=0.14 are listed in

Table 4-8. As expected, a larger correction value is required for higher opposing volumes and larger standard deviations.

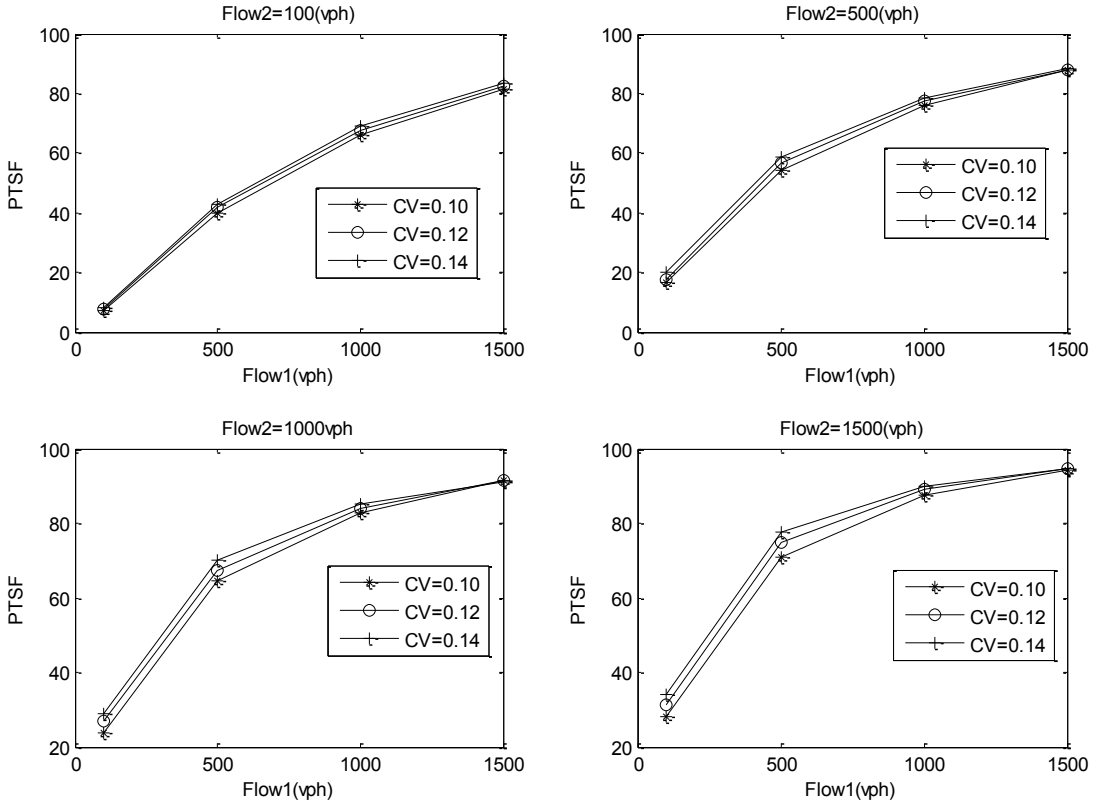

Figure 4-5- Percent time spent following versus volume for three standard deviation of speeds

Table 4-7- PTSF coefficients for base condition

	PTSF coefficients (CV=0.10) $100(1-\exp(av_d{}^b))$	
v_o Opposing volume (pc/h)	a	b
100	-0.0004884	1.116
500	-0.00297	0.896
1000	-0.00666	0.809
1500	-0.00837	0.800

Table 4-8- PTSF adjustment factors for coefficient of variation of free-flow speed

v_o Opposing direction volume (pc/h)	v_d Analysis direction volume (pc/h)	$f_{PTSD-CV}$ (CV=0.12)	$f_{PTSD-CV}$ (CV=0.14)
100	100	0	1
	500	2	3
	1000	1	3
	1500	1	2
500	100	1	3
	500	3	5
	1000	2	3
	1500	0	0
1000	100	3	5
	500	3	6
	1000	1	2
	1500	0	0
1500	100	3	6
	500	4	7
	1000	2	3
	1500	0	0

4.2 Safety Measures as an Alternative for Level-of-Service

As introduced previously, head-on TTC and overtaking rate (OTrate) are considered as two measures of safety for two-lane highways in this research. These safety measures can be used alternatively in determination of LOS. Morrall and Werner (1990) used overtaking ratio (ratio of accomplished overtakes to the estimated desired number) as an alternative measure for level-of-service for two-lane highways. In this section, based on OTSIM simulated outputs, mathematical expressions are proposed for these measures that can be potentially used as an indication of safety performance on two-lane highways. Similar to the previous section, four levels of volumes and three levels of standard deviation of speeds are considered in the simulation case study. Figure 4-6 illustrates the simulation results. A polynomial model of the following form was found to represent the overtaking rate appropriately.

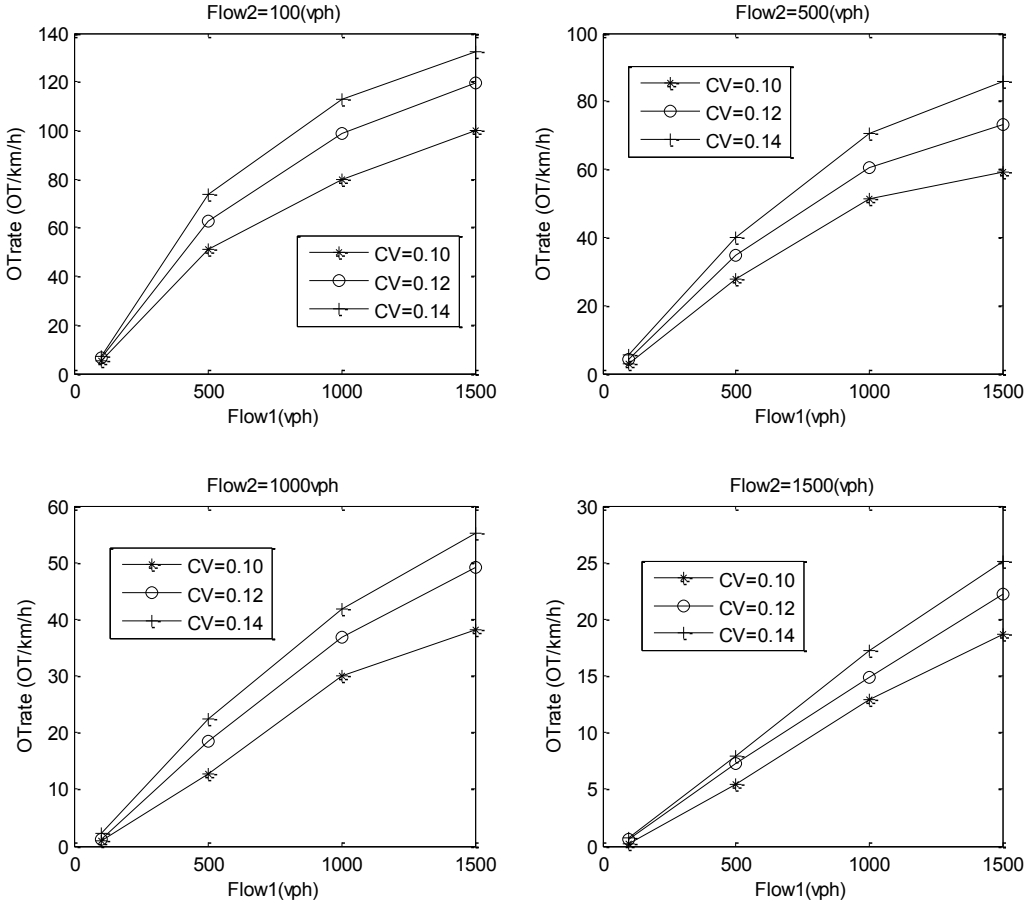

Figure 4-6-Overtaking rate versus volume for three standard deviation of speeds

$$OTrate_d = av_d^2 + bv_d + c + f_{OT-CV} \quad \text{Eq. 4-8}$$

where, f_{OT-CV} = OTrate adjustment factor for the standard deviation of free-flow speeds

Table 4-9 provides a list of coefficients, calculated from a regression analysis, for OTrate base condition. Similar to ATS and PTSF, adjustment factors are provided to compensate the effect of standard deviation of speeds in overtaking rate (Table 4-10).

Table 4-9- OTrate coefficients for base condition

	OTrate coefficients (CV=0.10) $OTrate_d = av_d^2 + bv_d + c$		
v_o, opposing volume (pc/h)	a	b	c
100	-3.645e-005	0.1247	-5.742
500	-2.464e-005	0.08014	-5.269
1000	-7.783e-006	0.03992	-3.686
1500	-1.14e-006	0.01517	-1.464

Table 4-10- OT-rate adjustment factors for coefficient of variation of free-flow speed

v_o Opposing direction volume (pc/h)	v_d Analysis direction volume (pc/h)	f_{OT-CV} (CV=0.12)	f_{OT-CV} (CV=0.14)
100	100	1	2
	500	12	23
	1000	19	33
	1500	20	33
500	100	1	2
	500	7	12
	1000	9	20
	1500	14	27
1000	100	0	1
	500	6	10
	1000	7	12
	1500	11	17
1500	100	0	1
	500	2	3
	1000	2	4
	1500	4	6

The effect of standard deviation is to increase overtaking rate. This effect is not very significant at low analysis direction volumes, where the catch-up rate is still insignificant; i.e., no adjustment is required. However, as volume increases larger adjustment values must be used.

Another overtaking frequency based measure is the overtaking rate per vehicle (OTperVeh). This measure can be calculated by dividing the overtaking rate by traffic volume of the analysis direction. Figure 4-7 illustrates OTperVeh as a function of volume for three standard deviations of speed. Unlike OTrate, OTperVeh does not continuously increase with volume. There is a volume at which this measure reaches its maximum. For the range of opposing volume up to 500 vph, the maximum OTperVeh is around 500 vph.

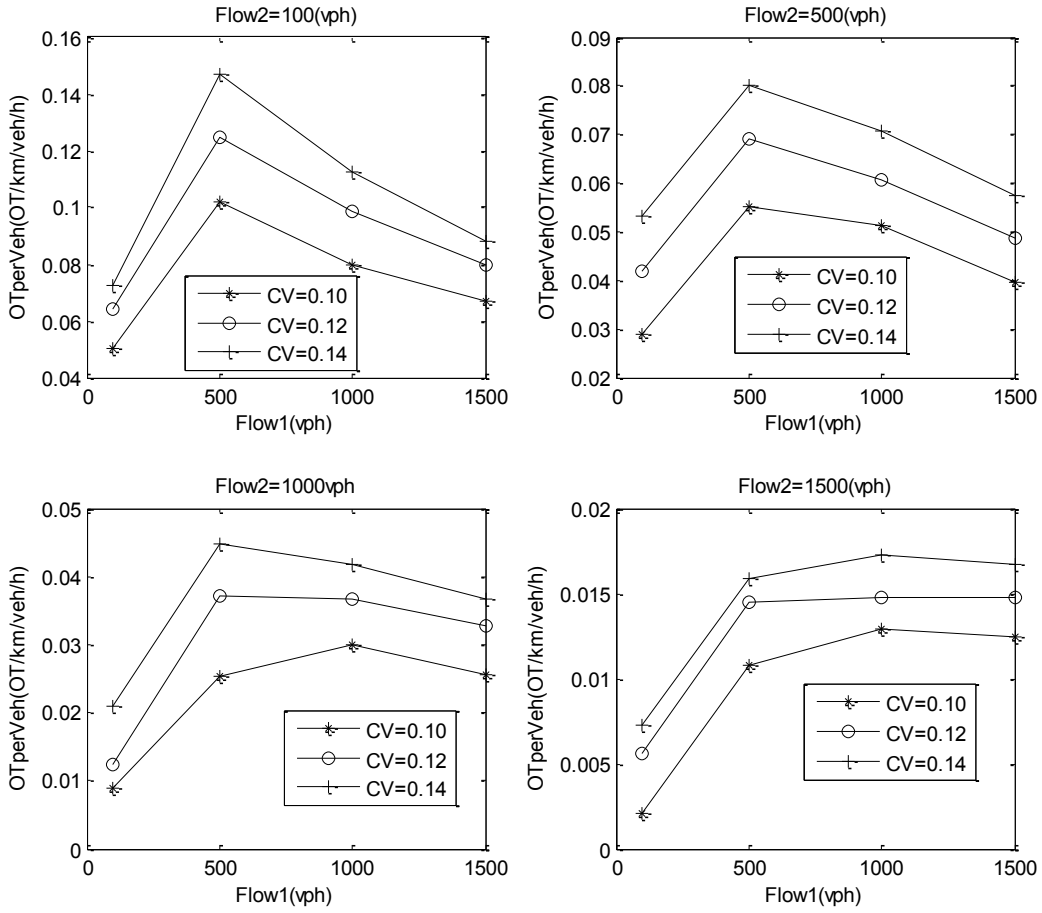

Figure 4-7- Overtaking rate per vehicle versus volume for three standard deviation of speeds

Similar to OTrate, a polynomial function is used to represent OTperVeh:

$$OTperVeh_d = av_d^2 + bv_d + c + f_{OTveh-CV} \quad \text{Eq. 4-9}$$

where, $f_{OTveh-CV}$ = OTperVeh adjustment factor for the standard deviation of free-flow speeds

Table 4-11 provides list of coefficients calculated from regression analysis for OTperVeh base condition. The corresponding adjustment factors are provided in Table 4-12. The correction factors are significant for the whole range of volume considered.

Table 4-11- OTperVeh coefficients for base condition

	OTperVeh coefficients (CV=0.10) $OTperVeh_d = av_d^2 + bv_d + c$		
v_o, opposing volume (pc/h)	a	b	c
100	-2.884e-007	0.0004797	0.1795
500	-1.759e-007	0.0003021	0.09503
1000	-1.024e-007	0.0002089	0.01758
1500	-4.574e-008	0.0001007	0.0004223

Figure 4-8 illustrates TTC as a function of volume for three standard deviations of speeds. TTC increases linearly with analysis direction volume while sharply decreases with the opposing volume. A linear function is used to represent TTC in our analysis:

$$TTC_d = a + bv_d + f_{OT-TTC} \quad \text{Eq. 4-10}$$

f_{OT-TTC} = TTC adjustment factor for the standard deviation of free-flow speeds

Table 4-12- OT-rate per vehicle adjustment factors for coefficient of variation of free-flow speed

v_o Opposing direction volume (pc/h)	v_d Analysis direction volume (pc/h)	$f_{OTveh-CV}$ (CV=0.12)	$f_{OTveh-CV}$ (CV=0.14)
100	100	0.0139	0.0728
	500	0.0189	0.1085
	1000	0.0232	0.1471
	1500	0.0210	0.1281
500	100	0.0190	0.1127
	500	0.0152	0.1031
	1000	0.0131	0.0882
	1500	0.0138	0.0706
1000	100	0.0128	0.0533
	500	0.0118	0.0663
	1000	0.0139	0.0800
	1500	0.0121	0.0746
1500	100	0.0094	0.0707
	500	0.0102	0.0650
	1000	0.0092	0.0573
	1500	0.0070	0.0396

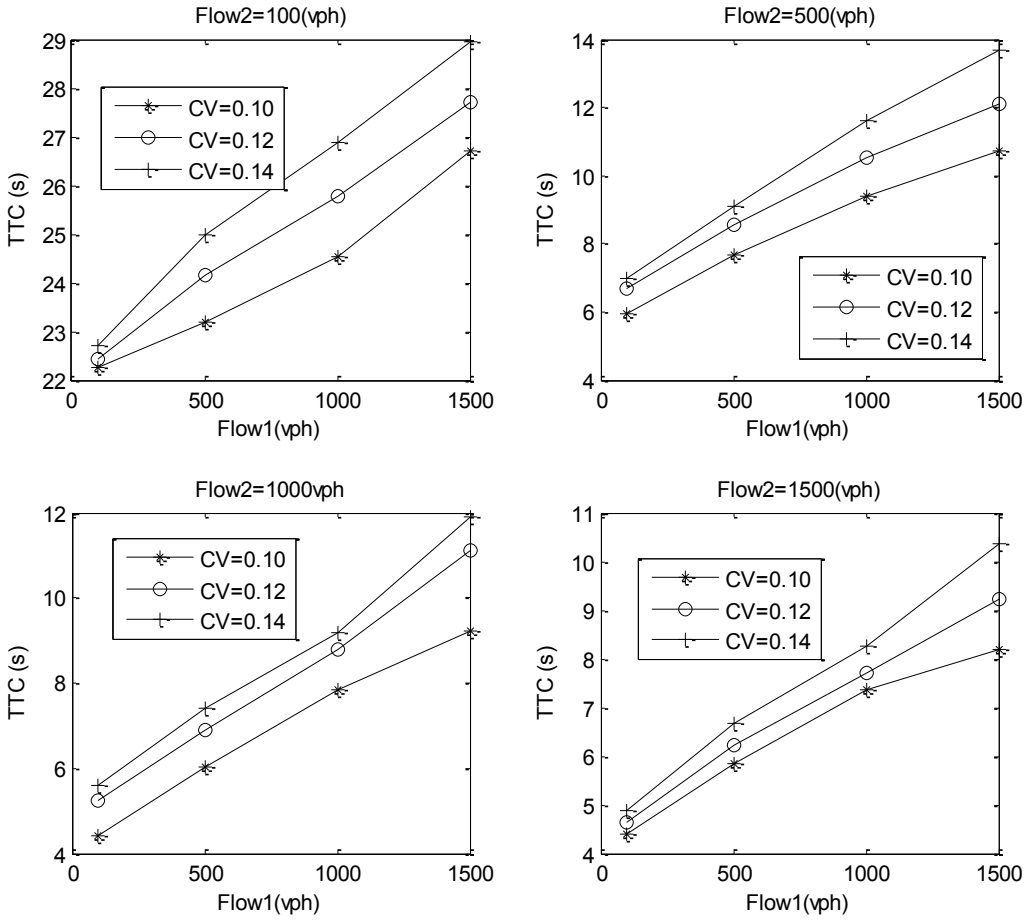

Figure 4-8- TTC versus volume for three standard deviation of speeds

The coefficients for the base condition and adjustment factors are listed in Table 4-13 and Table 4-14, respectively. The effect of standard deviation is to increase TTC. This can be indirectly the effect of lower average speed for higher standard deviation of desired speeds. Normally, at lower speeds, overtaking requires less time. In addition, the speed of opposing vehicle can be lower. This leaves more gap time when overtaking maneuver is finished (higher TTC).

Table 4-13- TTC coefficients for base condition

	TTC coefficients (CV = 0.10) $TTC_d = a + bv_d$	
v_o Opposing volume (pc/h)	a	b
100	21.6	0.00325
500	5.8	0.00341
1000	4.2	0.00344
1500	4.5	0.00260

Table 4-14- TTC adjustment factors for standard deviation of free-flow speed

v_o Opposing direction volume (pc/h)	v_d Analysis direction volume (pc/h)	f_{OT-TTC} (CV=0.12)	f_{OT-TTC} (CV=0.14)
100	100	0.2	0.4
	500	0.9	1.8
	1000	1.2	2.3
	1500	1.0	2.3
500	100	0.7	1.1
	500	0.9	1.5
	1000	1.1	2.2
	1500	1.4	3.0
1000	100	0.9	1.2
	500	0.9	1.4
	1000	0.9	1.4
	1500	1.9	2.7
1500	100	0.3	0.5
	500	0.4	0.8
	1000	0.3	0.9
	1500	1.0	2.2

4.3 Conclusion

In this section, OTSIM model was used to provide estimates for average travel speed (ATS) and percent time spent following (PTSF) measures used to establish level-of-service (LOS) for two-lane highways in the Highway Capacity Manual (HCM). The results obtained from the simulation model were compared to published values in the HCM 2000 and HCM 2010. Estimates of ATS as reported in HCM 2000 and HCM 2010 were found lower than those obtained from the simulation. A new nonlinear model was suggested to replace the current linear function relating volume to ATS in HCM. PTSF obtained from HCM 2010 closely matches simulated results at low opposing volumes. A new adjustment factor was introduced to take into account the effect of standard deviation of unimpeded speeds on ATS and PTSF. Three safety indicators including overtaking rate, overtaking rate per vehicle, and time-to-collision (TTC) were estimated as an alternative measure of level-of-service for two-lane highways. The underlying model coefficients for these indicators along with the adjustment factors for standard deviation of speeds were calculated.

Chapter 5
Safety and Traffic Implications of Truck/Car Speed Limit Strategies for Two-lane Highways (Model Application 2)

5.1 Introduction

While differential car/truck speed limits have been mainly applied to freeways and divided highways, where the speeds are relatively high, there is also a potential of using differential speed limit strategies for two-lane undivided highways. The implementation of differential speed limit strategies on two-lane highways can have significant effects on interactions between cars and trucks especially in overtaking maneuver and the special safety intervention this may pose. The objective of the research in this chapter is to use OTSIM to assess the safety and traffic implications of three speed control strategies applied to two-lane highway operations including uniform speed limits (USL), discretionary differential speed limits (DSL) and differential speed controls with truck mandated speed limiters (MSL). The major issue separating DSL from MSL is separate compliance assumptions for trucks and the effect this has on vehicle interactions. Safety and traffic performance of USL, DSL and MSL specifically for overtaking are evaluated. Similar to the previous OTSIM model application, the developed overtaking model plays an important role in this analysis. The content of this chapter is published in Ghods and Saccomanno (2013b) and Ghods and Saccomanno (2012).

5.2 Literature Review

A number of researchers have argued that speed is the single most important factor affecting the frequency and severity of highway accidents (Evans, 1991; Elvik, 2005). The deterrence of unsafe operating speeds is viewed as being a key objective for reducing both the frequency and severity of crashes, and the conventional way to do this is through “posted speed limits”. Highway design or geometric restrictions are the main factors in setting appropriate posted speed limits that are normally applied to all types of vehicles. Given size and weight differences between cars and trucks and special maneuverability characteristics associated with these two types of vehicles, uniform speed limits (USL) may be inappropriate to account for all the potential safety problems. Recognizing the more restrictive maneuverability of large trucks, differential speed limit (DSL) strategies are used to address this issue. DSL normally sets the maximum speeds for trucks at about 10 – 20 km/h lower

than for cars for the same highway conditions. For instance, in Michigan the posted speed limit for trucks has been set at 16km/h lower than for cars (cars: 60 mph versus trucks: 70mph) on rural interstates highways (GHSA, 2012).

In most jurisdictions, DSL control strategies tend to be discretionary in nature, in that they invariably depend on compliance among target drivers in the traffic stream. Compliance with speed limits depends on many factors including degree of enforcement, limit level, road and traffic conditions, etc. Johnson and Pawar (2007) found that, in certain DSL jurisdictions in U.S., compliance rates were low (similar speed distributions as per USL state) while in other DSL states compliance was found to be higher. Lack of compliance can have a significant effect on safety for both compliant and non-compliant vehicles. The effect of discretionary differential speed limits on safety has been widely studied. However, the results reported have been often inconclusive or sometimes contradictory. Some studies show negative safety impacts while others indicate positive or negligible impacts (Johnson and Pawar, 2005, Neeley and Richardson Jr, 2009, Garber et al., 2003). Most of these studies concerning the impact of DSL on road safety have adopted statistical before-and-after approaches. One of the major flaws of the statistical approach concerns limitations placed on the analysis by the available data, especially as it relates to levels of compliance to speed limits. The use of microscopic traffic simulation platforms in conjunction with surrogate safety measures provides an alternative approach for studying the safety of uniform and differential speed limits. Saccomanno et al. (2009) discuss the advantages of this approach in their speed limit study applied to freeway operations.

Given the severity of accidents involving large trucks, truck compliance to DSL is especially important. A study carried out by FMCSA (2008) in the U.S. noted that excessive speeds were the primary factor in 22% of fatal crashes involving trucks. Recently, a number of jurisdictions have recognized this issue and have required all trucks to be equipped with mandated speed limiters (MSL). A limiter is a built-in microchip that limits the maximum revolutions that an engine can achieve, thereby restricting the maximum operating speed of the vehicle. Trucks equipped with limiters are assumed to be 100% compliant with truck speed limit.

A common belief is that DSL/MSL increases speed variance in the traffic stream, and this becomes more pronounced where trucks are equipped with limiters. Solomon 1964 found a U-shaped relationship between the crash involvement rate and the amount of deviation from the average speed. Increased variance may lead to increased number of accidents, especially accidents involving (non-

compliant) cars and (compliant) trucks. However, other factors may act to mitigate the effect of speed variance on safety, for example, lower crash severity, improved lane discipline on freeways and changes in the pattern of overtaking for two-lane highway operations. In a recent study by Hanowski et al. (2012), more than 15,000 truck crash data from 20 truck fleets (approximately 138,000 trucks) were analyzed to investigate the effect of MSL on truck crashes that could have been avoided with activation of the speed limit device. The findings showed a significant reduction in speed limit related crashes (approximately 50%) for trucks equipped with the speed limiter compared to trucks without the speed limiter.

In spite of the above mentioned findings the potential implications of using differential speed limiters for two-lane highway operations have been unknown to date. Differential speed limits may impact the number of overtakes and safety of overtaking. Hauer (1971) has shown that increase in the number of overtaking maneuvers correlates with increase in accidents probability. In addition, vehicles seeking to overtake can be more at risk of rear-end accident due the tendency of drivers to maintain shorter headways prior to overtaking. This is suggested by Hegeman (2008) who found that the headway between the overtaking and overtaken vehicles prior to overtaking can be as low as 7.7m (~0.35s). This has not been researched adequately so far.

It must be noted that the current mandated speed limit thresholds set for trucks (105 kmh in Canada and 68 mph in U.S.) are relatively high for operation speed of two-lane highways. However, some two-lane highways with higher posted speed can be still affected by these speed limit thresholds. For example in Nebraska posted speed limits for rural two-lane highway can be as high as 65 mph (Schurr et al., 2002). Nevertheless, in this study a lower value of truck mandated speed limit is used (presumably this affects a larger proportion of rural two-lane highways around the world).

5.3 Distribution of Free-flow Speeds for Car/Truck Speed Limit Scenarios

In order to simulate the three candidate speed limit scenarios in OTSIM, it is crucial to determine the distribution of vehicles (car/truck) free-flow speeds (desired speeds) based on the USL/DSL posted limit and MSL maximum speed threshold for trucks. This includes the shape of the distributions as well as the corresponding means and standard deviations. As discussed previously, in micro-simulation the free-flow operating speed of individual vehicles speeds are sampled from an assumed desired speed distribution of the corresponding vehicle class.

The relationship between posted speed and operating speed has been an issue for many years. This has been extensively studied by Fitzpatrick (2003) for different types of roads. This study demonstrated that 85th percentile operating speeds normally exceed posted speed limits while the 50th percentile operating speed is usually near or above the posted speed limit. Although this does not distinguish passenger-cars and trucks, the mean operating speed is usually lower for trucks. Johnson and Murray (2007) found that the operating speed of trucks was 5% lower than that of cars for four posted USL sites (car: 70 mph; truck: 70 mph) on rural interstate highways in U.S.. In the same study, car speeds was 10% higher than that of trucks for three posted DSL sites (car: 70 mph; truck: 60 mph). McLean (1989) stated that for motorized countries normal distribution with mean of about 90 to 100 km/h and coefficient of variation between 0.11 to 0.14 can represent the distribution of desired speeds for two-lane highways.

These findings will justify the assumption made in this study about the distribution of car and truck speeds for USL and DSL scenarios; i.e., a normal distribution with the mean equating the posted speed can represent the actual operating driving speed of passenger-cars on two-lane highways. In addition, the truck average speed can be assumed to be 5% and 10% lower than that of passenger-car for USL and DSL scenarios, respectively. Nevertheless, the truck speed distribution for MSL scenario is still undetermined and discussed in the followings.

Figure 5-1 illustrates the distribution of free-flow speeds for heavy trucks obtained from a Weigh-In-Motion (WIM) station on Highway 401, Ontario, Canada (Vaziri et al., 2013). In Ontario, all large trucks (with Gross Vehicle Weight (GVW) greater than 11,794kg) must be equipped with a maximum allowable speed threshold set uniformly at 105 km/h. As seen the shape of this distribution does not follow a standard distribution curve e.g. normal. This is mainly due to the concentration of speed at the maximum limit (105 km/h) which creates a skew-shaped distribution. In this figure, the other proportion of trucks with speeds higher than 105 km/h can be trucks from other jurisdictions e.g. U.S. (at the time of data collection truck speed limiter was not mandatory in U.S.) or trucks from non-compliance common carriers in Canada. In this research, a custom distribution is fitted to the truck speed when mandated speed limit is in effect.

The best distribution found for this purpose is a linear combination of two distributions (Weibull and Cauchy), which is itself a probability distribution function, i.e.:

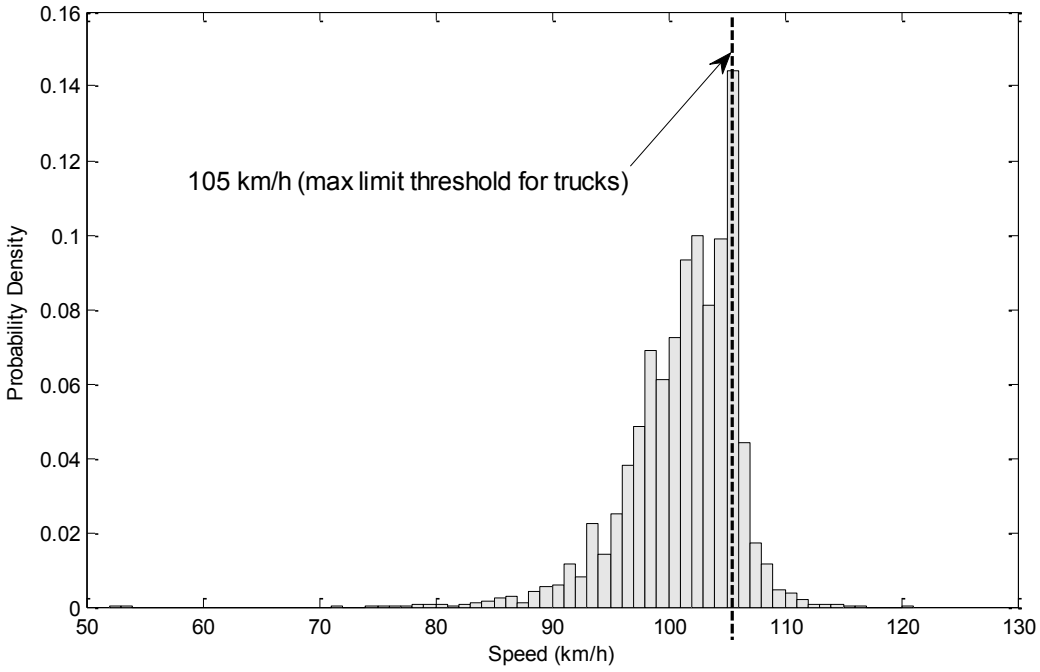

Figure 5-1- Distribution of trucks free-flow speeds with mandated speed limiters set at 105 km/h (Ontario, Canada)

$$f(x;p,\beta,\delta,x_0,\gamma) = p * \underbrace{\frac{\beta}{\delta}\left(\frac{x}{\delta}\right)^{\beta-1}}_{Weibull} + (1-p) * \underbrace{\frac{1}{\pi}\left[\frac{\gamma}{(x-x_0)^2+\gamma^2}\right]}_{Cauchy} \quad \text{Eq. 5-1}$$

where,

$p =$ weighting parameter

$\beta, \delta, x_0, \gamma =$ probability distribution parameters

The maximum likelihood method is used to determine the five unknown parameters of the above distribution such that it fits the speed data presented in Figure 5-1.

Figure 5-2 illustrates the fitted distribution of trucks speeds with their corresponding optimal parameter values. It is interesting to note that the median of the Cauchy distribution (x_0) was found to be 105 km/h which is actually the truck maximum mandated speed. Additionally, the sigma parameter in the Weibull distribution can logically be assumed as the mean of truck distribution speed if MSL had not been applied. Although this finding is based on dataset from a freeway section, with

reasonable assumption, it can be extended to lower operating speed for two-lane highways. Considering the findings and assumption made previously, one can determine the distribution of desired speeds for the three speed limit scenarios for our hypothetical two-line highway segment.

5.4 Case Study and Simulation Inputs

Table 5-1 presents the distribution of car and truck free-flow operating speeds (desired speed) assumed in this research for the three speed control strategies. For the USL strategy, the maximum posted speed is set at 90 km/h for both cars and trucks. In this case, we assume that the distribution of speeds has a mean of 90 km/h for cars and 85 km/h for trucks (5% lower). As a result, 50% of cars and 31% of trucks exceed the posted limits.

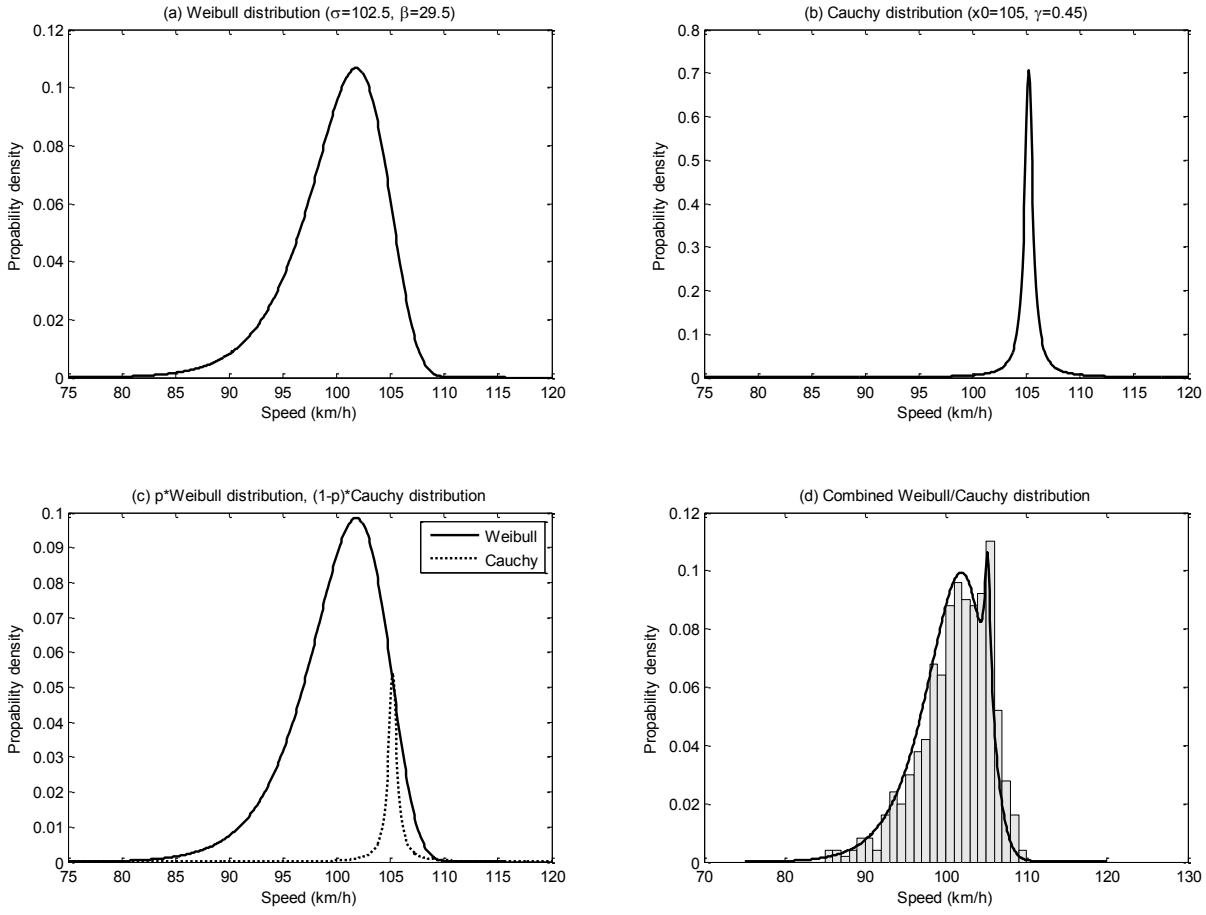

Figure 5-2- Linearly combined probability distribution functions fitted to distribution of truck speed with mandated speed limiters, a) Weibull distribution, b) Cauchy distribution, c) Scaled Weibull and Cauchy distributions, d) Linearly combined distribution

Table 5-1-Distribution of free-flow speeds for car and truck for the three speed limit strategies

		Car	Truck	
USL	Posted Speed (km/h)	90	90	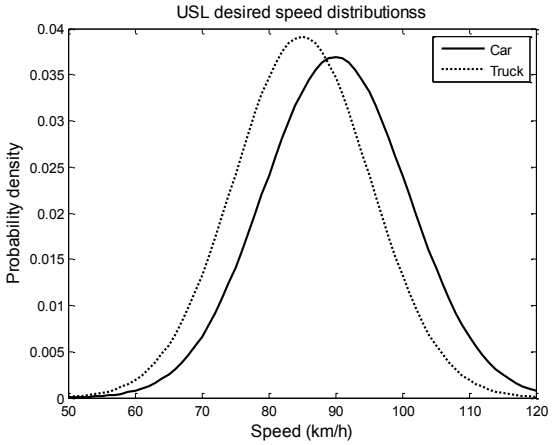
	Mean Operating Speed (km/h)	90	85	
DSL		**Car**	**Truck**	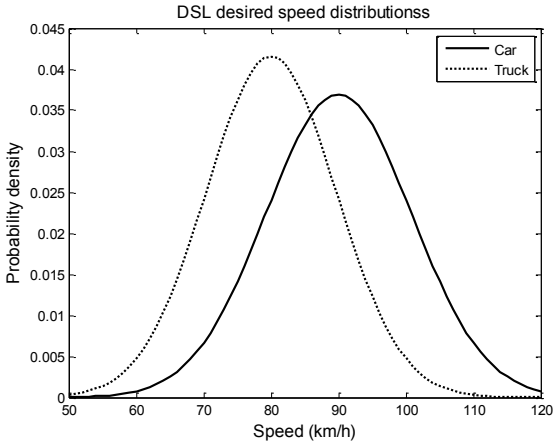
	Posted Speed (km/h)	90	80	
	Mean Operating Speed (km/h)	90	80	
MSL		**Car**	**Truck**	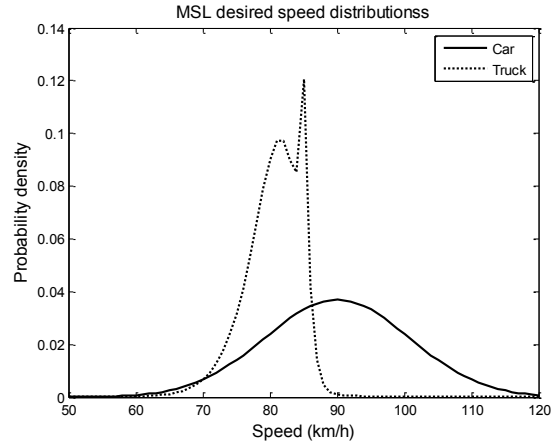
	Posted Speed (km/h)	90	80	
	Mean Operating Speed (km/h)	90	Skewed (Max:85)	

For the DSL scenario, the maximum posted speeds are set at 90km/h for cars and 80km/h for trucks with the corresponding operating mean speeds of 90km/h for cars and 80km/h for trucks. DSL does not change the percentage non-compliant cars, but it increases the non-compliance trucks to 50%. The effect of the DSL is assumed to reduce the truck mean speed by 5km/h (10% lower than that of cars). The introduction of MSL has the effect of shifting the DSL non-compliant trucks that are above 85km/h (MSL threshold) into a skewed speed distribution shown in Table 5-1.

Similar to the previous simulation studies, the case study for the simulation of speed limits is carried out for a six kilometers segment of two-lane highway with overtaking permitted in both directions. The first one kilometer on each end of the segment is considered as the warm-up zones and will not be considered in the simulation results. The simulation period is 70 minutes in duration, including a 10 min warm-up interval. A simulation experimental design was developed to optimize the results with minimum number of simulation runs. The design consists of four factors including analysis direction flow (Flow1), opposing direction flow (Flow2), percentage of trucks (PT), and the speed limit scenarios (SL). Table 5-2 presents the list of the four factors with their corresponding level values. Ten runs were carried out for each combination of experiment. Therefore, a total of 1440 (4×4×3×3×10) simulations were conducted (full factorial design). For each simulation run, the average travel speed (ATS), percent time spent following (PTSF), overtaking rate (OTrate), and average time-to-collision (TTC) were recorded.

Table 5-2-Factors included in the experimental design

Variable Name	Flow1	Flow2	PT	SL
Level values	100, 500, 1000, 1500	100, 500, 1000, 1500	5%, 10%, 15%	USL, MSL, DSL

5.5 Analysis of Variance

In this section we conduct an ANOVA test to discover the possible main and interaction effects of the factors (Flow1, Flow2, PT, SL) on the four output measures. In this analysis, three-way and higher interactions are ignored. Table 5-3 presents the ANOVA tests conducted for ATS. As seen, all the factors and their interactions effects are highly significant. Figure 5-3 illustrates a multiple comparison graph based on Tukey's honestly significant difference criterion. As shown, all the four factors at all levels show significant effect on ATS. ATS decreases with increase in both Flow1 and

Flow2 factors. As Percentage Truck (PT) increases ATS decreases. ATS drops as speed limit scenarios (SL) changes from USL to DSL and finally to MSL. The lowest ATS corresponds to the MSL scenario.

Table 5-4 presents the ANOVA table for PTSF. In this analysis all the main and interaction effects except that of Flow1*SL appear to be significant. As Figure 5-4 shows both Flow1 and Flow2 increased PTSF. This effect appears to be linear for Flow2 and nonlinear for Flow1. This is consistent with the relation between PTSF and analysis direction flow observed previously. PTSF increases with PT. This indicates that increased truck percentage results in more catch-up rates and less overtaking opportunities. USL and MSL resulted in lowest and highest PTSF values, respectively. This effect also appears to be nonlinear.

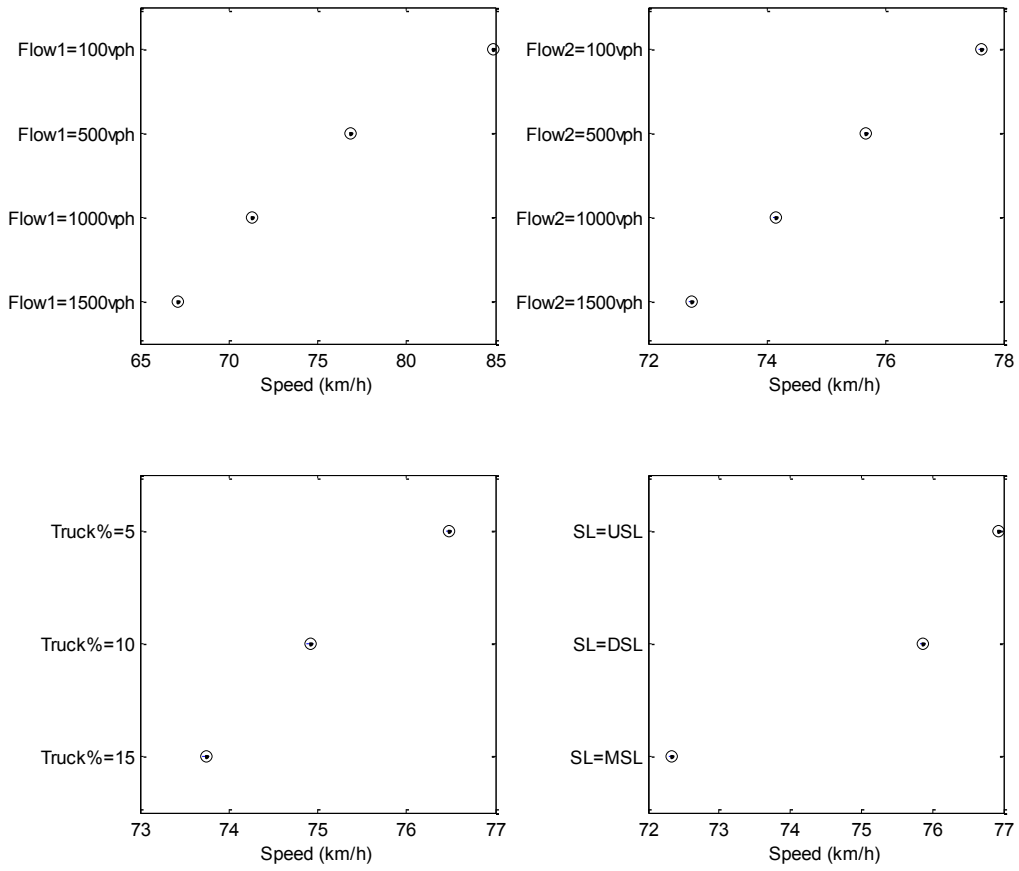

Figure 5-3- Multilevel comparison of factor effects on average travel speed (ATS)

Table 5-3- ANOVA table for average travel speed (ATS)

Source	Sum Sq.	d.f.	Mean Sq.	F	Prob>F
Flow1	6343.17	3	2114.39	33967.26	0
Flow2	476.74	3	158.91	2552.94	0
PT	181.62	2	90.81	1458.88	0
SL	560.65	2	280.33	4503.4	0
Flow1*Flow2	15.39	9	1.71	27.48	0
Flow1*PT	7.15	6	1.19	19.14	0
Flow1*SL	66.87	6	11.15	179.05	0
Flow2*PT	1.31	6	0.22	3.52	0.0034
Flow2*SL	4.61	6	0.77	12.34	0
PT*SL	82.04	4	20.51	329.49	0
Error	5.98	96	0.06		
Total	7745.55	143			

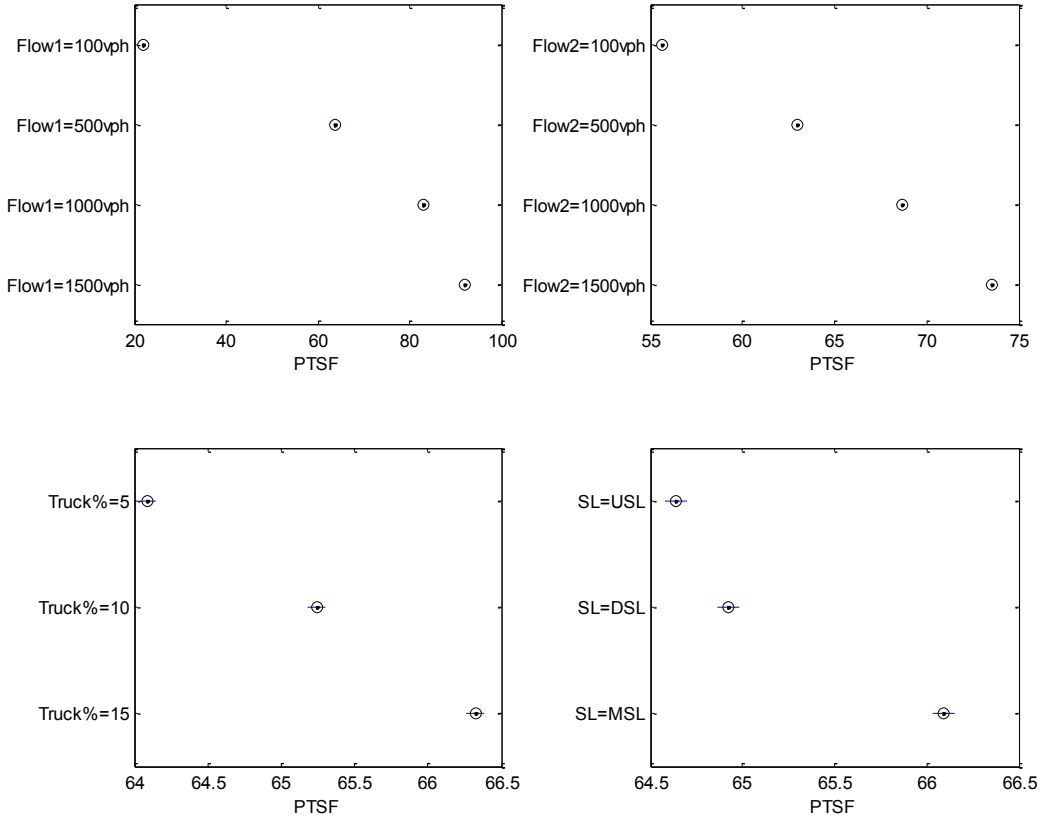

Figure 5-4- Multilevel comparison of factor effects on percent time spent following (PTSF)

Table 5-4- ANOVA table for percent time spent following (PTSF)

Source	Sum Sq.	d.f.	Mean Sq.	F	Prob>F
Flow1	105064.9	3	35021.6	204223.28	0
Flow2	6400	3	2133.3	12440.19	0
PT	120	2	60	349.89	0
SL	57	2	28.5	166.09	0
Flow1*Flow2	1072.8	9	119.2	695.08	0
Flow1*PT	4.1	6	0.7	3.97	0.0013
Flow1*SL	6.3	6	1	6.1	0
Flow2*PT	3.2	6	0.5	3.09	0.0081
PT*SL	10.1	4	2.5	14.71	0
Error	17.5	102	0.2		
Total	112755.7	143			

The overtaking rate is analyzed in three different categories: Overtaking rate between car and car (OTrate-carcar), overtaking rate between car and truck (OTrate-cartruck) and total overtaking rate. Since truck-truck and truck-car overtakes are scarce, they are omitted from the analysis. The ANOVA table for OTrate-carcar, presented in Table 5-5, demonstrates that all main effects and interactions are significant. As illustrated in Figure 5-5, OTrate-carcar increases nonlinearly with Flow1. This is due to the increased overtaking demand in the traffic stream. In an opposite way, an increase in Flow2 leads to decreased OTrate-carcar. This in an indication of reduced overtaking supply as volume in the opposing direction increases. Interestingly, higher PT resulted in lower number of car-car overtakes.

Table 5-5- ANOVA table for overtaking rate between car and car (OTrate-carcar)

Source	Sum Sq.	d.f.	Mean Sq.	F	Prob>F
Flow1	35283.4	3	11761.1	1654.91	0
Flow2	27056.6	3	9018.9	1269.04	0
PT	4338.5	2	2169.3	305.24	0
SL	2255.8	2	1127.9	158.7	0
Flow1*Flow2	8467.6	9	940.8	132.39	0
Flow1*PT	1941.2	6	323.5	45.53	0
Flow1*SL	1561.9	6	260.3	36.63	0
Flow2*PT	741.7	6	123.6	17.39	0
Flow2*SL	304.8	6	50.8	7.15	0
PT*SL	169.3	4	42.3	5.95	0.0003
Error	682.3	96	7.1		
Total	82803.1	143			

In addition, MSL resulted in lowest number of overtakes between cars. However, this trend is opposite for OTrate between car and trucks (Figure 5-6). OTrate-cartruck increases with percentage

truck. The highest number of overtakes between car and truck was observed when MSL was used. The effect of volumes (Flow1 and Flow2) on OTrate-cartruck is similar to that of carcar.

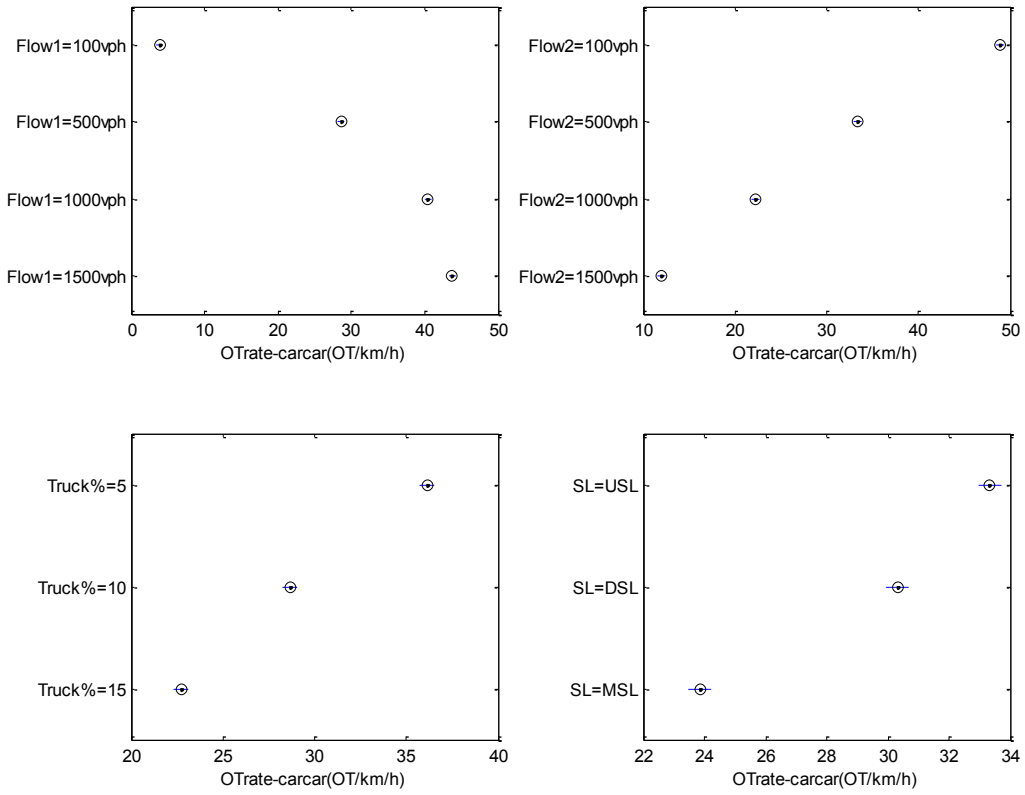

Figure 5-5- Multilevel comparison of factor effects on overtaking rate between car and car (OTrate-carcar)

Table 5-6- ANOVA table for overtaking rate between car and truck (OTrate-cartruck)

Source	Sum Sq.	d.f.	Mean Sq.	F	Prob>F
Flow1	7012.9	3	2337.64	296.43	2.14997e-48
Flow2	4908.5	3	1636.17	207.48	8.09517e-42
PT	1927	2	963.5	122.18	4.13057e-27
SL	3996.5	2	1998.27	253.4	5.02189e-39
Flow1*Flow2	1705.9	9	189.54	24.04	5.64865e-21
Flow1*PT	538.5	6	89.75	11.38	1.41402e-09
Flow1*SL	1329.4	6	221.57	28.1	3.73829e-19
Flow2*PT	458.9	6	76.49	9.7	2.46827e-08
Flow2*SL	993.7	6	165.61	21	1.3595e-15
PT*SL	452.7	4	113.19	14.35	3.20453e-09
Error	757	96	7.89		
Total	24081.2	143			

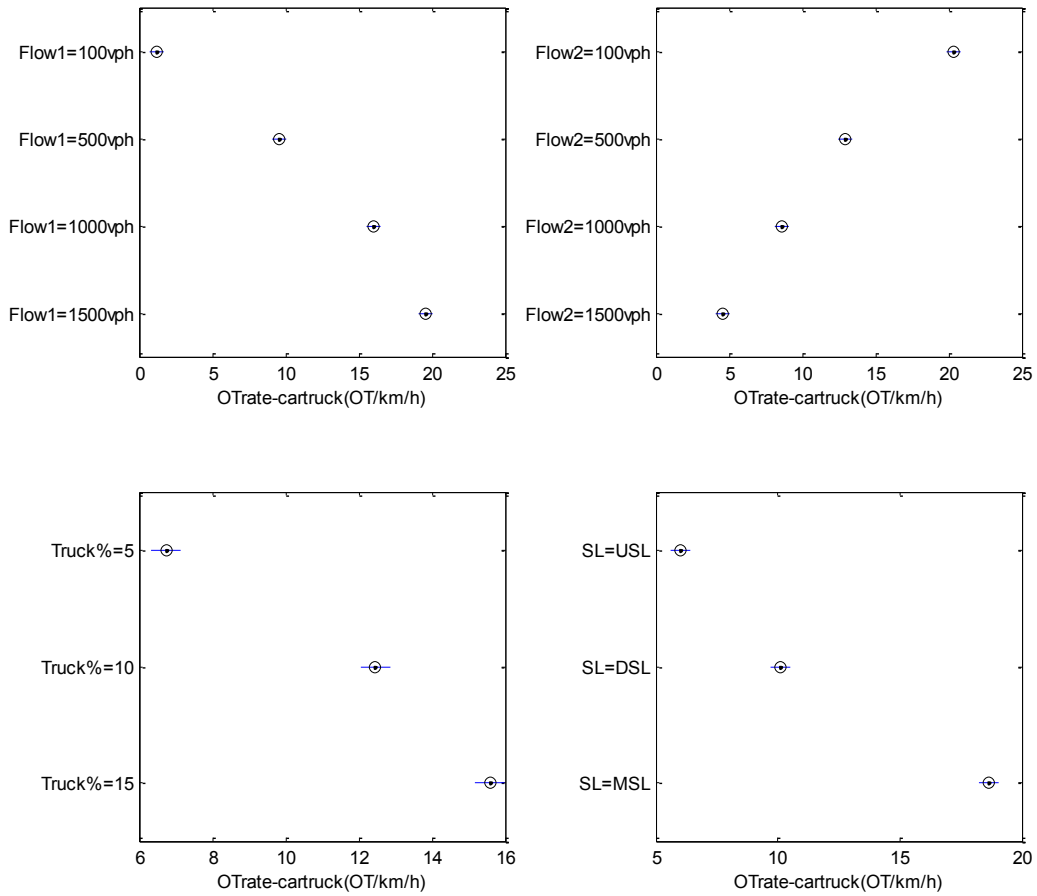

Figure 5-6- Multilevel comparison of factor effects on overtaking rate between car and truck (OTrate-cartruck)

The total overtaking rate is an aggregation of the two carcar and cartruck categories. As expected, the OTrate increases with Flow1 and decreases with Flow2. Total OTrate decreases with PT (similar to OTrate-carcar case) and is highest when MSL is used (similar to OTrate-cartruck case). For the three overtaking rate categories the effects are significant at all range of levels considered.

Table 5-8 presents the ANOVA table for average overtaking TTC. In this analysis, the main four effects and four interaction terms are significant. As illustrated in Figure 5-8, TTC increases with Flow1 volume. However, Flow2 has an opposite effect; i.e., TTC decreases sharply with initial increase in the opposing volume (from 100 to 500 vph). This is an indication of increased head-on risk when the opposing volume increases from low to middle range values. TTC remains almost constant with further increase in Flow2. Higher percentage truck led to higher TTC values for

overtakes. MSL scenario resulted in higher TTC values compared to USL and DSL. The difference between the effects of USL and DSL on TTC is not significant.

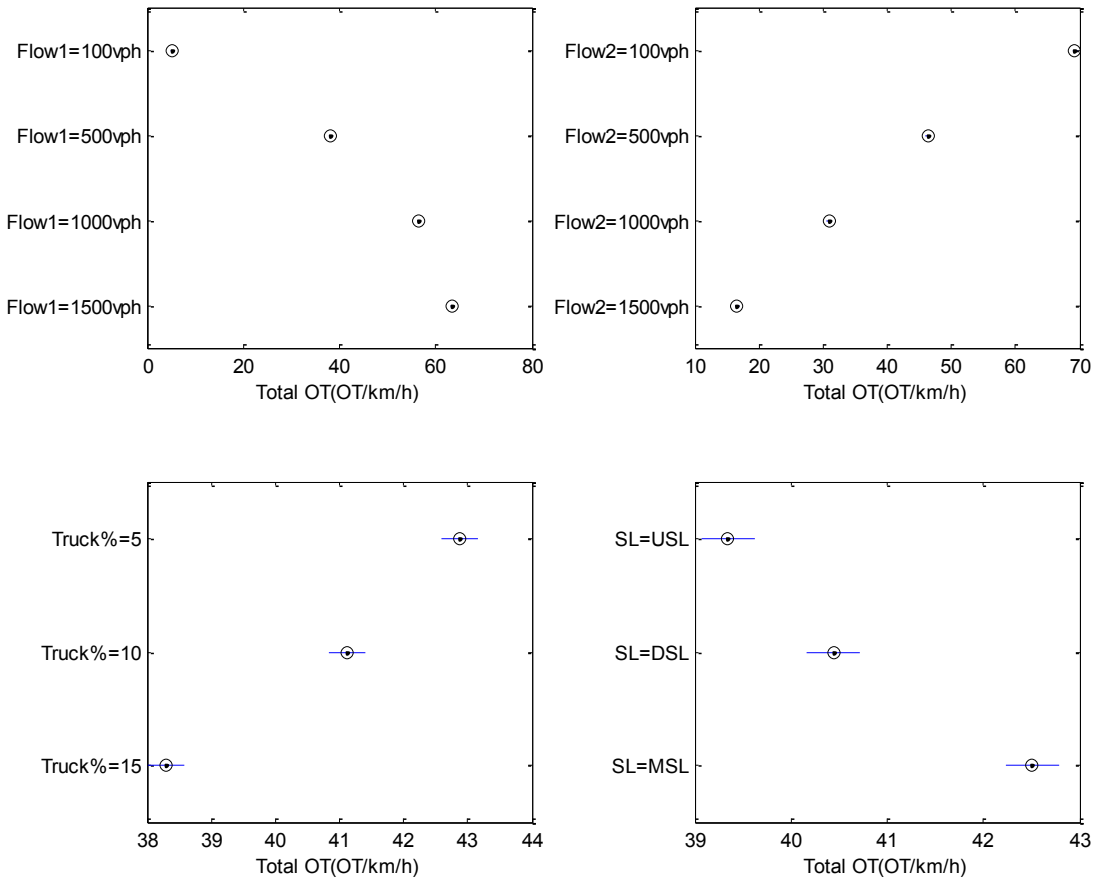

Figure 5-7- Multilevel comparison of factor effects on total overtaking rate (OTrate)

Table 5-7- ANOVA table for total overtaking rate (OTrate)

Source	Sum Sq.	d.f.	Mean Sq.	F	Prob>F
Flow1	73234.9	3	24411.6	6585.69	0
Flow2	54982.1	3	18327.4	4944.29	0
PT	513.1	2	256.6	69.21	0
SL	247.4	2	123.7	33.37	0
Flow1*Flow2	17722.9	9	1969.2	531.25	0
Flow1*PT	536.6	6	89.4	24.13	0
Flow1*SL	210.5	6	35.1	9.47	0
Flow2*PT	83.5	6	13.9	3.75	0.0021
Flow2*SL	228.8	6	38.1	10.29	0
PT*SL	80.9	4	20.2	5.46	0.0005
Error	355.9	96	3.7		
Total	148196.6	143			

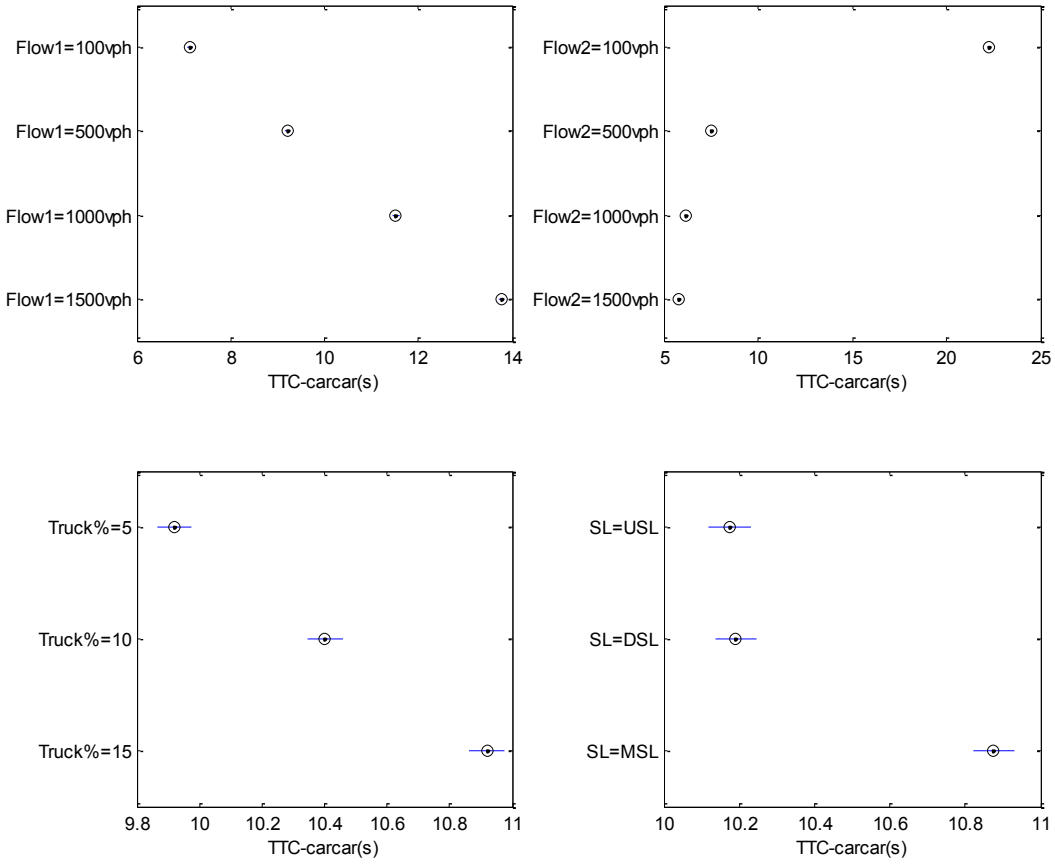

Figure 5-8- Multilevel comparison of factor effects on average time-to-collision (TTC)

Table 5-8- ANOVA table for average time-to-collision (TTC)

Source	Sum Sq.	d.f.	Mean Sq.	F	Prob>F
Flow1	892.9	3	297.63	1996.53	0
Flow2	6776.69	3	2258.9	15152.72	0
PT	23.96	2	11.98	80.35	0
SL	15.38	2	7.69	51.58	0
Flow1*Flow2	4.62	9	0.51	3.44	0.0009
Flow1*PT	6.84	6	1.14	7.65	0
Flow1*SL	3.18	6	0.53	3.55	0.003
Flow2*PT	4.4	6	0.73	4.92	0.0002
Error	15.8	106	0.15		
Total	7743.76	143			

Table 5-9 summarizes the effect of the four factors (Flow1, Flow2, PT, SL) on the six output measures. In the ANOVA analysis, all the main factors were found to have significant effect on all measures. The difference between all the factor levels was also significant with the exception of USL and DSL effect on TTC.

Table 5-9- Summary of the factors' effects on the output measures

Measures	Analysis direction flow (Flow1)	Opposing direction Flow (Flow2)	Percentage truck (PT)	Speed limit strategy from USL to DSL and MSL (SL)
Average travel speed (ATS)	-	-	-	-
Percent time spent following (PTSF)	+	+	+	+
Overtaking rate between car-car (OTrate-carcar)	+	-	-	-
Overtaking rate between car-truck (OTrate-cartruck)	+	-	+	+
Overtaking rate total (OTrate)	+	-	-	+
Time-to-collision (TTC)	+	-	+	+ (no difference between USL and DSL)

+/-: increase/decrease in the measure

5.6 Model Development

In the previous section, the ANOVA tables provided valuable information regarding the relationship between the independent variables and the measures in the study. In this section, mathematical models are developed to predict the changes in output measures (ATS, PTSF, OTrate, and TTC) as a function of input factors (Flow1, Flow2, PT, SL). In the regression analysis proposed here, speed limit strategy is treated as a nominal variable. The following polynomial function was found to be appropriate for estimating ATS as a function of independent variables.

$$ATS = a_0 + a_1\text{Flow1} + a_2\text{Flow2} + a_3\text{PT} + a_4\text{SL} + a_5\text{Flow1}\times\text{PT} + a_6\text{Flow1}^2 \quad \text{Eq. 5-2}$$

$$Adjusted\ R^2 = 0.972$$

Table 5-10 presents list of coefficients and the corresponding estimates, standard errors, t-Stats and p-Values. As it is shown, all variables are significant in the model. The adjusted R^2 corresponding to this model was 0.972 showing good model predictability. Figure 5-9 provides analysis of residuals for the regression. In this figure, three tests including residual plot, normal plot, and probability density plot are shown for this regression. The residuals are appeared to be randomly and normally distributed and no systematic trend is observed. Figure 5-10 illustrates actual (as per simulation) versus estimated (as per regression) for the ATS measure. As seen, MSL scenario significantly reduced ATS as compared to USL while the difference is slight when comparing USL and DSL.

Table 5-10- List of model coefficients from regression of ATS

Coefficient	Estimate	SE	t-Stat	p-Value
a_0	93.283	0.55146	169.16	5.3562e-160
a_1	-0.020685	0.00092277	-22.416	1.6486e-47
a_2	-0.0034309	0.00019347	-17.733	3.485e-37
a_3	-0.19571	0.044393	-4.4085	2.0962e-05
a_4_DSL	-1.0687	0.24936	-4.2855	3.4275e-05
a_4_MSL	-4.6165	0.24936	-18.513	5.493e-39
a_5	-0.00010121	4.739e-05	-2.1357	0.034496
a_6	5.7976e-06	4.7751e-07	12.141	1.9492e-23

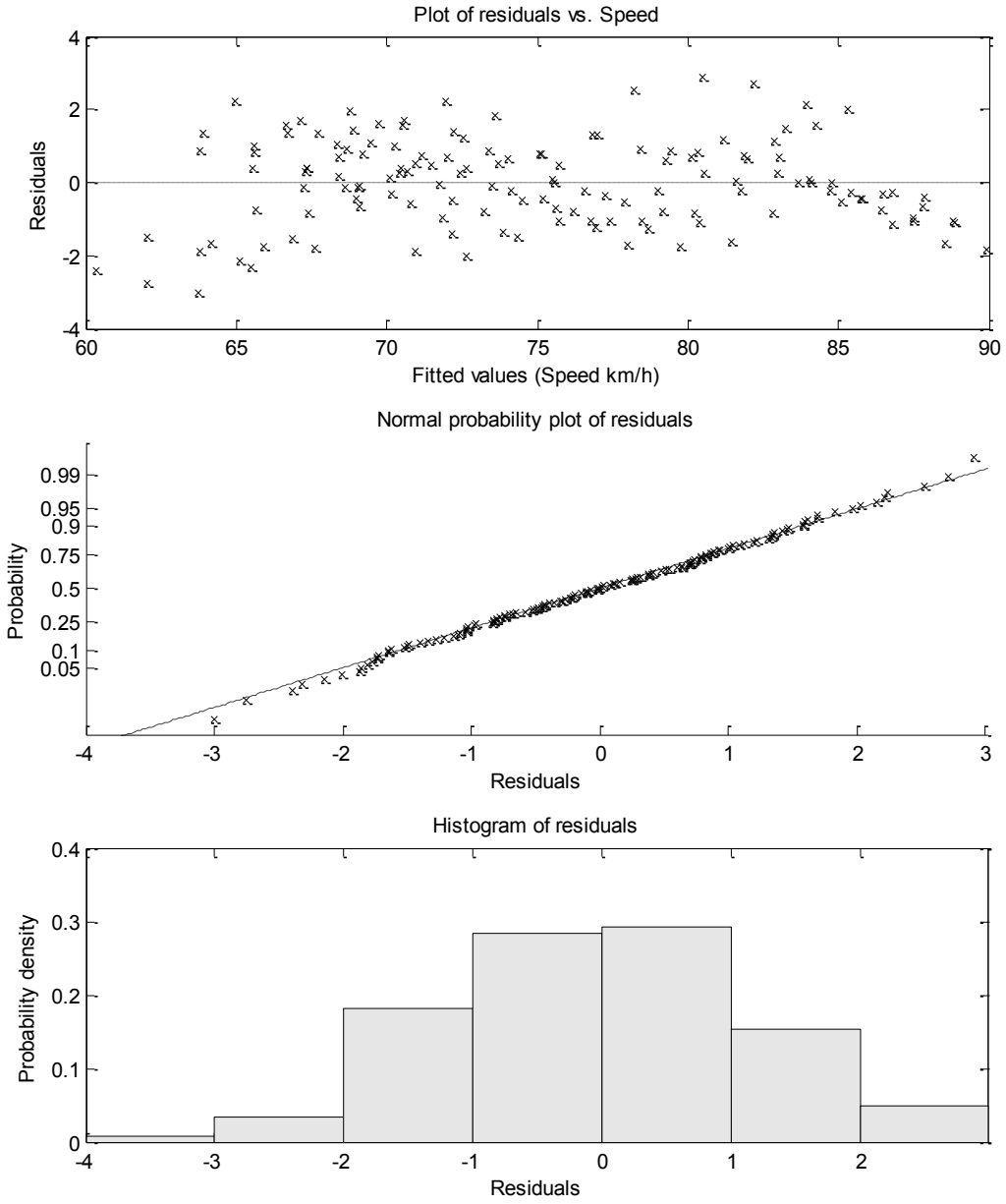

Figure 5-9- Analysis of residuals for ATS regression

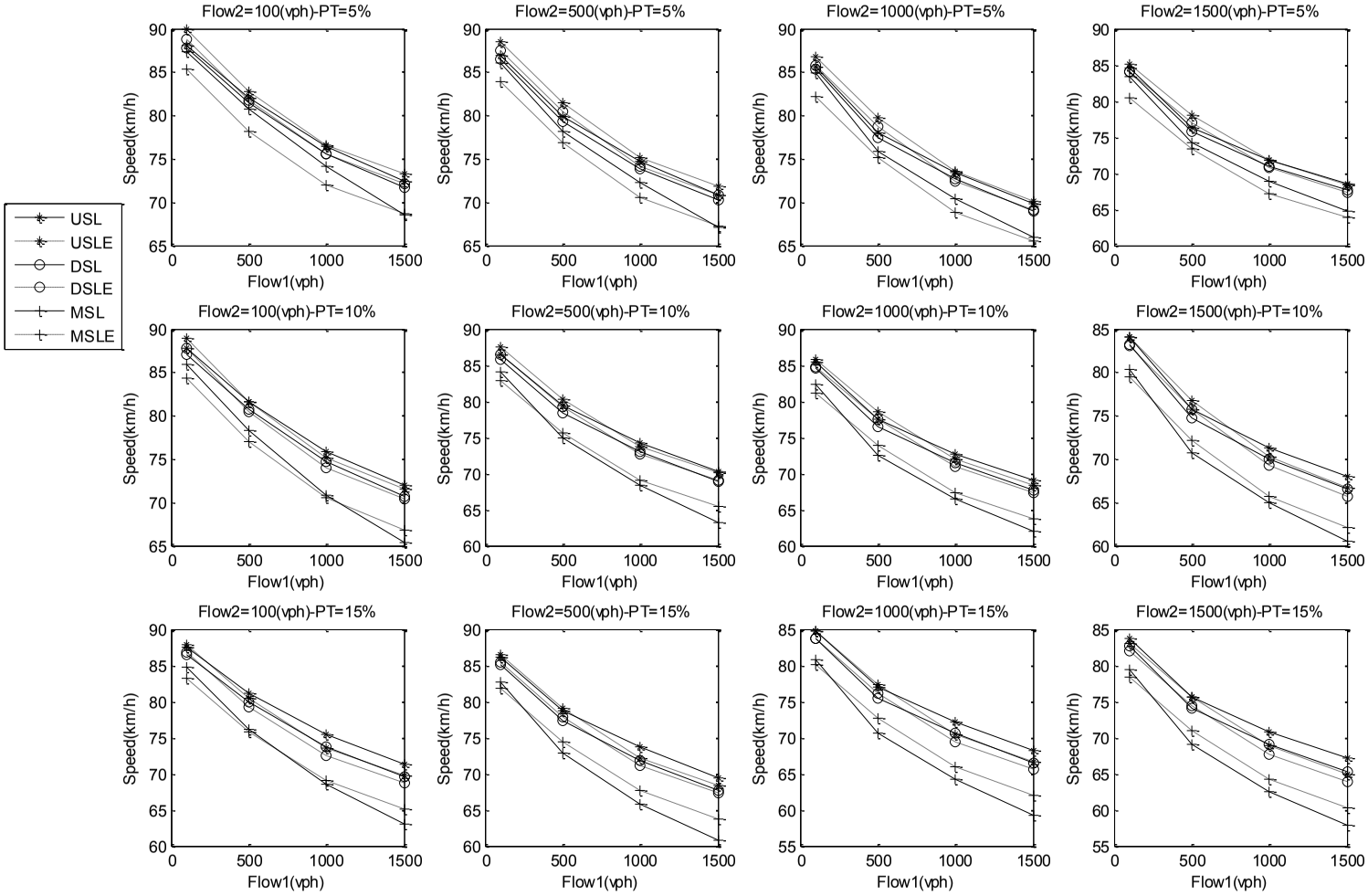

Figure 5-10- Actual versus estimated Average Travel Speed (ATS), letter "E" denotes "Estimated"

To model PTSF, a nonlinear form of function with exponential and polynomial expressions provides an appropriate fit for PTSF. Although the effect of percentage truck (PT) and speed limit type (SL) were found to be statistically significant, their contribution to PTSF was very marginal and, hence eliminated.

$$PTSF = 100(1 - \exp(a_0 \text{Flow1} \times \text{Flow2}^{a_1})) + a_2 \text{Flow1}^2 + a_3 \text{Flow2}^2 + a_4 \text{Flow1 Flow2} \quad \text{Eq. 5-3}$$

$$Adjusted\ R^2 = 0.996$$

Table 5-11 presents list of coefficients estimated for PTSF. As shown, all variables are significant in the model. The adjusted R^2 corresponding to this model was 0.996 showing good model predictability. Figure 5-11 provides analysis of residuals for regression of PTSF. The residuals are appeared to be randomly and normally distributed without any systematic trend. Figure 5-12 illustrates actual versus estimated PTSF.

Table 5-11- List of model coefficients from regression of PTSF

Coefficient	Estimate	SE	t-Stat	p-Value
a_0	-0.00053427	2.6365e-05	-20.265	2.4854e-43
a_1	0.19986	0.0084433	23.671	1.2923e-50
a_2	1.3273e-06	2.7736e-07	4.7854	4.3079e-06
a_3	6.0507e-06	2.861e-07	21.149	2.7784e-45
a_4	-8.4521e-06	4.934e-07	-17.13	4.514e-36

Similar to ATS a polynomial function is used to represent overtaking rates between cars (OTratecarcar) i.e.:

$$OTrate - carcar = a_0 + a_1 \text{Flow1} + a_2 \text{Flow2} + a_3 \text{SL} + a_4 \text{Flow1} \times \text{Flow2} + a_5 \text{Flow1} \times \text{PT} +$$
$$a_6 \text{Flow1} \times \text{SL} + a_7 \text{Flow1}^2 + a_8 \text{Flow1} \times \text{Flow2} \times \text{PT} + a_9 \text{Flow1} \times \text{Flow2} \times \text{SL} +$$
$$a_{10} \text{Flow1} \times \text{PT} \times \text{SL} + a_{11} \text{Flow1}^2 \times \text{Flow2} + a_{12} \text{Flow1}^2 \times \text{PT} + a_{13} \text{Flow1} \times \text{Flow2}^2 \quad \text{Eq. 5-4}$$
$$+ a_{14} \text{Flow1}^3$$

$$Adjusted\ R^2 = 0.991$$

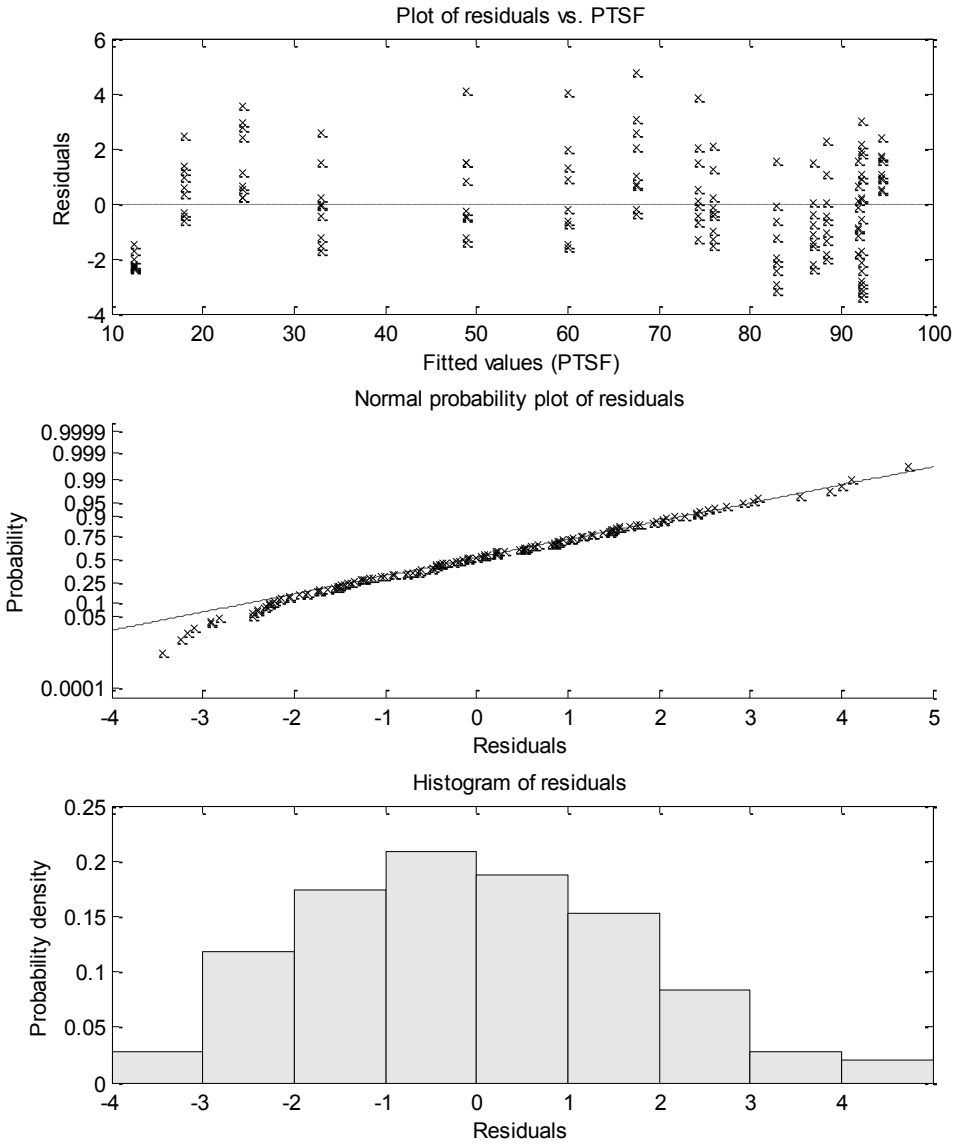

Figure 5-11- Analysis of residuals for PTSF regression

Table 5-12 presents list of coefficients for OTratecarcar regression. The adjusted R^2 corresponding to this model was 0.991 showing good model predictability. Figure 5-14 provides analysis of residuals for this variable. The residuals are appeared to be randomly and normally distributed without any systematic trend. Figure 5-14 illustrates actual versus estimated OTratecarcar. As seen, the effect of differential speed limit is to reduce number of overtakes between cars. This reduction is more significant with MSL scenario.

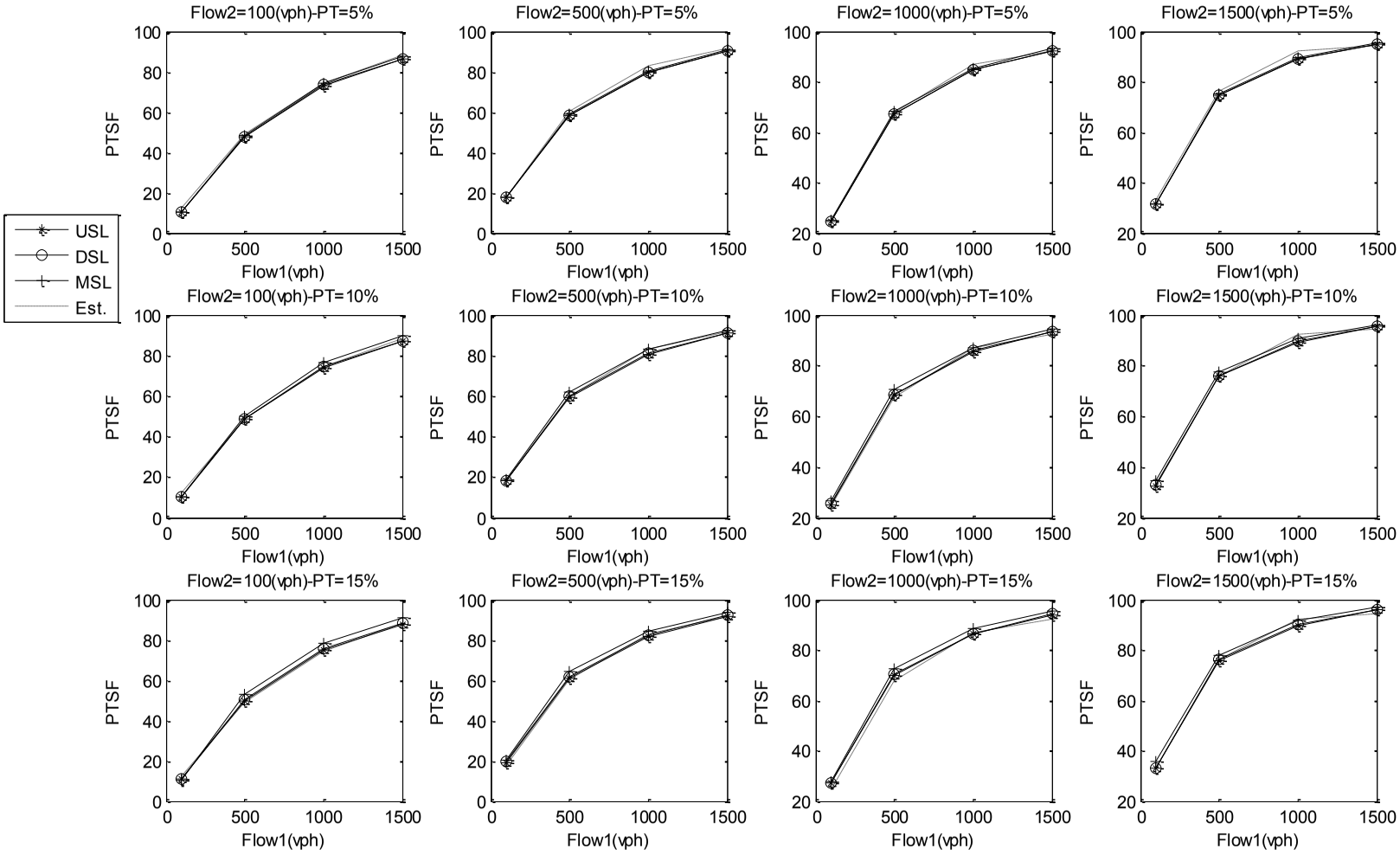

Figure 5-12- Actual versus estimated Percent Time Spent Following (PTSF), "Est." denotes "Estimated"

Table 5-12- List of model coefficients from regression of OTratecarcar

Coefficient	Estimate	SE	t-Stat	p-Value
a_0	-7.7377	1.0534	-7.3452	2.3244e-11
a_1	0.18901	0.005308	35.609	2.7079e-67
a_2	0.0020794	0.00088848	2.3404	0.020846
a_3_DSL	0.21341	0.82147	0.25979	0.79545
a_3_MSL	1.9814	0.82147	2.412	0.017316
a_4	-9.5645e-05	3.35e-06	-28.551	1.3032e-56
a_5	-0.0028748	0.00022844	-12.585	5.7634e-24
a_6_DSL	-0.0047532	0.0016587	-2.8656	0.0048845
a_6_MSL	-0.014908	0.0016587	-8.9876	3.313e-15
a_7	-9.2714e-05	6.7993e-06	-13.636	1.6865e-26
a_8	1.3046e-06	9.3615e-08	13.936	3.2355e-27
a_9_DSL	2.8375e-06	9.3615e-07	3.031	0.0029631
a_9_MSL	9.2383e-06	9.3615e-07	9.8684	2.4574e-17
a_{10}_DSL	-0.00016184	0.00012066	-1.3413	0.18226
a_{10}_MSL	-0.00070516	0.00012066	-5.8442	4.1517e-08
a_{11}	2.2073e-08	1.6793e-09	13.145	2.5501e-25
a_{12}	3.3931e-07	1.5526e-07	2.1854	0.030726
a_{13}	1.0992e-08	9.4328e-10	11.653	1.0678e-21
a_{14}	1.8451e-08	2.6835e-09	6.8756	2.6182e-10

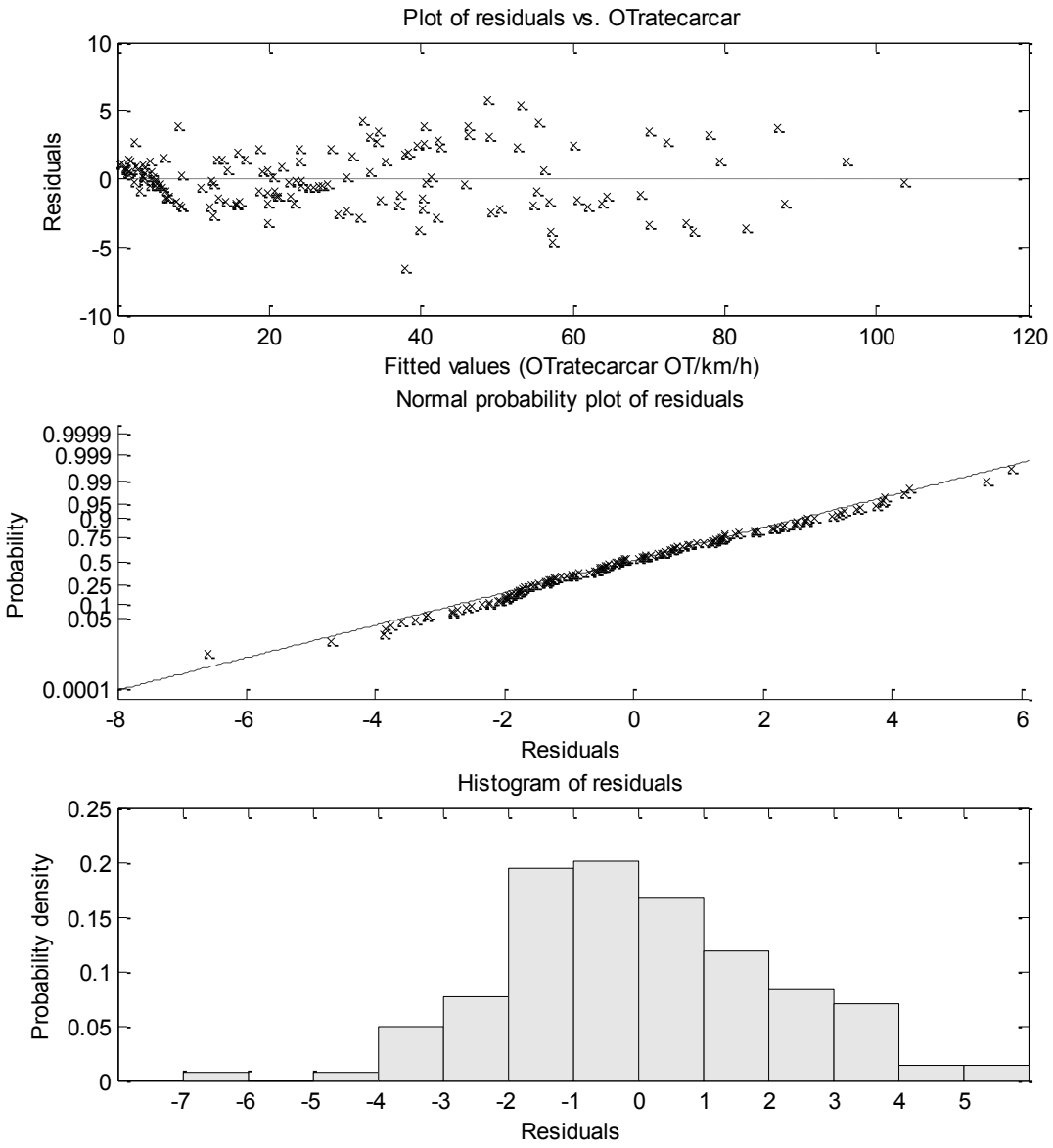

Figure 5-13- Analysis of residuals for OTratecarcar regression

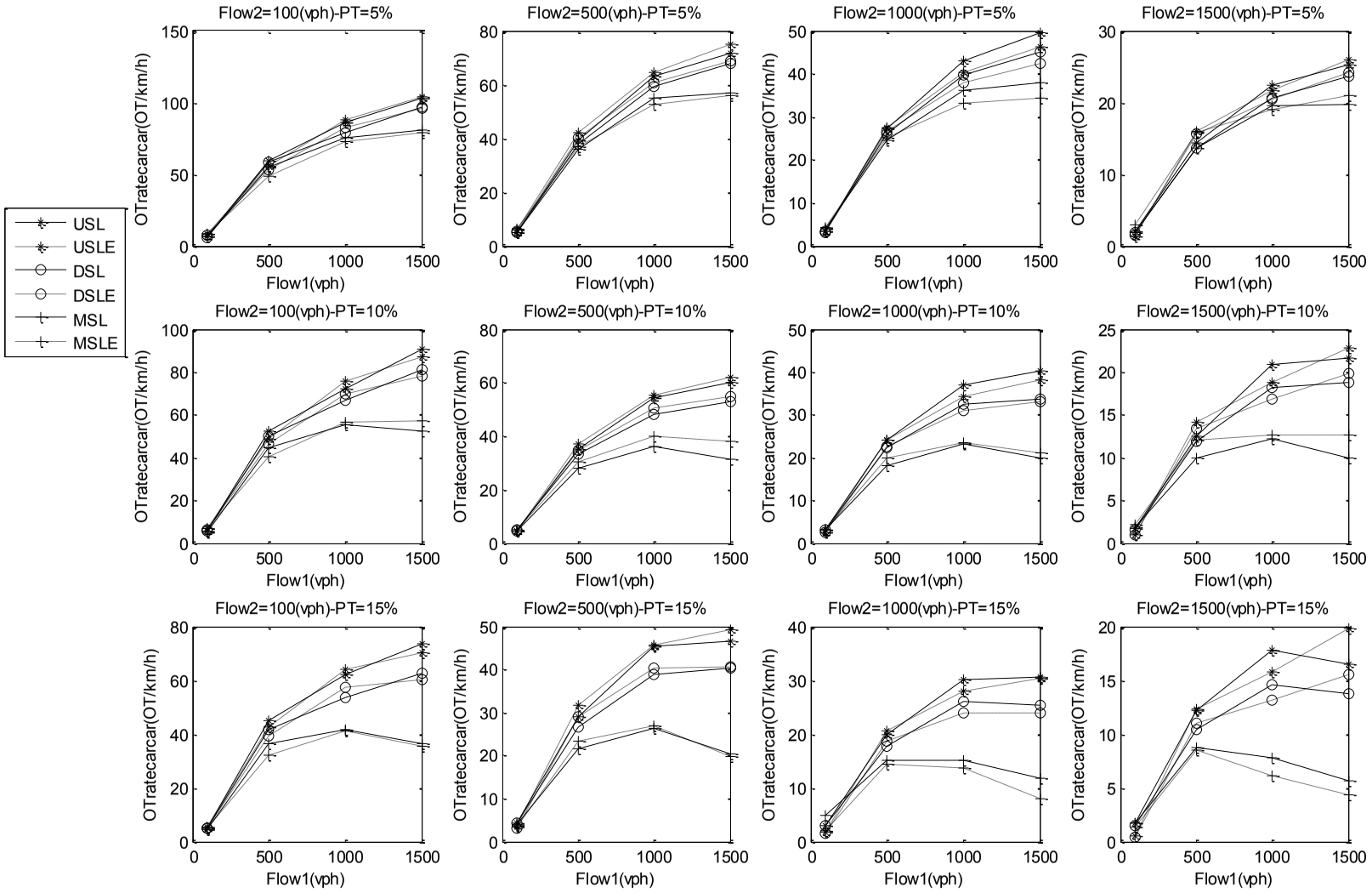

Figure 5-14- Actual versus estimated OTcarcar rate, letter "E." denotes "Estimated"

The regression model to represent overtaking rates between car and truck (OTratecartruck) is given as:

$$OTrate-cartruck = a_0 + a_1\text{PT} + a_2\text{Flow1}\times\text{PT} + a_3\text{Flow1}\times\text{SL} + a_4\text{Flow2}\times\text{SL} + a_5\text{Flow1}\times\text{Flow2}\times\text{PT} + a_6\text{Flow1}\times\text{Flow2}\times\text{SL} + a_7\text{Flow1}\times\text{PT}\times\text{SL} + a_8\text{Flow1}^2\times\text{PT} + a_9\text{Flow2}^2\times\text{SL} + a_{10}\text{Flow1}\times\text{Flow2}\times\text{PT}\times\text{SL} + a_{11}\text{Flow1}^2\times\text{Flow2}\times\text{SL} + a_{12}\text{Flow1}^2\times\text{PT}\times\text{SL} \quad \text{Eq. 5-5}$$

$$Adjusted\ R^2 = 0.97$$

The adjusted R^2 associated with this model is 0.97. Table 5-13 provides the list of coefficients used in the regression, which were found to be statistically significant. Figure 5-15 illustrates the residuals analysis for this regression. The residuals appear to be normally distributed, although with presentation of some outliers. Figure 5-16 illustrates estimation of OTratecartruck variable as obtained from the regression versus simulated values. The impact of differential speed limit strategies

Table 5-13- List of model coefficients from regression of OTratecartrcuk

Coefficient	Estimate	SE	t-Stat	p-Value
a_0	1.5616	0.6471	2.4132	0.017287
a_1	-0.16189	0.070477	-2.297	0.023309
a_2	0.0016784	0.00018637	9.0057	3.3487e-15
a_3_DSL	0.0065971	0.0016394	4.024	9.925e-05
a_3_MSL	0.011895	0.0016394	7.2558	3.9242e-11
a_4_DSL	-0.0051564	0.0019599	-2.631	0.0096015
a_4_MSL	-0.010976	0.0019599	-5.6003	1.3277e-07
a_5	-6.9301e-07	5.5823e-08	-12.414	1.9336e-23
a_6_DSL	-9.6287e-06	3.6015e-06	-2.6735	0.0085246
a_6_MSL	-2.2036e-05	3.6015e-06	-6.1185	1.16e-08
a_7_DSL	0.0010561	0.00028045	3.7656	0.00025616
a_7_MSL	0.0040122	0.00028045	14.306	6.1139e-28
a_8	-3.0721e-07	1.1518e-07	-2.6672	0.0086772
a_9_DSL	3.4572e-06	1.2899e-06	2.6801	0.0083675
a_9_MSL	7.8779e-06	1.2899e-06	6.1072	1.2245e-08
a_{10}_DSL	-8.9708e-08	1.5789e-07	-0.56816	0.57096
a_{10}_MSL	-8.5495e-07	1.5789e-07	-5.4148	3.0907e-07
a_{11}_DSL	4.3948e-09	2.0668e-09	2.1263	0.035475
a_{11}_MSL	1.1549e-08	2.0668e-09	5.588	1.4051e-07
a_{12}_DSL	-5.6868e-07	1.7729e-07	-3.2076	0.0017063
a_{12}_MSL	-1.7896e-06	1.7729e-07	-10.094	8.0633e-18

(DSL and MSL) is to increase number of overtakes between car and trucks. The effect of percentage truck is also to increase number of overtakes for this variable. These findings are also accordance with the ANOVA study presented in the previous section.

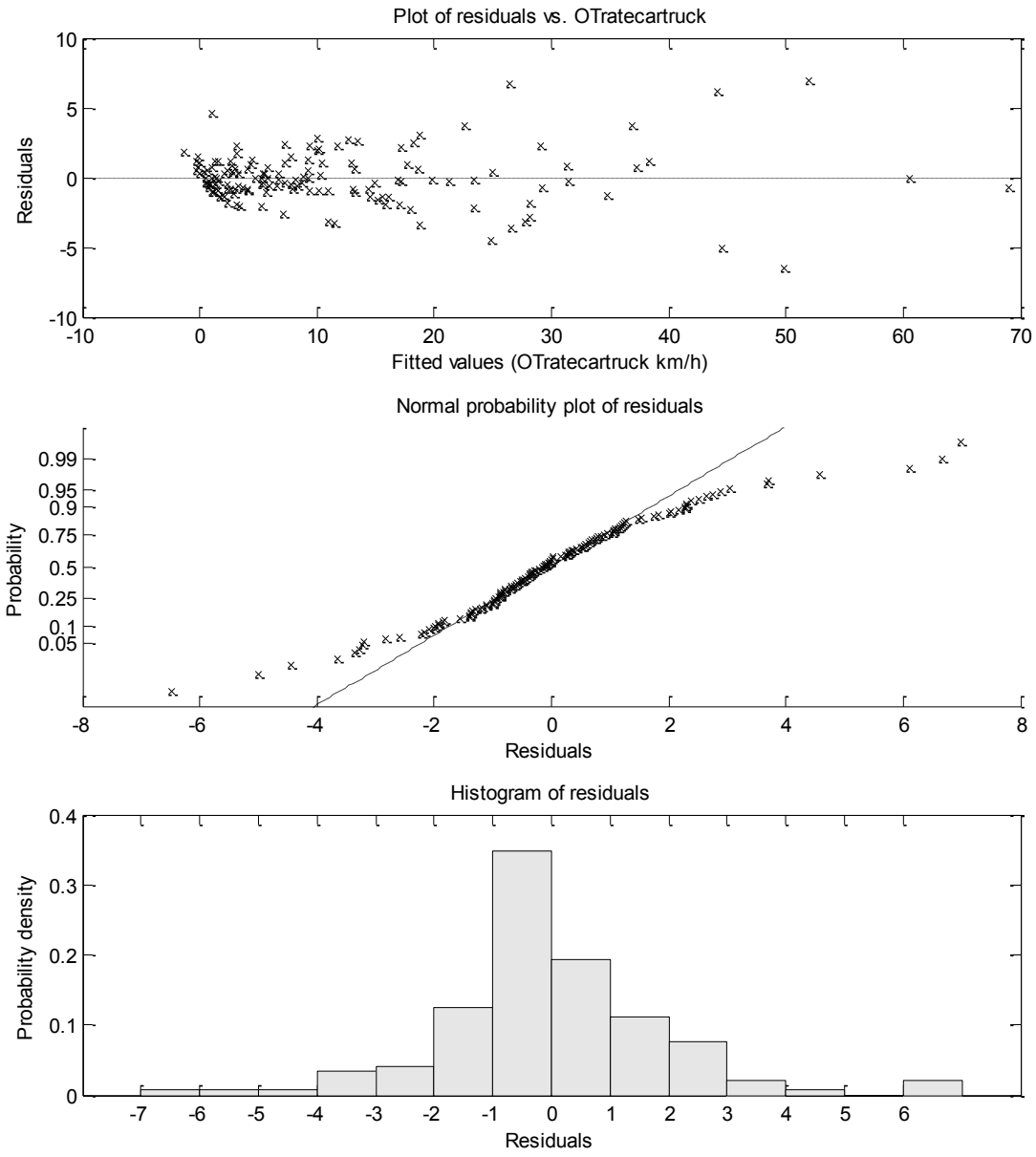

Figure 5-15- Analysis of residuals for OTratecartruck regression

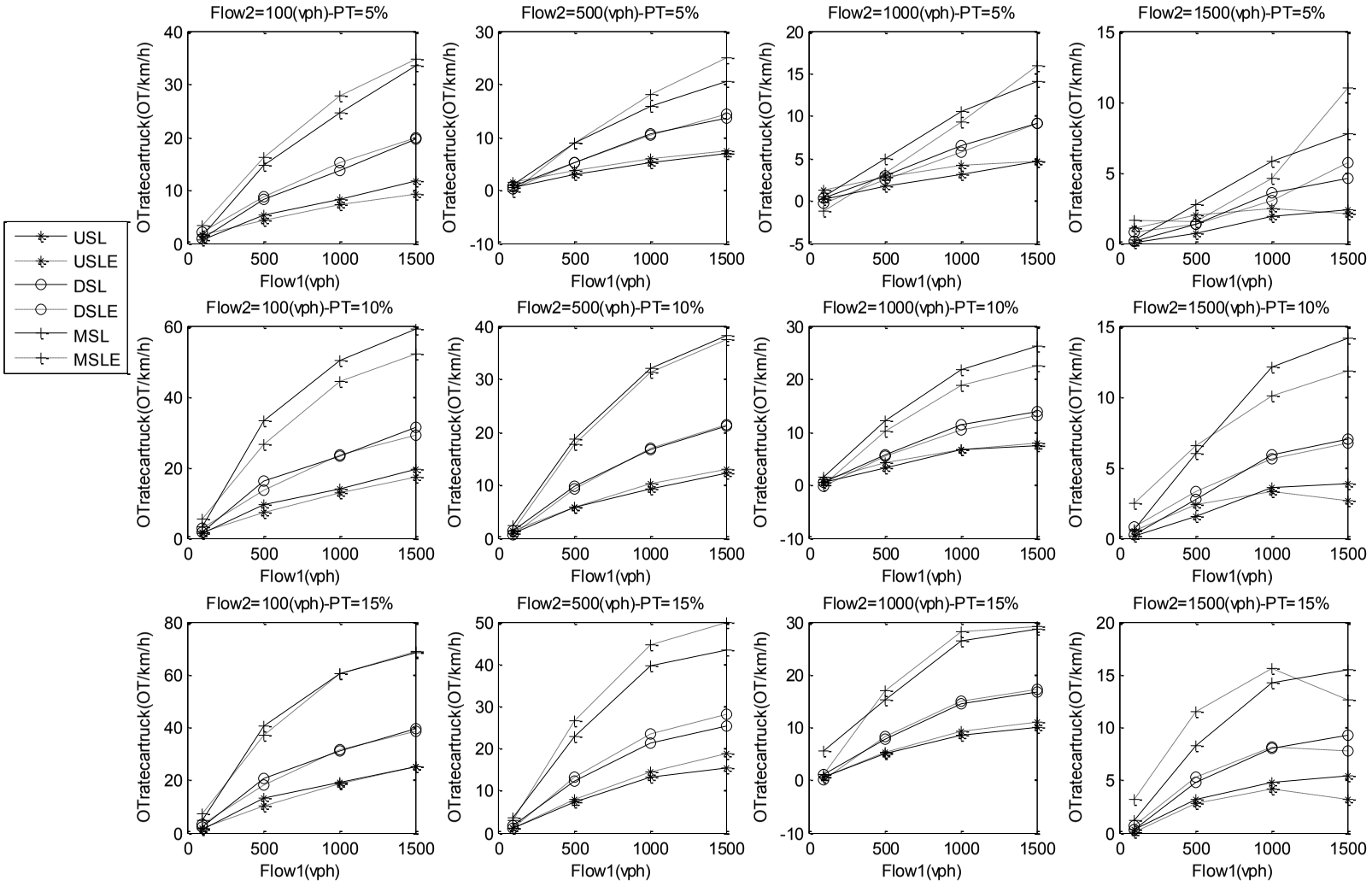

Figure 5-16- Actual versus estimated OTcartrcuk rate, letter "E." denotes "Estimated"

A similar polynomial equation form is used to model total overtaking rate. This model yielded adjusted R^2 of 0.97. Table 5-14 shows the corresponding coefficient values for this model. As shown in Figure 5-17, residuals are normally distributed with no systematic trend. As ANOVA study showed previously, the total overtaking rate is slightly higher for differential speed limits. This is opposite for percentage of trucks; i.e., higher number of trucks in the traffic stream led to fewer number of overtakes.

$$OTrate = a_0 + a_1 \text{Flow1} + a_2 \text{Flow1} \times \text{Flow2} + a_3 \text{Flow1} \times \text{PT} + a_4 \text{Flow2} \times \text{PT} + a_5 \text{Flow1} \times \text{SL} + a_6 \text{PT} \times \text{SL} + a_7 \text{Flow1}^2 + a_8 \text{Flow2} \times \text{PT} \times \text{SL} + a_9 \text{Flow1}^2 \times \text{Flow2} + a_{10} \text{Flow1} \times \text{Flow2}^2 + a_{11} \text{Flow1}^2 \times \text{SL} + + a_{12} \text{Flow1}^3 \quad \text{Eq. 5-6}$$

$$Adjusted\ R^2 = 0.97$$

Table 5-14- List of model coefficients from regression of total OTrate

Coefficient	Estimate	SE	tStat	pValue
a_0	-10.443	1.2168	-8.5826	2.7944e-14
a_1	0.20182	0.0070517	28.62	3.154e-57
a_2	-0.0001094	3.7669e-06	-29.043	6.2528e-58
a_3	-0.0010049	9.9792e-05	-10.07	6.8371e-18
a_4	0.0003986	9.4034e-05	4.2389	4.2852e-05
a_5_DSL	0.0024046	0.0040311	0.59652	0.55189
a_5_MSL	0.012911	0.0040311	3.2029	0.0017198
a_6_DSL	0.07616	0.1301	0.5854	0.55932
a_6_MSL	0.52098	0.1301	4.0045	0.00010511
a_7	-0.00010268	9.5245e-06	-10.781	1.2177e-19
a_8_DSL	-9.2075e-05	0.00011151	-0.82572	0.41051
a_8_MSL	-0.00046743	0.00011151	-4.1919	5.1454e-05
a_9	2.8038e-08	2.0241e-09	13.852	3.7072e-27
a_{10}	1.7118e-08	1.3498e-09	12.681	2.5727e-24
a_{11}_DSL	-9.7177e-07	2.634e-06	-0.36893	0.7128
a_{12}_MSL	-9.3327e-06	2.634e-06	-3.5431	0.0 0055401
a_{13}	2.054e-08	3.84e-09	5.3488	3.9841e-07

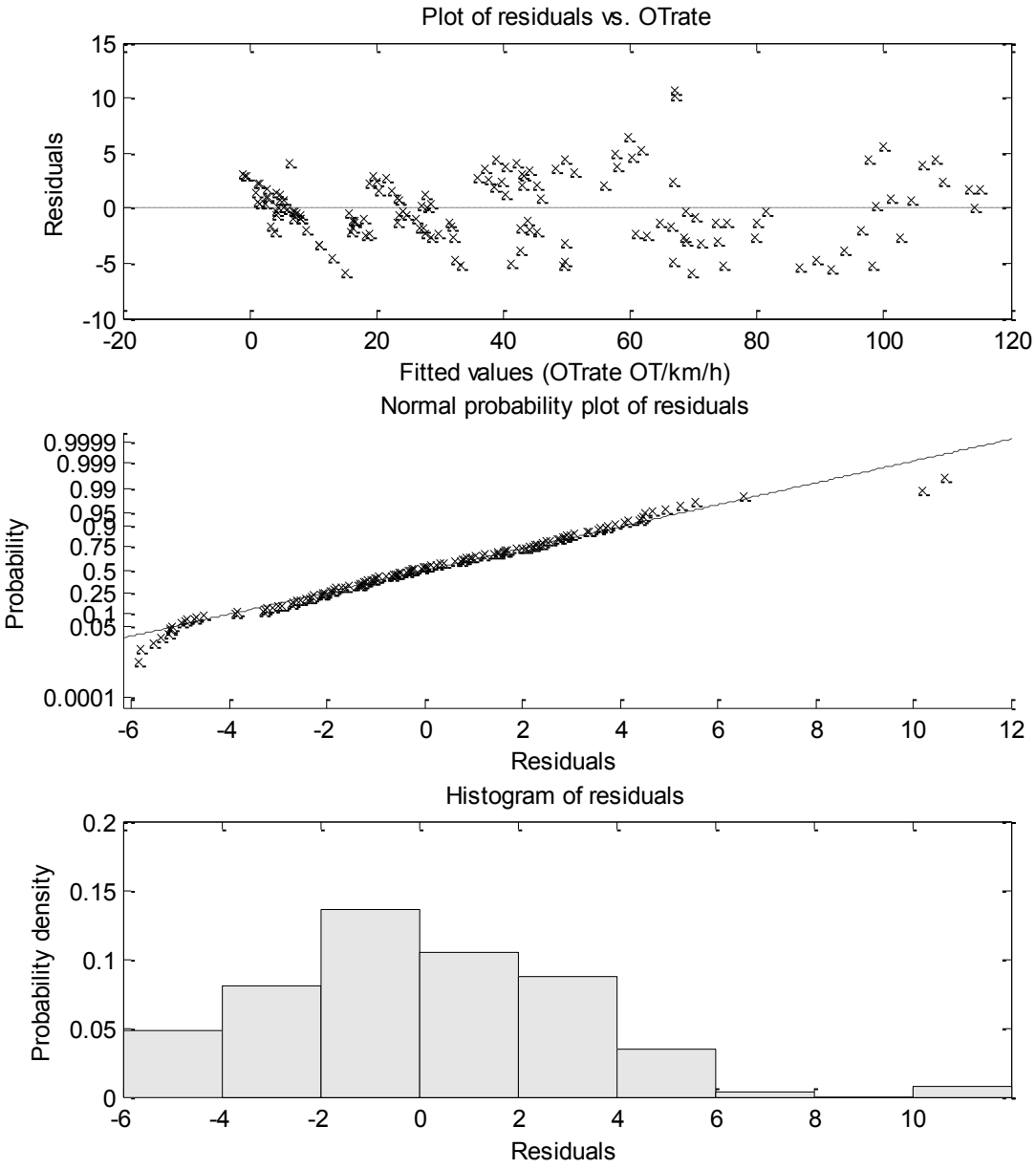

Figure 5-17- Analysis of residuals for total OTrate regression

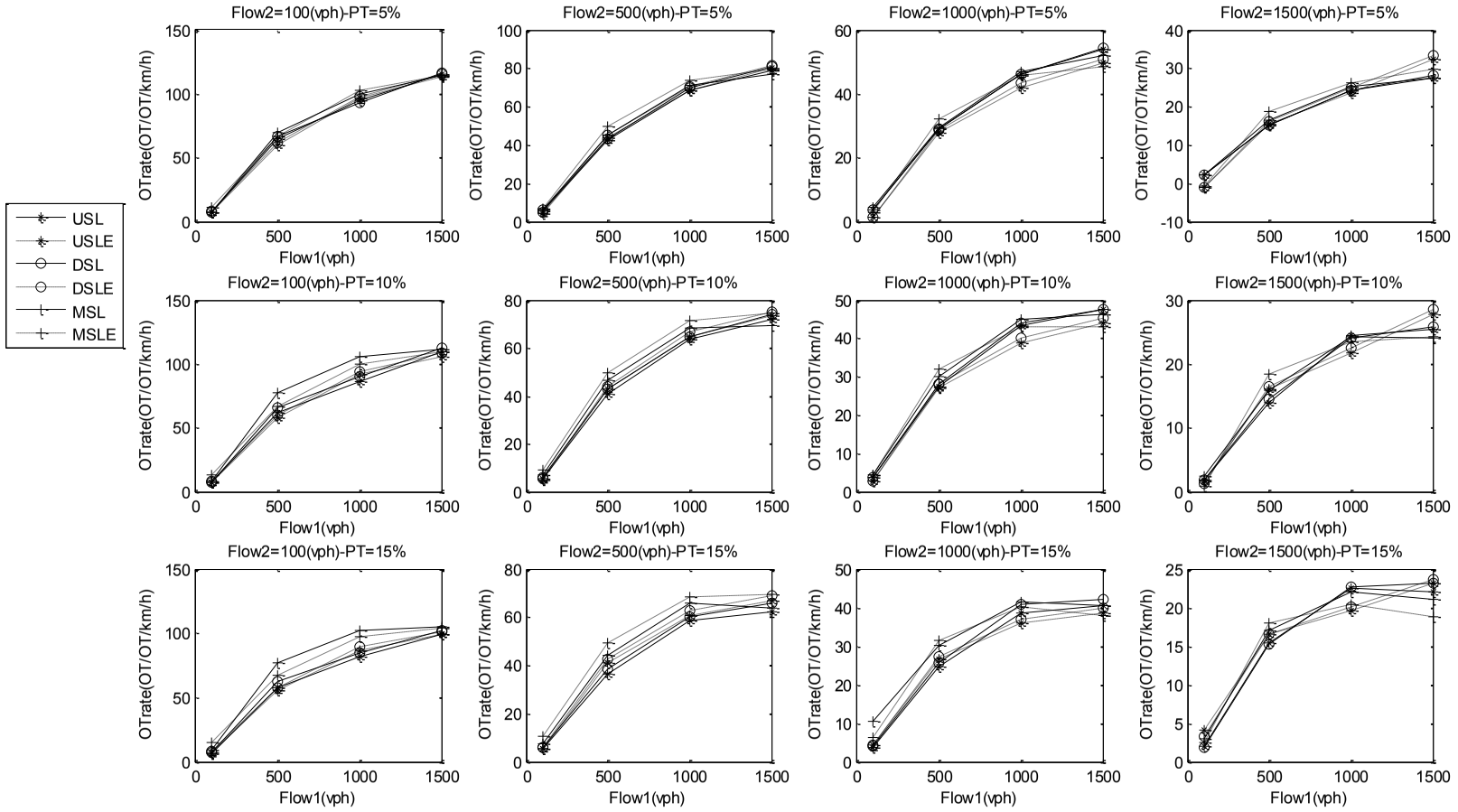

Figure 5-18- Actual versus estimated total OTrate, letter "E." denotes "Estimated"

A nonlinear equation is used as a regression model for TTC with adjusted $R^2 = 0.991$ representing a good predictability property of the model. Table 5-15 presents the list of coefficients for this variable. The SL variable is not in the proposed model since the effect of speed limit was to increase TTC marginally. Figure 5-19 shows the residual analysis for this regression. TTC estimated versus simulated is illustrated in Figure 5-20.

$$TTC = a_0 + a_1\text{Flow1} + a_2 Flow2^{a_3} + a_4\text{PT} \qquad \text{Eq. 5-7}$$

$$Adjusted\ R^2 = 0.991$$

Table 5-15- List of model coefficients from regression of TTC

Coefficient	Estimate	SE	t-Stat	p-Value
a_0	0.62208	0.23167	2.6852	0.0081308
a_1	0.0047059	0.00010258	45.875	7.8218e-86
a_2	6457.4	1806.4	3.5747	0.00048265
a_3	-1.281	0.062575	-20.472	8.6055e-44
a_4	0.10746	0.013222	8.1273	2.1582e-13

5.7 Discussion of Results

In summary, it can be concluded that ATS decreases with volume of both directions. This is due to increased interactions between vehicles in the analysis direction and reduced overtaking opportunities in the opposing direction when volume is increased. The increased number of trucks in the traffic stream is also contributing to lower speeds. This is mainly due to the fact that trucks desired speeds are normally lower than that of cars. The MSL showed highest impact on reducing the average travel speed. PTSF increases with volume, reflecting higher number of rear-end interactions between overtaking and overtaken vehicles. The effect of percentage truck and differential speed limit is to increase PTSF, although marginal. Overtaking rate increases with analysis flow and decreases with opposing flow. The impact of speed limit scenarios on overtaking rate is twofold. Differential speed limit decreases number of car-car overtakes while increases number of car-truck overtakes. The effect of slower moving trucks in DSL and MSL seems to be acting as a kind of speed calming factor on the traffic stream resulting in fewer interactions between cars (resulting in fewer car-car overtakes) while creating more interactions between cars and trucks (resulting in more car-truck overtakes). In a similar way, percentage truck decreases/increases car-car/car-truck overtakes, respectively. The total

overtake rate is statistically higher for differential speed limit strategies although very marginal. TTC drops rapidly with initial increases in opposing volume. This is a reflection of increased head-on risk. The effect of speed control strategies and truck percentage on TTC is negligible. Two-dimensional multi-level comparison graphs for the above analysis are provided in Appendix C. From these graphs, one can determine the effect of each factor at different level of another factor(s) e.g. effect of speed limit strategies at different volumes.

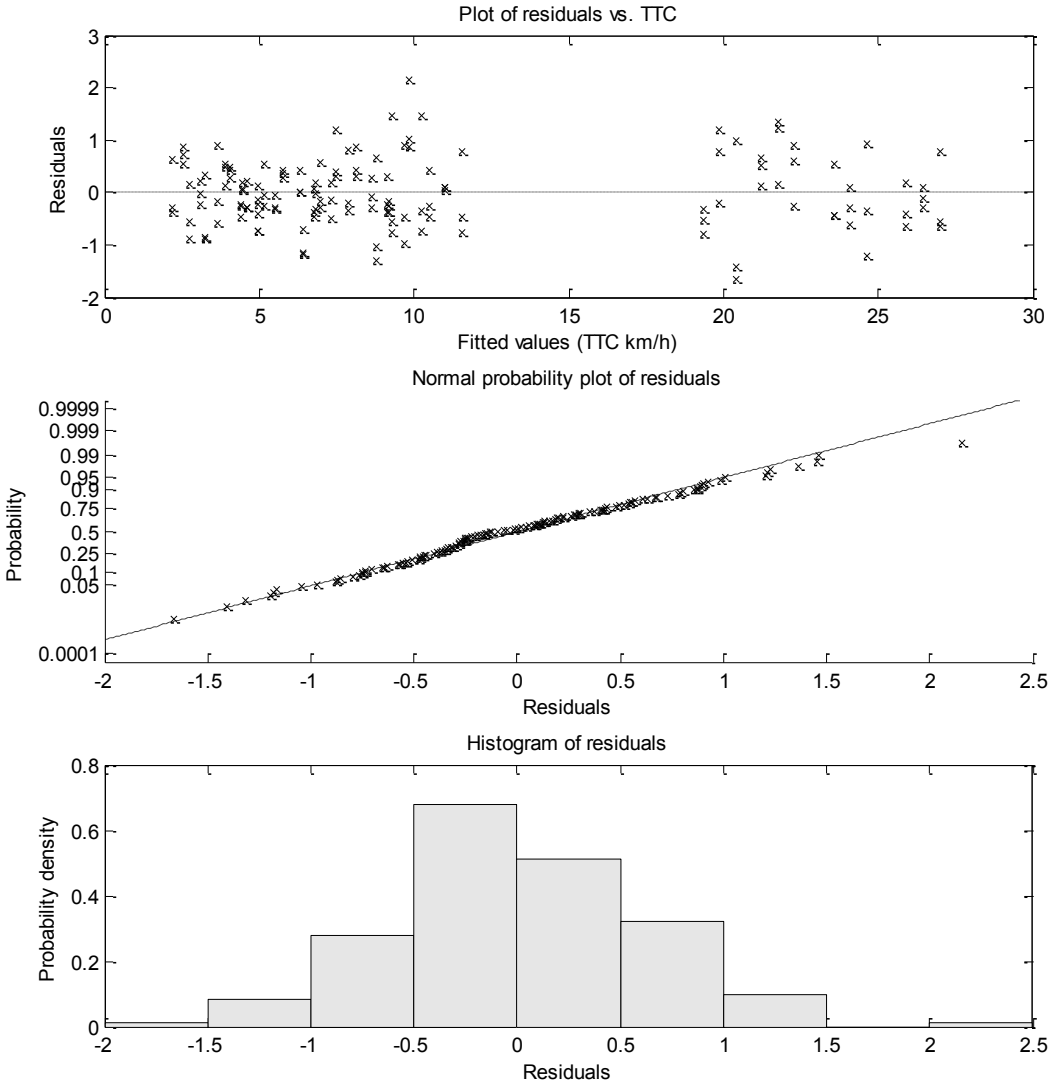

Figure 5-19- Analysis of residuals for TTC regression

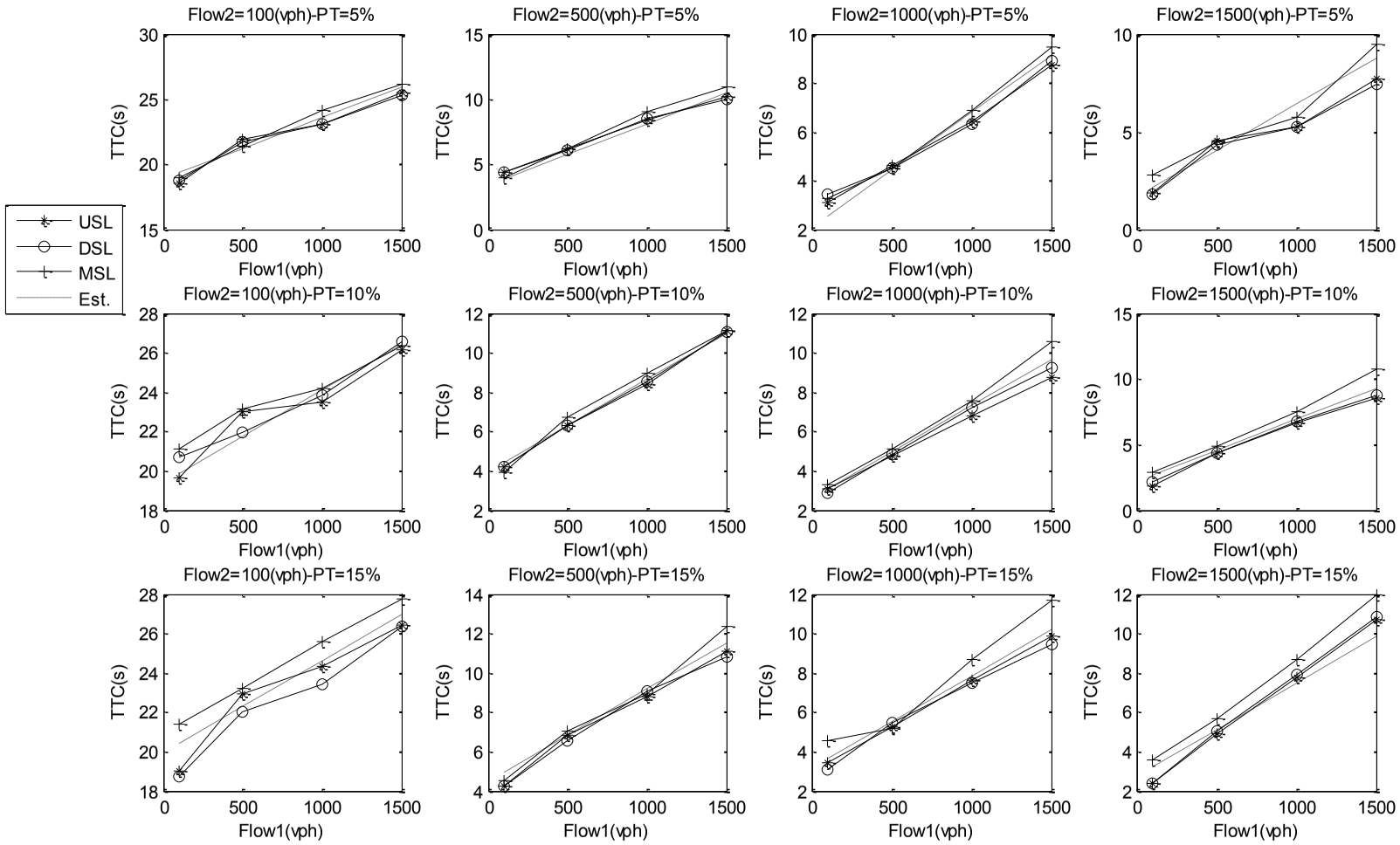

Figure 5-20- Actual versus estimated TTC, letter "Est." denotes "Estimated"

5.8 Conclusion

In this chapter, the traffic and safety implications of car-truck differential speed limit (DSL), truck mandated speed limits (MSL), and uniform speed limits (USL) were investigated. Differential speed limit strategies (DSL and MSL) reduced the average travel speed of the traffic stream. This is associated with increased traffic delay. No significant effect was observed concerning differential speed control strategies and PTSF. Although differential speed strategies (DSL and MSL) were observed to have a minimal increase in the total number of overtake maneuvers, the effect on the nature of the overtakes; i.e., car-car versus car-truck was significant. Differential speed strategies increased the rate of car-truck overtakes over the range of volumes considered in this analysis. This suggests a negative effect on safety resulting from differential speed strategy applied to two-lane rural highways. On a positive side, DSL and MSL strategies reduced the number of car-car overtakes at different volumes, hence increasing safety. This latter relationship suggests a calming effect of slower trucks on the speed of the traffic stream, which results in fewer interactions between cars. TTC sharply dropped with increases in the opposite volume. Similar to PTSF, the impact of differential speed limit strategies on TTC was minimal. For the cases that differential speed limit contributed to significant changes to the traffic and safety measures, the impact of MSL was larger than that of DSL.

Chapter 6
The Impact of Adaptive Cruise Control on Overtaking Maneuver (Model Application 3)

6.1 Introduction

A number of in-vehicle driving systems have been recently introduced to increase safety and reliability of vehicles. Stability control, blind spot detection, lane keeping, collision avoidance, and adaptive cruise control (ACC) are some examples of these systems. An ACC system is intended to maintain a safe distance between the following and the preceding (lead) vehicle through space adjustment in a car-following situation. In the absence of any preceding vehicle, ACC acts as the standard cruise control system to keep the speed of the vehicle at a user preset speed. The system makes use of radar technology to detect the vehicle in front and switch from speed control to space control mode if necessary.

The objective of this section is to assess the traffic and safety implication of adaptive cruise control for two-lane highway operations especially those related to overtaking maneuver. The traffic and safety indicators are evaluated using OTSIM. Safety and traffic performance are evaluated using the following indicators: average travel speed (ATS), percent time spent following (PTSF), overtaking rate (OTrate), and time-to-collision (TTC) of the overtaking vehicle to the opposing vehicle prior to return to normal travel lane.

6.2 Literature Review

Rear-end collision account for a large percentage of total accidents and this is known to be highly dependent on human factors. The ACC can help reduce this type of accidents by providing safe time headway between vehicles in the traffic stream. In addition, ACC with low headway thresholds can increase road's capacity. The first generation of ACC was introduced in Japan and Europe in 1997 (Watanabe et al., 1995) and then became available in North America (Fancher et al., 1997; Reichart et al., 1996; Woll, 1997). Currently, vehicles from different manufacturers come with an optional laser based adaptive cruise control system.

A number of studies have been conducted to evaluate the impact of ACC on comfort, safety, and traffic flow. Touran et al. (1998) used simulation and found that the probability of accidents between ACC controlled vehicles and leading vehicles can be significantly reduced while ACC slightly

increased the probability of accidents between ACC vehicles and their non-ACC following vehicles. Liang and Peng (1999) found that the vehicles equipped with ACC can contribute to improved average speed and reduced average acceleration. These can be translated to improved traffic flow and lower fuel consumption and smoother rides. Bose and Ioannou (2001) found that air pollution can be reduced by 60%, if 10% of vehicles are equipped with ACC. In Marsden et al. (2001), ACC showed reduction in the standard deviation of acceleration of the following vehicles between 44% and 52%. This indicated ACC contributed to better driving comfort and reduced fuel consumption. A more detailed discussion of ACC impacts on safety and traffic are provided in Vahidi and Eskandarian (2003).

In spite of these findings, the potential impacts of ACC on two-lane two-way highway traffic operation are not well understood. On one hand, larger headways can reduce the risk of rear-end accidents between the lead and following vehicles. This is especially beneficial when the following vehicle desires to overtake and tend to keep shorter headways than he/she would normally do in a following situation. On the other hand, the increased initial overtaking headway can increase the overtaking time (time spent by the overtaken vehicle to pull-out, pass, and return to normal travel lane) and cause other types of safety issues such as increased risk of head-on collision. To date, there is no research investigating the possible influence of ACC on overtaking maneuver safety.

6.3 Car-following Model

As discussed in section 2.7.2 of the thesis, OTSIM makes use of two car-following models. The first model, which is used for simulation of normal car-following driving is a collision avoidance type model borrowed from the Gipps car-following formulation. The car-following model, which is aimed to maintain a fixed time-headway between lead and following vehicles in the adaptive cruise control system, is borrowed form Ioannou and Chien (1993) model. In this mode of driving, the ACC system adjusts the speed of the following vehicle such that a constant time-gap is maintained between the lead and following vehicles. Ioannou and Chien (1993) provided a stable control law for the ACC system. In this model, the speed differential between the lead and following vehicles is denoted as:

$$\Delta_n^v = v_n - v_{n-1} \qquad \text{Eq. 6-1}$$

and the spacing error is defined as:

$$\delta_n^x = x_n - x_{n-1} - L_{n-1} - hv_n \quad \text{Eq. 6-2}$$

where,

h =desired time-gap as determined in ACC system

The control law can be represented such that:

$$a_n = \frac{1}{h}(\Delta_n^v + \lambda\delta_n^x) \quad \text{Eq. 6-3}$$

where,

a_n = acceleration/deceleration of the following vehicle in ACC headway control mode

λ = model parameter

To illustrate the difference between the two car-following models, a pair of lead and following vehicles is simulated in a car-following situation. The initial speed of the lead and following vehicles are assumed to be 70 and 80 km/h respectively and the initial distance between the two vehicles is 100 meters. The lead vehicle keeps the constant speed of 70 km/h for about 100 seconds and then decelerates to 57 km/h. Then, after about 50 seconds, it accelerates to the speed of around 77 km/h. The following vehicle changes its speed based on the two car-following model formulations, accordingly. The model parameters (default), used for simulation of the two models, are presented in Table 6-1.

Figure 6-1 illustrates the results of the Gipps car-following model simulation for the two simulated vehicles. At the beginning, the following vehicle decelerates slowly to match the speed of the lead vehicle. Afterward, the two vehicles continue with the same speed until the time that the lead vehicle starts decelerating. The following vehicle accordingly uses an appropriate deceleration, based on the Gipps car-following rule, to match the speed of the lead vehicle again. Finally, acceleration of the lead vehicle causes the following vehicle to react and accelerate accordingly. As shown, in the Gipps model, the equilibrium time-headway between the two vehicles is shorter at higher speeds.

Figure 6-2 illustrates the simulation results for the same pair of vehicles in a car-following situation using the ACC car-following rule with desired time-headway of 2 seconds ($h = 2s$). Similarly, the following vehicle was able to track the speed of the lead vehicle by choosing appropriate

acceleration/deceleration. As opposed to the Gipps model, the ACC always kept a 2-second headway to the lead vehicle at different speeds.

Table 6-1- Default parameters used in the simulation of the Gipps and ACC car-following models

Parameter	$a_n^{max}(m/s^2)$	$d_n^{max}(m/s^2)$	$\hat{d}_{n-1}(m/s^2)$	$L_{n-1}(m)$	$T(s)$	$s(m)$
Gipps	1.7	-3	-3	4.9	1	2
Parameter	$h(s)$			$\lambda(1/s)$		
ACC	2			0.2		

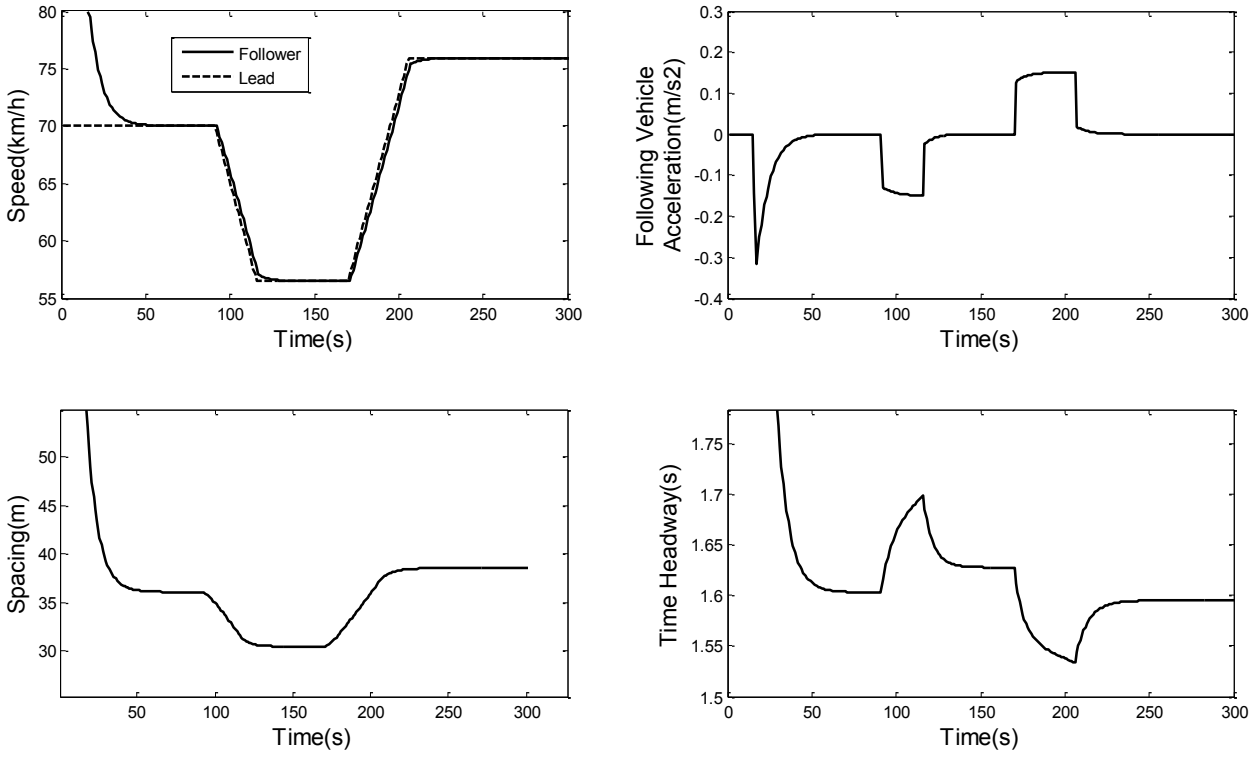

Figure 6-1- Simulation of a lead-following pair interaction (Gipps car-following model)

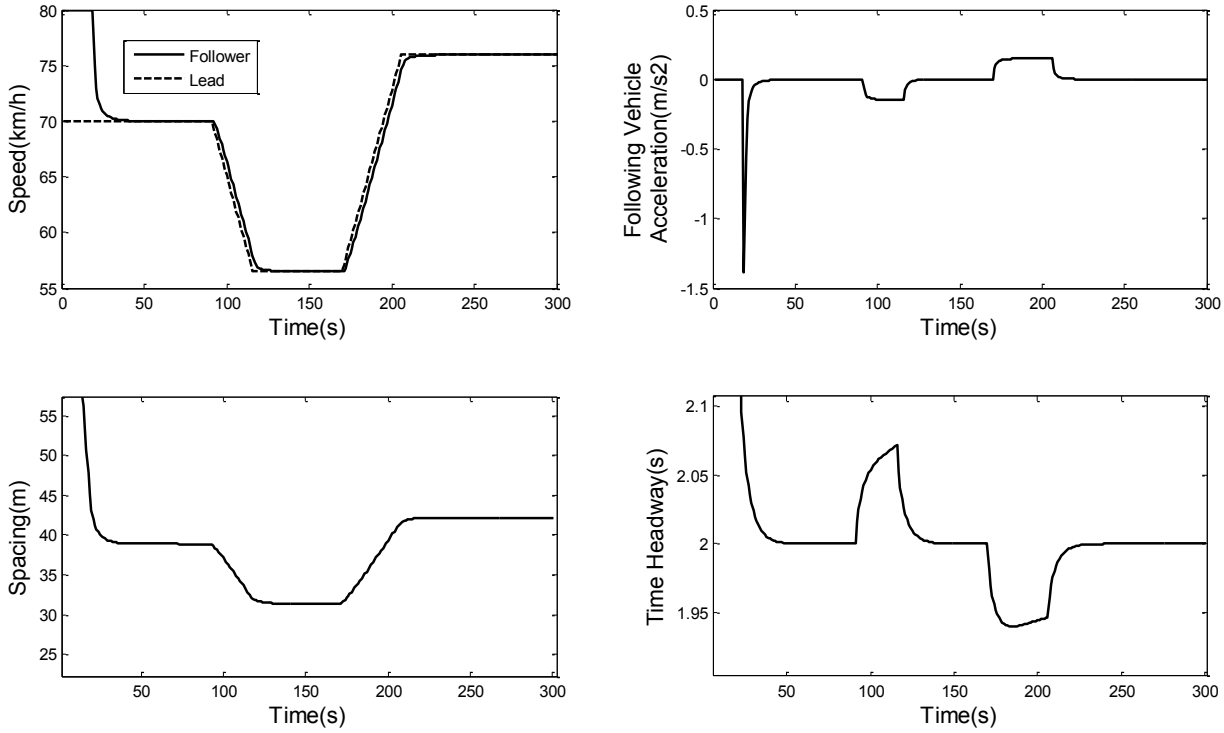

Figure 6-2- Simulation of a lead-following pair interaction (ACC car-following model)

6.4 Effect of Adaptive Cruise Control on Overtaking Time and Distance

As shown in calculation of the overtaking time (T_{OT}) in section 3.4.1, the initial headway between the overtaking and overtaken vehicle (HW^{init}) is one of the influencing variables in calculation of overtaking time and distance. This variable is the key point in assessing the effect of ACC on overtaking maneuver. The ACC system is supposed to keep this headway between overtaking and overtaken vehicles at a preset value. In this section, a sensitivity analysis is conducted to determine the effect of different ACC headway thresholds (h) in estimation of the overtaking time and distance. Three headways of 1, 1.5, and 2 seconds are tested, where the corresponding initial space headway is given by:

$$HW^{init} = hv_n \qquad \text{Eq. 6-4}$$

where, $v_n =$ speed of overtaking vehicle

Using Eq. 3-9, T_{OT} and D_{OT} can be calculated for a given HW^{init}. Figure 6-3 illustrates the changes in overtaking distance and time as a function of time-gap headway threshold for four posted speeds. As can be seen, the overtaking duration and distance increase linearly when time-gap headway is increased. Moreover, as expected, higher speeds resulted in larger overtaking time and distance. This directly reduces the resultant TTC which was assumed to be central in the decision to overtake logic in our model. Once an available TTC gap is small, the gap may not be accepted by drivers or if accepted the resultant TTC will be short and unsafe. Therefore, depending on effect of ACC on TTC (decrease or increase depending on the headway threshold), the number of accomplished overtakes and their average TTC can be influenced significantly. This can be evaluated and quantified through OTSIM simulation of traffic when ACC is in effect. The following section provides details about the simulation case study and its results.

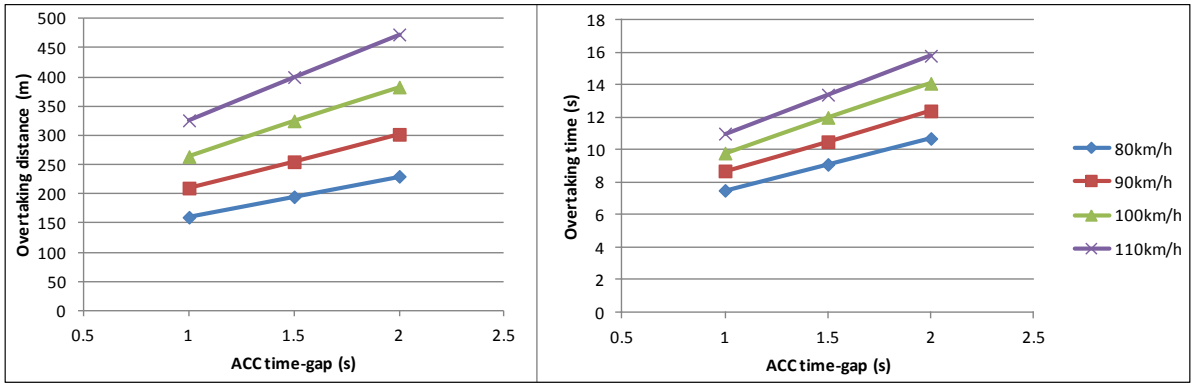

Figure 6-3- Overtaking time and distance vs. time-gap headway threshold in ACC system

6.5 Case-study and Simulation Inputs

Here, we report on the results of a simulation case study carried out for a six kilometers segment of a two-lane highway with overtaking permitted in both directions. A simulation experimental design consists of four factors including analysis direction flow (Flow1), opposing direction flow (Flow2), ACC headway threshold (HW), and ACC penetration rate among vehicles (PenRate). Table 6-2 presents the list of the four factors with the corresponding level values. An assumption is made that overtaking drivers keep ACC active before and during the overtaking process. However, the overtaking driver can exceed his/her cruise speed when passing; i.e., the desired overtaking speed can be higher than the cruise speed (if required). In addition, the driver can also use his/her manual comfortable acceleration during the passing phase. Average travel speed (ATS), percent time spent

following (PTSF), overtaking rate (OTrate), and time-to-collision (TTC) are obtained from each simulation run.

Table 6-2-Factors included in the experimental design

Variable Name	Flow1 (vph)	Flow2 (vph)	HW (s)	PenRate (%)
Level values	100, 700, 1300	100, 700, 1300	1, 1.5, 2	20, 60, 100

6.6 Analysis of Variance

Table 6-3 presents the results of ANOVA test for ATS. As seen all the main and interaction factors are statistically significant except Flow2*HW and Flow2*PenRate. Figure 6-4 illustrates a multiple comparison graph based on Tukey's honestly significant difference criterion. As shown, all the four factors at all levels show significant effect on ATS. ATS decreases with increase in both Flow1 and Flow2 factors. As ACC headway threshold increases, ATS decreases. Higher penetration rate resulted in lower average travel speed. The relationship between penetration rate and headway threshold with average travel speed appears to be linear.

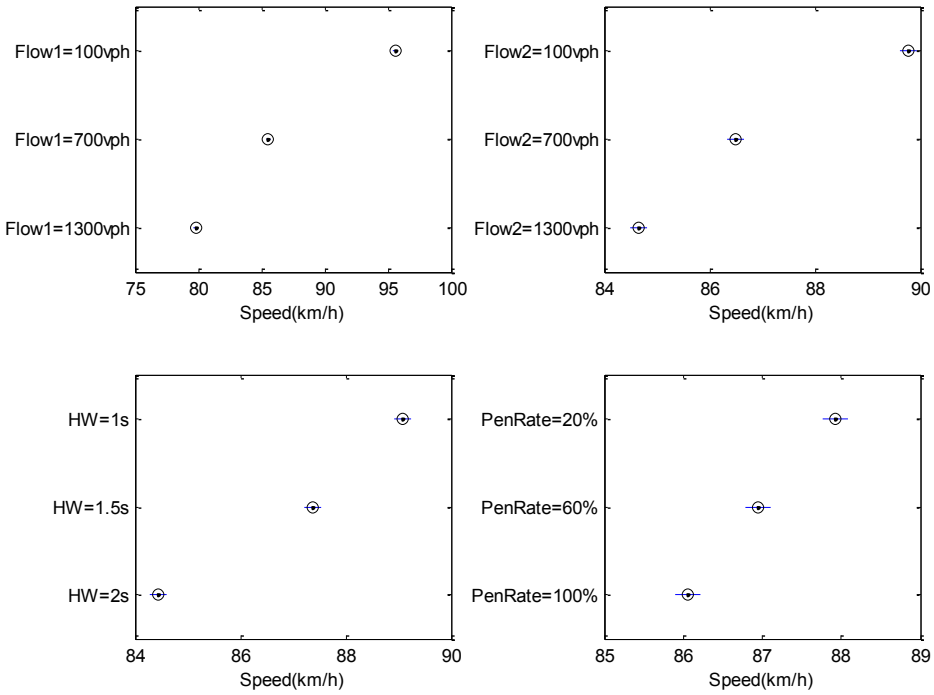

Figure 6-4- Multilevel comparison of factor effects on average travel speed (ATS)

Table 6-3- ANOVA table for average travel speed (ATS)

Source	Sum Sq.	d.f.	Mean Sq.	F	Prob>F
Flow1	3445.02	2	1722.51	2464.48	0
Flow2	361.61	2	180.8	258.69	0
HW	296.91	2	148.45	212.4	0
PenRate	47.08	2	23.54	33.68	0
Flow1*Flow2	19.2	4	4.8	6.87	0.0002
Flow1*HW	169.79	4	42.45	60.73	0
Flow1*PenRate	8.04	4	2.01	2.87	0.0326
Flow2*HW	5.45	4	1.36	1.95	0.1173
Flow2*PenRate	1.61	4	0.4	0.58	0.6805
HW*PenRate	30.35	4	7.59	10.86	0
Error	33.55	48	0.7		
Total	4418.61	80			

Table 6-4 presents the result of ANOVA test for PTSF. All factors except Flow1*PenRate, Flow2*HW and Flow2*PenRate were statistically significant. As shown in Figure 6-5, PTSF increases with both Flow1 and Flow2. Larger HWs resulted in increased PTSF. The role of ACC penetration rate is to increase PTSF. Except flow that shows nonlinear relationship with PTSF, the effect of HW and PenRate appears to be linearly related to PTSF.

Table 6-4- ANOVA table for percent time spent following (PTSF)

Source	Sum Sq.	d.f.	Mean Sq.	F	Prob>F
Flow1	57337.7	2	28668.9	13842.12	0
Flow2	6990.7	2	3495.4	1687.66	0
HW	1288.7	2	644.3	311.1	0
PenRate	169.6	2	84.8	40.95	0
Flow1*Flow2	558	4	139.5	67.35	0
Flow1*HW	492.9	4	123.2	59.5	0
Flow1*PenRate	6.1	4	1.5	0.74	0.572
Flow2*HW	14.4	4	3.6	1.74	0.1561
Flow2*PenRate	14.7	4	3.7	1.77	0.1496
HW*PenRate	30.5	4	7.6	3.68	0.0109
Error	99.4	48	2.1		
Total	67002.7	80			

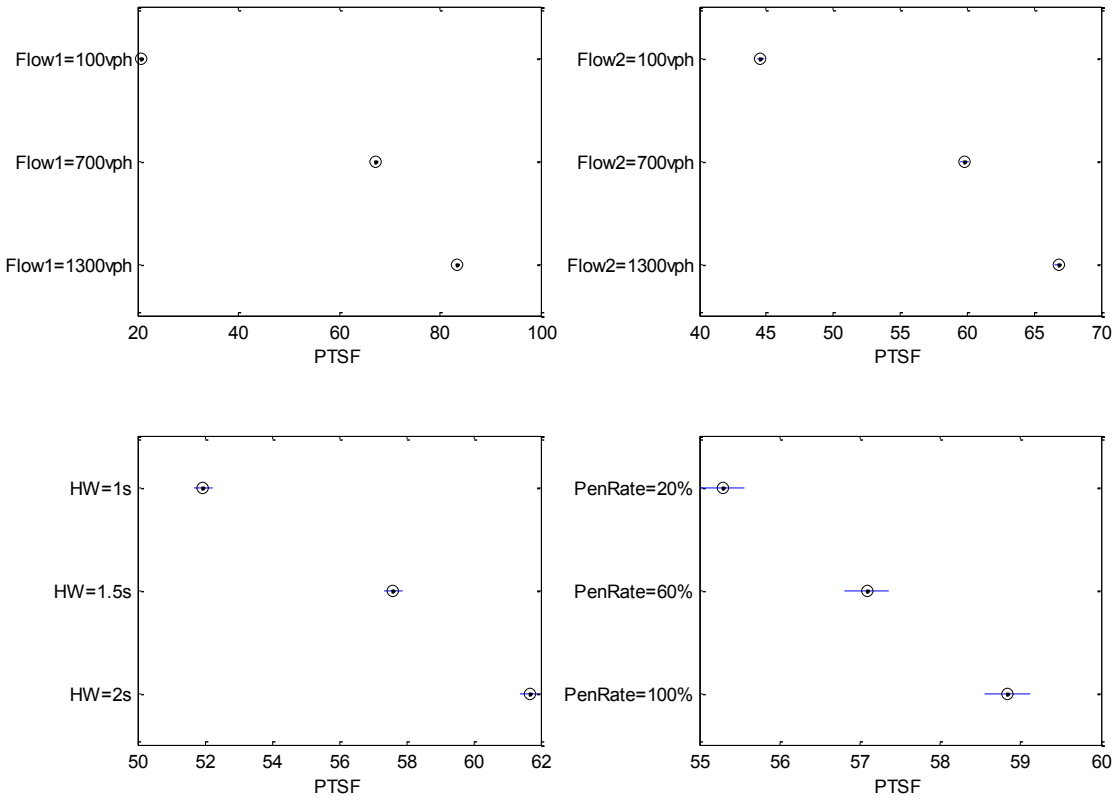

Figure 6-5- Multilevel comparison of factor effects on percent time spent following (PTSF)

The results of ANOVA test for overtaking rate (Table 6-5) shows statistically significant effect of factors except for Flow2*PenRate and HW*PenRate interactions. Figure 6-6 illustrates that OTrate increases and decreases with Flow1 and Flow2, respectively. The effect of HW is to reduce overtaking rate at all levels of HW. The difference, however, is less significant between HW=1.5s and HW=2s. OTrate decreases linearly with penetration rate.

For TTC, ANOVA test (Table 6-6) showed that the effect of PenRate rate and some interactions are not statistically significant, although TTC moderately increases with penetration rate. Figure 6-7 shows TTC increases with Flow1, but sharply decreases with initial increase in Flow2. The difference between HW=1s and HW=2s TTCs are not significant; while between these two and HW=1.5 are statically different (HW=1.5s resulted in lower TTC).

Table 6-7 summarizes the factors effects on simulation outputs as discussed above.

Table 6-5- ANOVA table for overtaking rate (OTrate)

Source	Sum Sq.	d.f.	Mean Sq.	F	Prob>F
Flow1	56575.1	2	28287.6	1009.16	0
Flow2	55792.5	2	27896.3	995.2	0
HW	2237.6	2	1118.8	39.91	0
PenRate	1522.2	2	761.1	27.15	0
Flow1*Flow2	23704.8	4	5926.2	211.42	0
Flow1*HW	1932	4	483	17.23	0
Flow1*PenRate	823.6	4	205.9	7.35	0.0001
Flow2*HW	313.3	4	78.3	2.79	0.0364
Flow2*PenRate	203.8	4	51	1.82	0.1408
HW*PenRate	211.8	4	52.9	1.89	0.1277
Error	1345.5	48	28		
Total	144662.3	80			

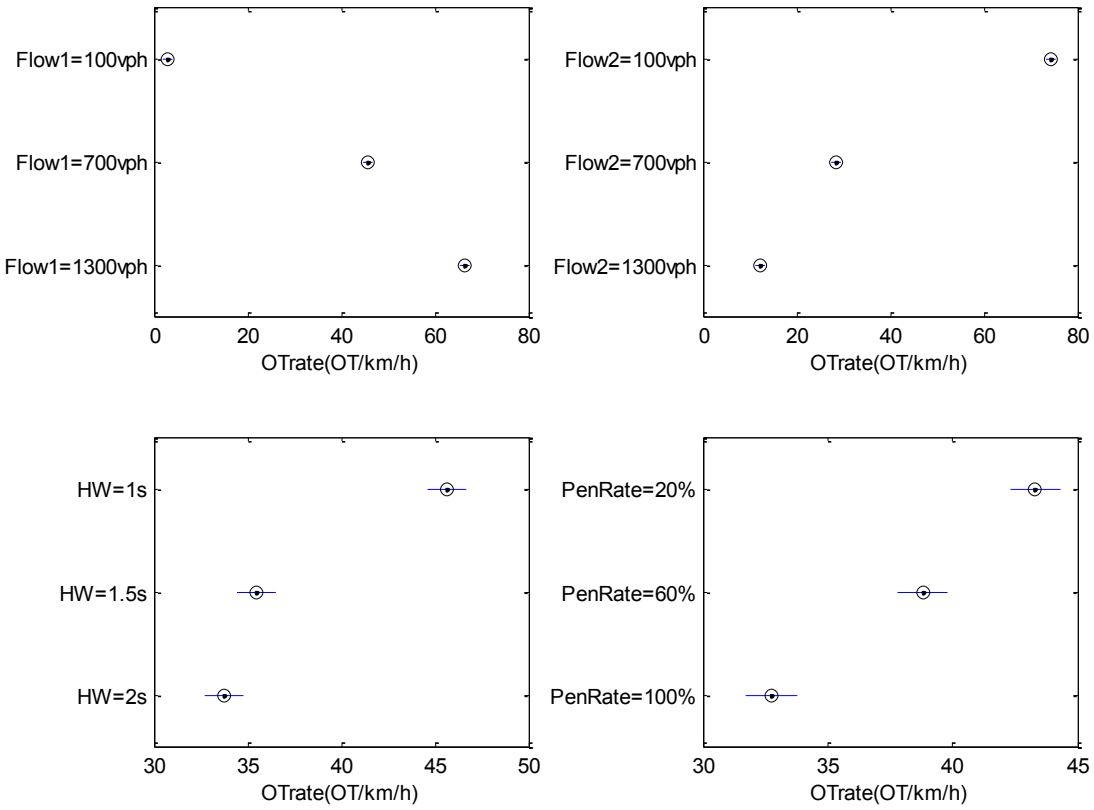

Figure 6-6- Multilevel comparison of factor effects on overtaking rate (OTrate)

Table 6-6- ANOVA table for average TTC

Source	Sum Sq.	d.f.	Mean Sq.	F	Prob>F
Flow1	283.25	2	141.63	261.52	0
Flow2	5670.74	2	2835.37	5235.74	0
HW	6.76	2	3.38	6.25	0.0039
PenRate	1.82	2	0.91	1.68	0.1979
Flow1*Flow2	10.6	4	2.65	4.89	0.0022
Flow1*HW	6.48	4	1.62	2.99	0.0278
Flow1*PenRate	0.41	4	0.1	0.19	0.9435
Flow2*HW	5.58	4	1.39	2.58	0.0493
Flow2*PenRate	0.33	4	0.08	0.15	0.9612
HW*PenRate	2.63	4	0.66	1.21	0.3168
Error	25.99	48	0.54		
Total	6014.59	80			

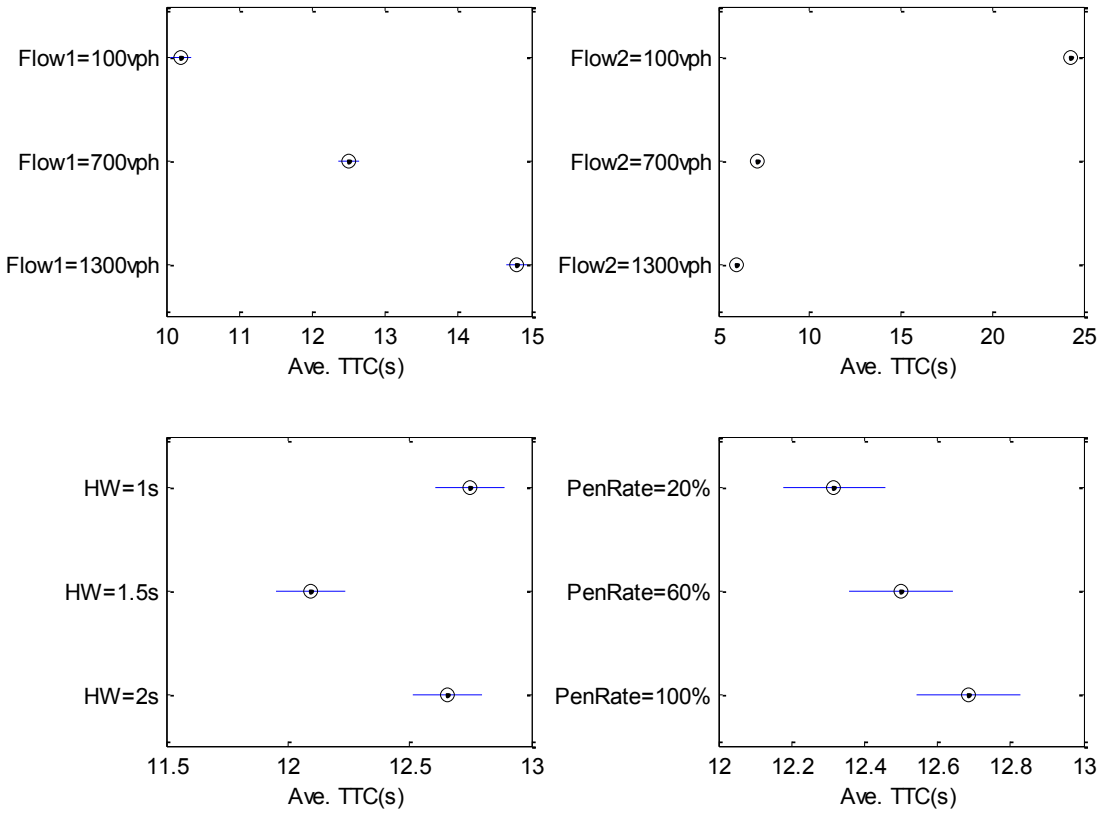

Figure 6-7- Multilevel comparison of factor effects on average TTC

Table 6-7- Summary of the factors effects on the output measures

Measures	Analysis direction flow (Flow1)	Opposing direction flow (Flow2)	ACC time headway (HW)	ACC penetration rate (PenRate)
Average travel speed (ATS)	-	-	-	-
Percent time spent following (PTSF)	+	+	+	+
Overtaking rate total (OTrate)	+	-	-	-
time-to-collision (TTC)	+	-	NC (lowest at HW=1.5s)	+

+/-: increase/decrease in the measure

NS: Not consistent

Figure 6-8 illustrate the comparison results between ACC (with 100% penetration rate) and Gipps (normal car-following mode). In simulation of Gipps car-following model calibration parameters, reported in Table 4-3, are used. These parameters, for vehicles in desired-to-overtake mode, yielded average headway of 0.7 second and for normal car-following mode (without overtaking desire) yielded average headway of 1.3 s. As seen previously, average travel speed decreases with increased ACC headway. HW=1s resulted in slightly higher speed as compared to Gipps. A similar pattern is observed for PTSF. PTSF increases with HW and is slightly higher for Gipps as compared to HW=1s. OTrate increases as HW decreases. The difference between Gipps and HW=1s is not statistically significant for OTrate. ACC does not appear to have consistent effect on average TTC for the range of HW considered. HW=1.5s resulted in lowest TTC and HW=1s resulted in highest TTC. The difference between Gipps and HW=2s and HW=1.5s is not statistically significant.

6.7 Discussion of Results

The most important effect of ACC was to reduce overtaking rate. This can be explained that larger controlled time gaps in ACC creates larger initial headways between overtaking and overtaken vehicles and this increases required overtaking time. This leads to increased overtaking distance, lower available TTC gaps and rejection of some gaps that would have been accepted if initial headways had been lower (e.g. No-ACC scenario).

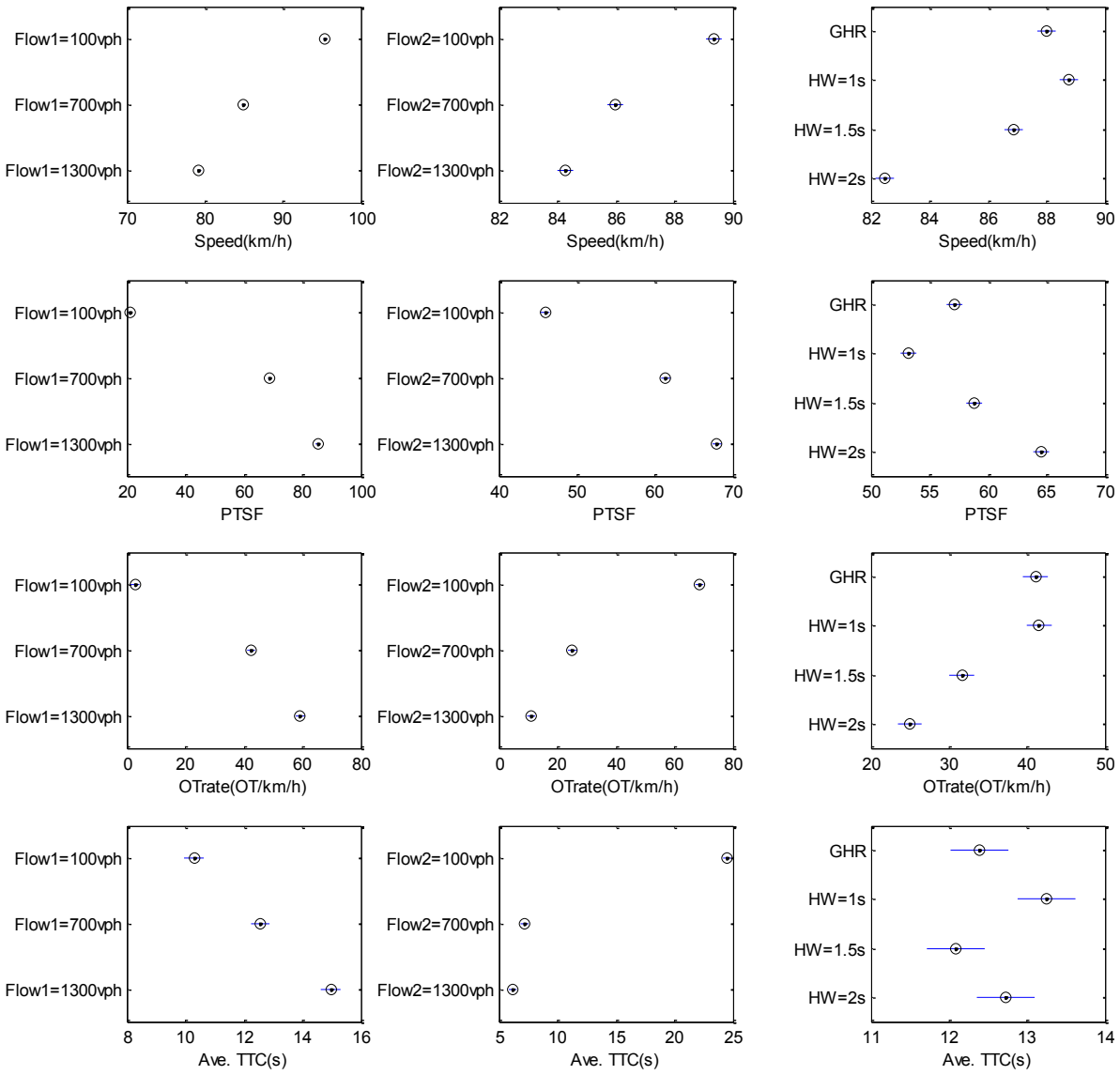

Figure 6-8- Multilevel comparison of factor effects for ACC versus GHR car-following model

The lowest and highest number of overtakes were observed for ACC with 2s time gap and No-ACC scenarios, respectively. The reduced number of overtakes resulted in decreased average travel speed, and increased PTSF. These effects are more significant as ACC time headways and/or penetration rate increases. If compared with no-ACC scenario (Gipps car-following), the results of ACC with one second headway are close to those of no-ACC. There was actually no significant difference between no-ACC scenario and ACC with 1-second control headway for overtaking rate. However, as

compared to ACC-1s scenario, average travel speed and PTSF were slightly lower and higher for no-ACC scenario, respectively.

The average accepted TTC drops rapidly with initial increase in volume. This is a reflection of risk. The highest risk is associated with volumes around 700 vph. As volume increases further, TTC increases slightly primarily due to slower moving vehicles in the traffic stream in particular opposing vehicles and overtaken vehicles. The effect of ACC on TTC is more complex. On one hand, the larger ACC time-gap headway increases the overtaking time and presumably decreases average available TTC gaps. On the other hand, when available TTC gaps become too short and unsafe (due to the headway control) they may not be accepted anymore. This can lead to lower number of unsafe overtakes and increased average TTC. The safest TTC (highest average TTC) was for ACC-1s scenario where the effect of reduced overtaking time increased safety. However, as ACC headway increases further to 1.5s, TTC decreases (presumably due to increased overtaking time). With further ACC headway increase to 2 second, TTC increases again (presumably due to decreased number of unsafe overtakes).

6.8 Conclusion

The potential impacts of adaptive cruise control (ACC) system on safety and traffic operation of two-lane two-way highways were investigated in this chapter. Traffic and safety measures including average travel speed, percent time spent following, number of overtakes, overtaking time, and times to collision (TTC) to the opposing vehicles were measured for a range of directional volumes. Three ACC scenarios with 2s, 1.5s, and 1s gap-time headways with three penetration levels as well as no-ACC onboard scenario were tested. The results showed that ACC significantly increases overtaking time duration. This led to reduction in the number of accomplished overtakes and consequently reduced average travel speed and increased average vehicle following time. These effects are more significant with larger time-gap thresholds set for ACC system and higher penetration rates. It appears that the impact of ACC on TTC, at different ACC headway levels, is different. The highest and lowest TTC corresponded to ACC-1s and ACC-1.5s scenarios, respectively. It must be noted that ACC always reduces the probability of rear-end collision by keeping larger headway between overtaking and overtaken vehicles. However, this can be sometimes compromised by increased risk of head-on collision and larger following time. The combination effect of these factors on head-on and rear-on crash risks require further investigation.

Chapter 7
Conclusion

7.1 Research Summary

In this research, an in-depth analytical and behavioral formulation of the overtaking gap-acceptance process for two-lane highway operations was presented. The decision to overtake was expressed as a function of the perception of time-to-collision (TTC) to the opposing vehicle at the end of maneuver and an established driver's gap-acceptance threshold. The perception error was determined based on difference between estimation of TTC at the beginning and measure of TTC at the end of maneuver for observed overtaking maneuvers. The gap-acceptance logic adopted in this research was assumed to encapsulate the full spectrum of physical variables influencing the gap-acceptance decision, resulting in reduced number of calibration parameters. Observational video data of a two-lane highway segment was used to estimate TTC perception error values and calibrate the gap-acceptance model.

From the observational video data, the mean of the TTC perception error was found to be around zero with corresponding standard deviations of 1.2 seconds. This shows drivers may underestimate or overestimate TTC in their perception of available gaps. The distribution of critical TTC gaps for a population of drivers was found to be normally distributed with a mean of 3.0 seconds and standard deviation of 0.7 s. This shows 95% of drivers have critical gap-acceptance thresholds between 1.6 and 4.4 seconds (mean±2*SD), and the corresponding headway distance thresholds from 80 to 220 meters, between the overtaking vehicle and the opposing vehicle, prior to returning to the normal travel lane (assuming average speeds of 90 km/h).

The gap-acceptance model was incorporated into a new simulation framework (OTSIM) and the simulation outputs were compared with independent aggregate field data as well as simulated results based on the TRARR, TWOPAS and HCM models. The overtaking model was found to yield both consistent and transferable results for PTSF, ATS, and overtaking rate when compared to field data and other simulation model values. In this research, it is demonstrated that in spite of complexity of overtaking maneuver and challenges in data collection process, it is possible to develop and calibrate a logical overtaking gap-acceptance model that yield both consistent and transferable results in two-lane highway operations.

The sensitivity of model outputs to the proposed calibration parameters was analyzed. For the range of values considered, critical TTC showed marginal impact on the traffic measures including average travel speed and percent time spent following. However, this impact is quite significant for safety measures including overtaking rates and average TTC.

The OTSIM model was applied to three different traffic and safety performance applications in which the proposed overtaking model played a crucial role. In the first application, OTSIM was used to provide estimates on level-of-service (LOS) measures for two-lane highways. The results obtained from the simulation model were compared to the published values in HCM 2000 and HCM 2010. Estimates of average travel speed (ATS) as reported in HCM 2000 and HCM 2010 were found to be lower than that of OTSIM. A new nonlinear model form was suggested to replace the current linear function relating volume to ATS in HCM. As found in this research and elsewhere, percent time spent following (PTSF) as obtained from the HCM 2000 was highly overestimated especially at low analysis direction volumes. PTSF from HCM 2010 compared well with simulated results at low opposing volumes, but was lower for higher opposing volumes than that of simulation. A new set of updated model parameters were provided for the PTSF expression. In addition, new adjustment factors were introduced to take into account the effect of standard deviation of speed on ATS and PTSF. Standard deviation of speed demonstrated a significant effect on LOS measures for two-lane highways.

Further simulation analysis was proposed to model three measures of safety performance for two-lane highways and accordingly the corresponding expressions versus directional traffic volume were formulated. These measures included overtaking rate, overtaking rate per vehicle, and average overtaking head-on time-to-collision (TTC). As expected overtaking rate (OT/km/h) increased with analysis direction volume and decreased with opposing direction volume. However, the overtaking rate per vehicle (OT/km/veh/h) hit a maximum value at around 500 vph volume. This volume may represent the maximum overtaking risk for drivers in terms of the expected number of overtaking maneuvers that they accomplish. Average overtaking TTC increased with analysis direction volume, but sharply decreased with opposing direction volume. This showed that for a given opposing volume, overtaking is safer at higher analysis direction volumes presumably due to lower speed of overtaken vehicles. However, an initial increase in opposing volume significantly reduced the average TTC.

In the second application of OTSIM, the model was used to assess the traffic and safety implication of car-truck differential speed limit (DSL) and truck mandated speed limit (MSL) as compared to uniform speed limit (USL) for cars and trucks. In this research overtaking was also a key component of the simulation process. Differential speed strategies (DSL and MSL) reduced the average travel speed of the traffic stream. This was associated with increased traffic delay. No significant effect was observed in PTSF using differential speed control strategies. Although differential speed strategies (DSL and MSL) were observed to have a minimal increase in the total number of overtake maneuvers in comparison to a uniform strategy (USL), the effect on the nature of the overtakes (i.e., car-car versus car-truck) was significant. Differential speed strategies increased the rate of car-truck overtakes over the range of volumes considered in this analysis. This suggested a negative effect on safety resulting from differential speed strategy applied to two-lane rural highways. On a positive side, the DSL and MSL strategies reduced the number of car-car overtakes at different volumes, hence increasing safety. TTC sharply dropped with increase in the opposition volume. Similar to PTSF, the impact of differential speed limit strategies on TTC was minimal. For the cases that differential speed limit contributed to significant changes in the traffic and safety measures, the impact of MSL was larger than that of DSL.

The last application of OTSIM concerned the potential impacts of adaptive cruise control (ACC) system on safety and traffic operation of two-lane two-way highways resulted from changes in overtaking behavior. Traffic and safety measures were estimated for three ACC scenarios with 2s, 1.5s, and 1s gap-time headways as well as no-ACC scenario. The results showed that ACC (with large headways greater than 1 second) significantly increased overtaking time duration due to larger headways at the beginning of the overtaking. This led to a reduction in the number of overtakes and average travel speed, and also an increase in the average following time of vehicles. These effects were more significant with larger time-gap thresholds set for the ACC system. The impact of ACC on TTC at different ACC headway levels was investigated. The highest and lowest TTC corresponded to ACC-1s and ACC-1.5s scenarios, respectively. It is noted that ACC always reduces the probability of rear-end collision by keeping larger headway between overtaking and overtaken vehicles. However, this can be sometimes compromised by increased risk of head-on collision at high volumes and increased following time.

7.2 Main Contributions

This research provided a number of significant contributions summarized as follows:

1. Introducing a new mechanistic and behavioral overtaking model for two-lane highway operation. This model was developed in such a way that unlike previous models, a few overtaking model parameters (e.g. distribution of critical TTC) are required to capture realistic overtaking behavior and true measure of traffic field. This provides a flexibility to calibrate the model based on either aggregate traffic data or disaggregate overtaking observational data.
2. Proposing an overtaking gap-acceptance logic based on the perception of driver to estimate overtaking time-to-collision (TTC) to the opposing vehicle.
3. Determining the perception error based on observation of overtaking maneuvers from overtaking field data.
4. Calibration and validation of the overtaking gap-acceptance model on observational overtaking data using a binary Probit model.
5. The application of the new model contributed to improved estimates for ATS and PTSF measures used in determination of level-of-service for two-lane highways. For the first time, the effect of standard deviation of speed was proposed as a correction factor to increase the accuracy of ATS and PTSF. Safety alternative measures including overtaking rate and average TTC were proposed as an alternative measure for the LOS analysis on two-lane highways.
6. The application of the model to evaluate safety and traffic implications of truck mandated speed limiter on two-lane highways was demonstrated in this thesis. This is the first research using micro-simulation to assess the potential effects of imposing mandated truck speed limiter for two-lane highways. Although previous studies proposed both statistical and simulation approaches to evaluate this countermeasure for freeways, using two-lane simulation to study safety and traffic consequences of using truck speed limiters especially on overtaking maneuver is a new approach in its kind.
7. The last contribution of this research regards the application of OTSIM to model safety and traffic implications of adaptive cruise control (ACC) if used in two-lane traffic flow and how this may specifically affect overtaking behavior.

7.3 Future Research

A number of potential research subjects are proposed as future works for this thesis. First is to improve the accuracy of the proposed overtaking model and extend its validity through more comprehensive field data collection. In addition, there are also a number of recommendations for future works regarding the model applications.

The inclusion of an impatience factor in overtaking decision logic can improve accuracy of the overtaking model. In the proposed data collection study, it was not possible to determine the driver's past driving circumstance e.g. number of rejected gaps or time spent in desire-to-overtake mode, although a general formulation was provided in Chapter 3 to calibrate the impatient function. As discussed, this could result in reduction in driver's critical TTC threshold and increased driver's aggression level. This data is normally difficult to obtain unless, a large section of two-lane highway is monitored, or a driving simulator is used.

The other improvement area, which is also related to model validation, is to collect aggregate traffic data at multiple locations of a two-lane highway with permitted overtaking. The traffic data can include spot speeds, vehicles headways, and occupancies. This data would be valuable to further check the transferability of the model in generating real world field data. This can also check whether simulation outputs will be consistent with field data through adjustment of the overtaking model parameters. This is not a very difficult data collection task since this type of traffic data can be easily obtained from ordinary traffic sensors e.g. loop detectors. The challenge remains to find an appropriate site location with minimum access points, minimum overtaking restriction and significant traffic volume.

In this research, the model parameters were determined as per calibration overtaking data for normal driving, road, and traffic conditions as well as good weather and clear visibility. Any changes to these conditions may change the calibration results; i.e., calibration parameters must be adjusted. It is also useful to collect overtaking and traffic data for two-lane highways on different conditions; e.g. bad weather, narrow lanes and shoulder at multiple locations. Given the availability of aggregate traffic data or disaggregate observational overtaking data for these locations, the proposed overtaking model can be recalibrated by adjusting the model calibration parameters.

In this research, the desire-to-overtake was simply modeled based on a speed differential threshold. This may be more complicated since drivers may change their tendency to overtake at different road

and traffic conditions. This requires more investigation and specific data collection effort, which was out of scope of this research.

The application of OTSIM in the study of car-truck differential speed limit was limited to the assumption made on distribution of speeds which were mostly borrowed from freeways and multi-lane highways. This was especially true about truck speed distribution with mandated speed limiters. New speed field data can be collected on two-lane highways to validate these assumptions.

It is known ACC always reduces the probability of rear-end collision by keeping larger headway between overtaking and overtaken vehicles. However, as shown in this study, this can be sometimes compromised by increased risk of head-on collision and larger percent time spent following. The combination of these factors and associated crash risks require further investigation.

In addition, it is also recommended to decrease the simulation time-step to 0.1 second to improve the accuracy of simulation outputs especially those related to surrogate safety performance measures. That would require implementing the software code in a faster language platform such as C++.

Finally with advancement in vehicles technologies, especially development and implementation of connected vehicles, more extensive overtaking data can be collected and used to improve the reliability and accuracy of overtaking simulation models in various driving and traffic conditions.

Appendix A

- OTSIM manual

In this appendix, the OTSIM manual is described. Figure A1 illustrate the OTSIM main interface window. The description of each section, numbered from 1 to 8, is as follow.

1: Simulation run control including “start”, “stop”, and “resume/pause” buttons. A slider bar below these buttons is designed to control the speed of animation.

2: This section is aimed to provide appropriate view of the simulation screen through “zoom in” and “zoom out” buttons. The “fit” button returns the screen view to the view of the entire road section.

3: In this section, user can disable/enable simulation animation, restrict/allow overtaking for the entire section, and disable/enable data logging.

4: Data logging information can be provided in this section. This includes the file and folder names for log files as well as number of runs for batch simulation.

5: Directional flow information is provided in this section. The traffic flow in vehicle per hour is given for both entry flows and actual randomly generated flows.

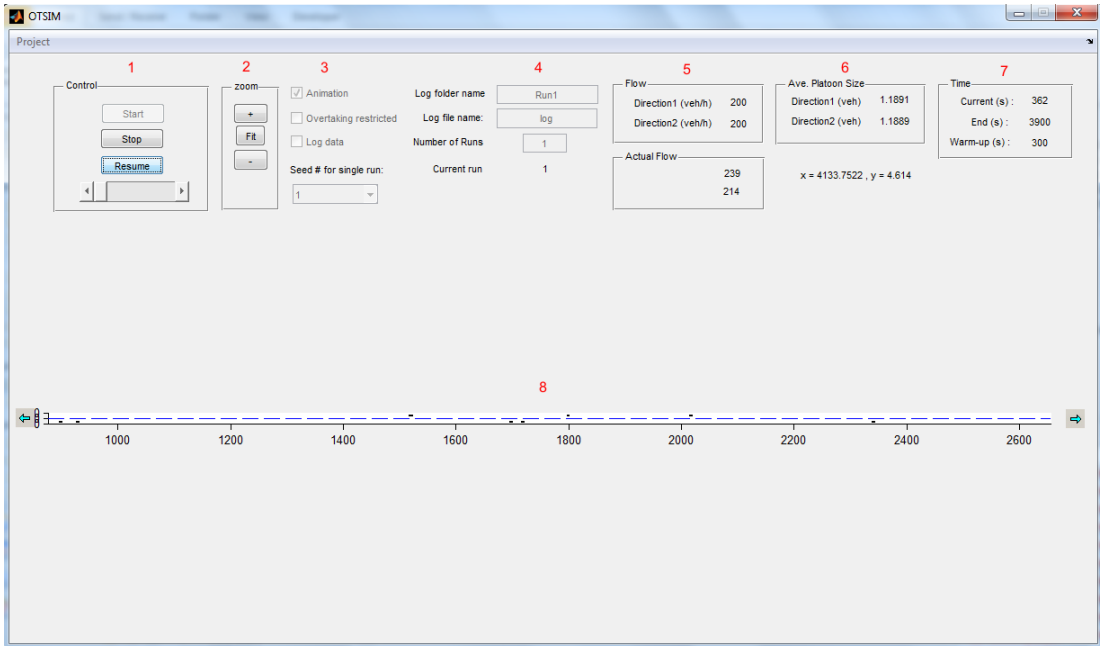

Figure A1- OTSIM software main interface window

6: Information regarding the average generated platoon size is given in section 6 in the simulation main interface.

7: Simulation time including current simulation time, simulation time period, and simulation warm-up time are provided in seconds.

8: View of the simulation section as well navigation to right and left can be performed using the left/right arrow buttons.

Figure A2 illustrates the flow entry menu designed in OTSIM. Directional flow, minimum generated headway, and percentage of vehicles can be entered by users through this mean. "Max time HW of platoon" is the maximum time headway between vehicle to be considered as a part of platoon. Vehicles with headways more than this value are considered as separate vehicles. This parameter plays role in multiple overtaking logic in OTSIM to determine whether the potential overtaking vehicle must overtake a platoon of vehicles or a single vehicle. The "platoon forming Eq. parameter (A)" is a calibration parameter playing role in the OTSIM's platoon generation model.

Distribution of desired speed for three classes of vehicles for each direction can be entered through the menu shown in Figure A3. The "Auto Generate" button create minimum and maximum of desired speeds based on the mean and standard deviation (min = mean – 3*SD, max = mena+3*SD). The distributions of desired speed are assumed to be normally distributed in OTSIM. Mandated speed limit for trucks can be activated by putting a check mark to the corresponding activation box and entering the desired maximum value.

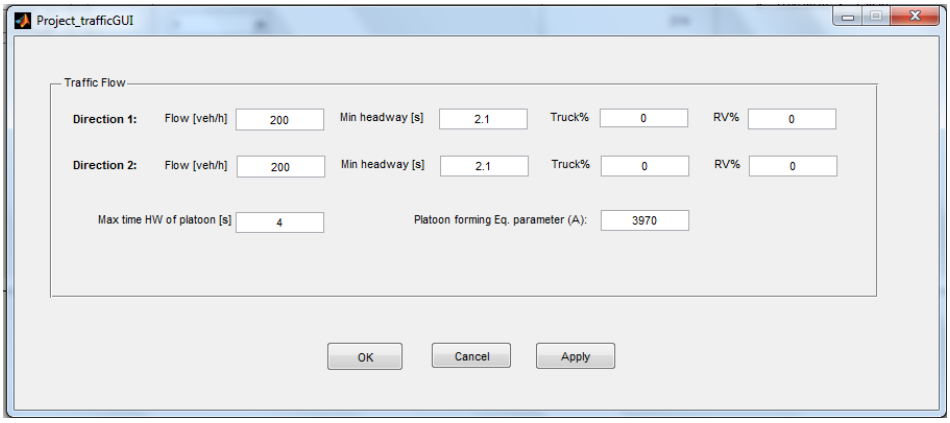

Figure A2- OTSIM flow entry menu

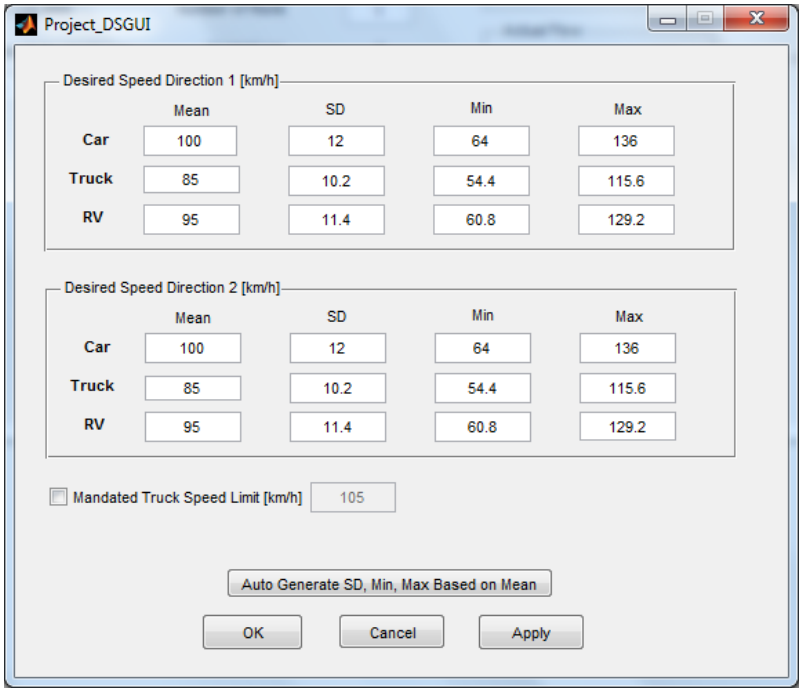

Figure A3- OTSIM desired speed distribution menu

Figure A4 illustrates the simulation time menu. Total simulation as well as warp-up time can be determined in this menu. The "Auto Generate" menu creates minimum warm-up time based on the length of the simulated section and average travel speed of vehicles.

Figure A5 shows the user interface menu for entering physical characteristics of vehicles. Care should be taken in changing the default parameter values since a significant impact may be observed on model outputs especially those related to overtaking maneuver.

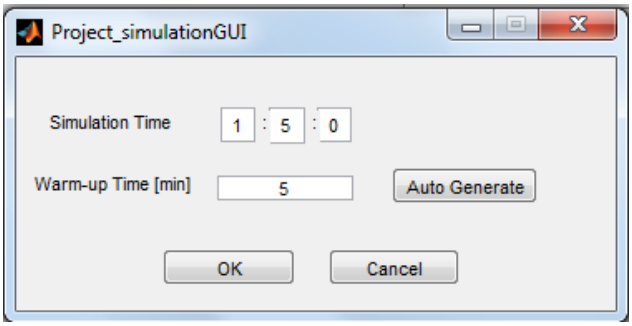

Figure A4- OTSIM simulation time control

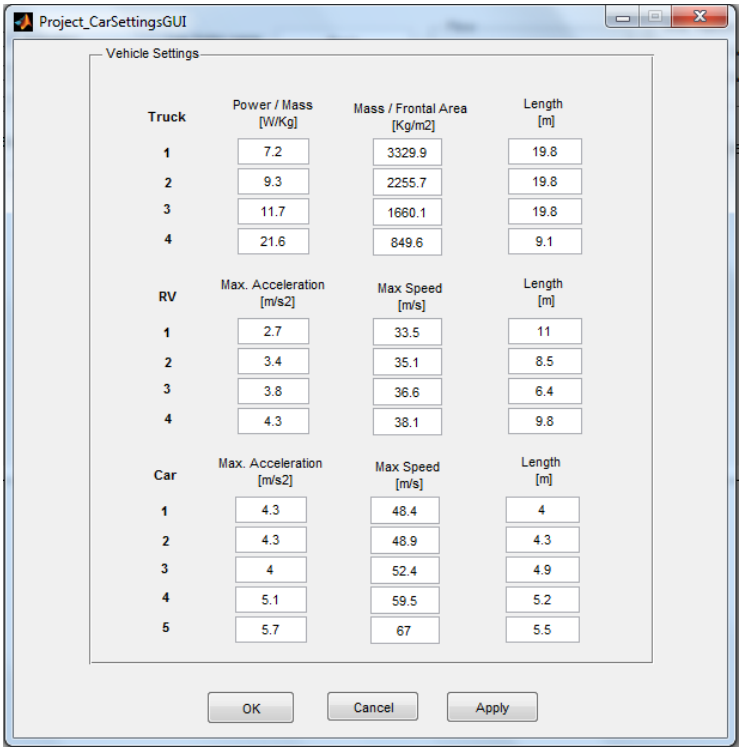

Figure A5- OTSIM simulation time control

Parameters related to driving behavior is shown in Figure A6 (driving behavior menu). The first section of this menu determines the desired deceleration rate of vehicles used in OTSIM. The second section provides the list of parameters playing rule in the overtaking decision logic. The Gipps car-following model parameters can be changes in section three and finally the last section is to activate the adaptive cruise control and change the corresponding penetration rate and desired time-gap headway for three classes of vehicles.

Figure A7 presents the menu used in OTSIM to enter road data. The road data include segment length, lane width, shoulder width, and elevation. Segment grade information as well as passing/no-passing information can be entered by users in this section.

A view of the post processing software developed to analyze and summaries the simulation log files generated by OTSIM is shown in Figure A8. The left section of this figure shows the log file information and the right side shows the summary of results. Detailed overtaking information as well as summary of results can be generated in spreadsheet format.

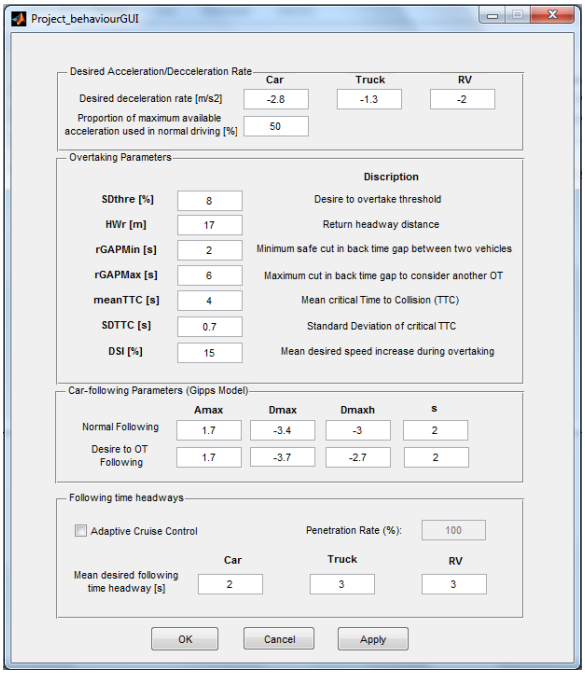

Figure A6- OTSIM simulation time control

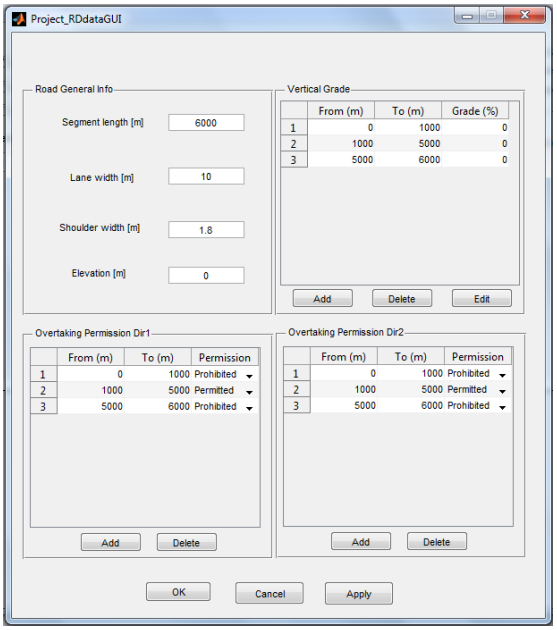

Figure A7- OTSIM road entry menu

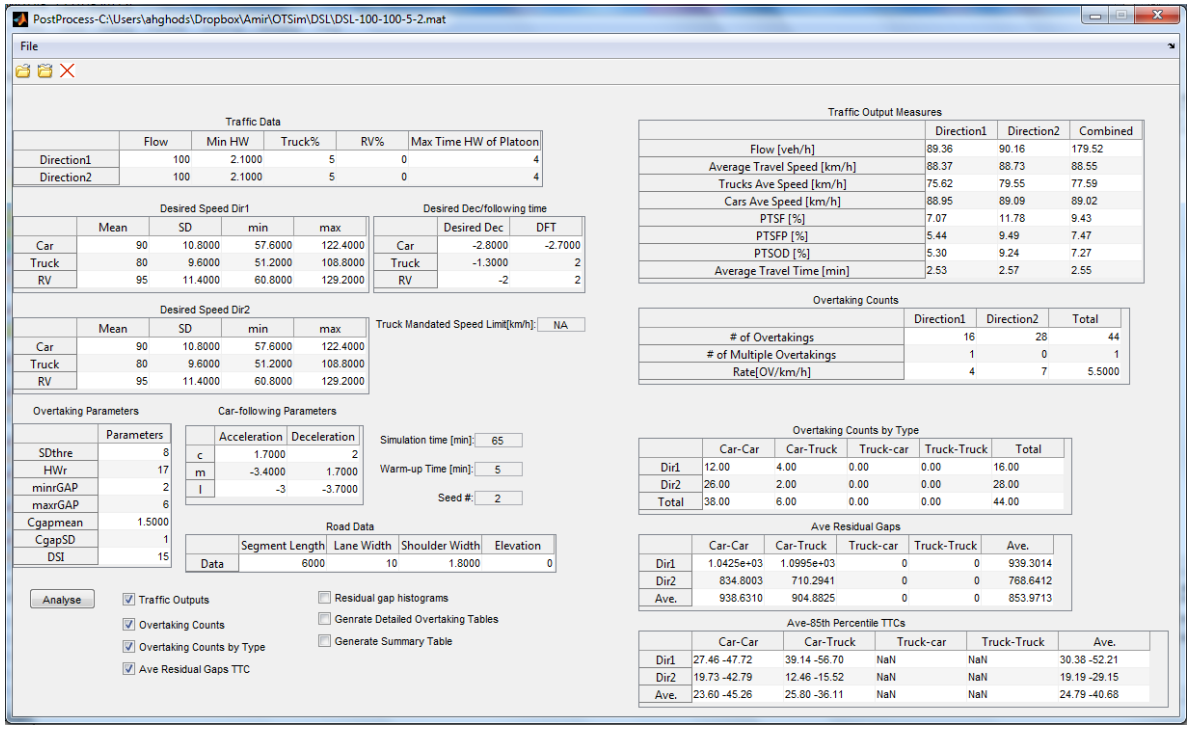

Figure A8- Post processing software used in OTSIM

Appendix B

- Calculation of distance covered by overtaking vehicle to reach the desired overtaking speed

The instant acceleration for light vehicles can be linearly approximated as a function instant speed of the vehicle such that:

$a(t) = \frac{dv(t)}{dt} = ka^{max}\left(1 - \frac{v(t)}{v^{max}}\right)$	**B1**

where,

v^{max} = maximum achievable speed

a^{max} = maximum achievable acceleration from the stopped position

k = porportion of maximum available acceleration employed by the driver

Eq. A1 is an ordinary differential equation (ODE) that can be solved as follow:

$v(t) = v^{max} - [v^{max} - v(0)]e^{-\frac{ka^{max}}{v^{max}}t}$	**B2**

where,

$v(0)$ = initial speed = v^{ini}

The time required to achieve the desired speed of v^{des} from initial speed of v^{ini} using k proportion of a^{max} can be determined from Eq. A2 as:

$T = -\frac{v^{max}}{ka^{max}} \times ln\left(\frac{v^{max} - v^{des}}{v^{max} - v^{ini}}\right)$	**B3**

The distance travel during T can be estimated as follow:

$\int_0^T v(t)dt = x(t)\Big\|_0^T \xrightarrow{replacing\ v(t)\ by\ Eq.A2}$ $\int_0^T \left(v^{max} - [v^{max} - v(0)]e^{-\frac{ka^{max}}{v^{max}}t}t\right)dt = x(T) - x(0)$	**B4**

Finally, the travel distance can be determined as:

$x(T) = v^{max}T + \frac{v^{max}}{ka^{max}}\left(v^{max} - v^{ini}\right)\left(e^{-\frac{ka^{max}}{v^{max}}T} - 1\right)$	**B5**

Appendix C

- Two-dimensional multi-level comparison graphs for speed limiters

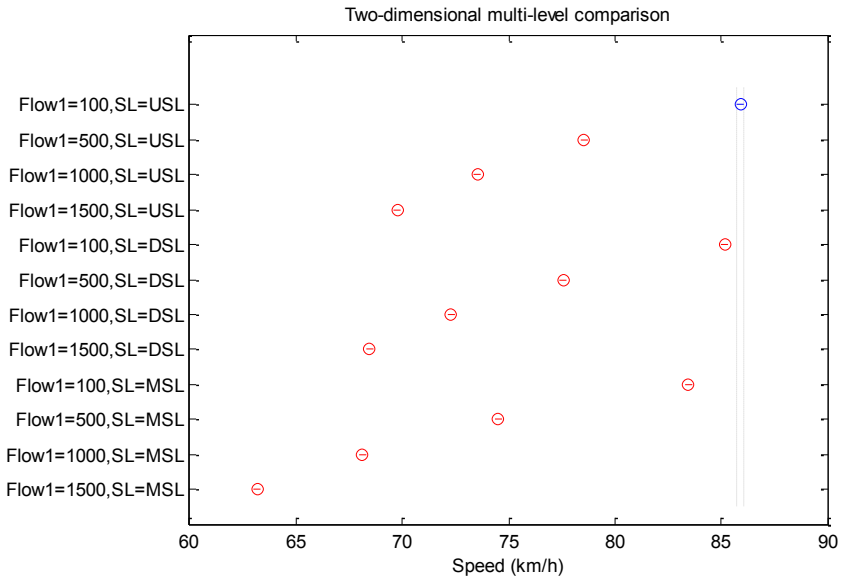

Figure C1- Flow1/SL versus Speed

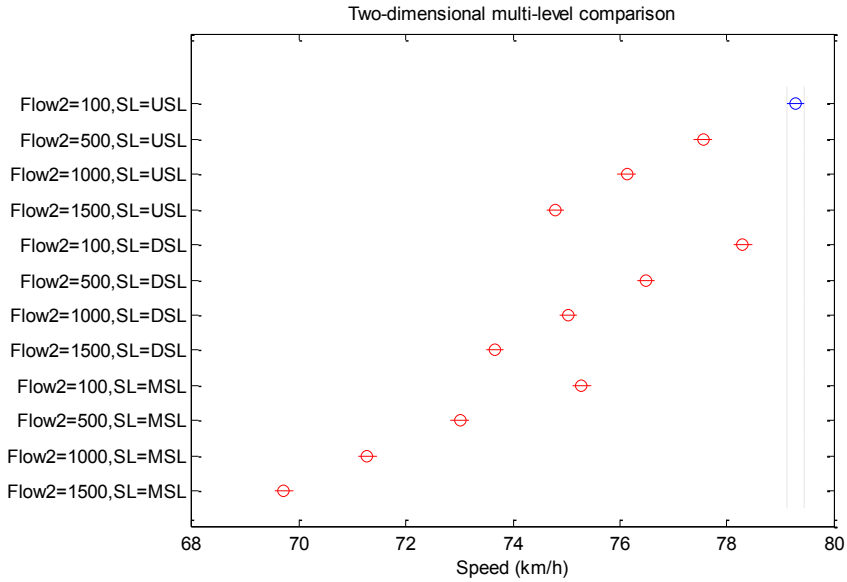

Figure C2- Flow2/SL versus Speed

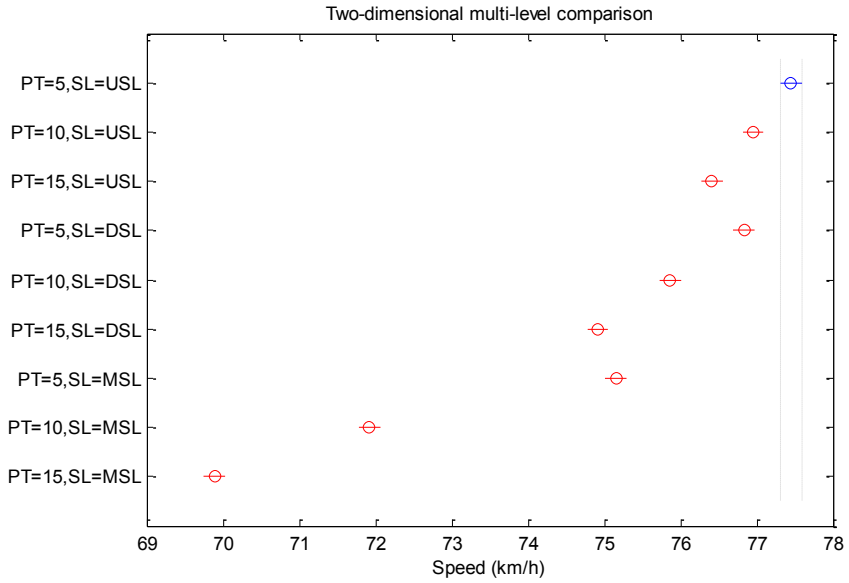

Figure C3- PT/SL versus Speed

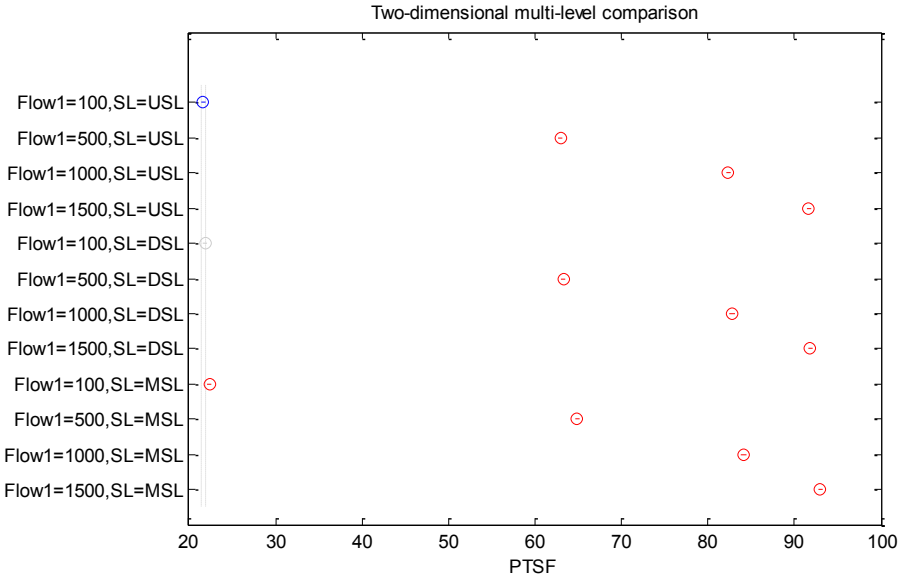

Figure C4- Flow1/SL versus PTSF

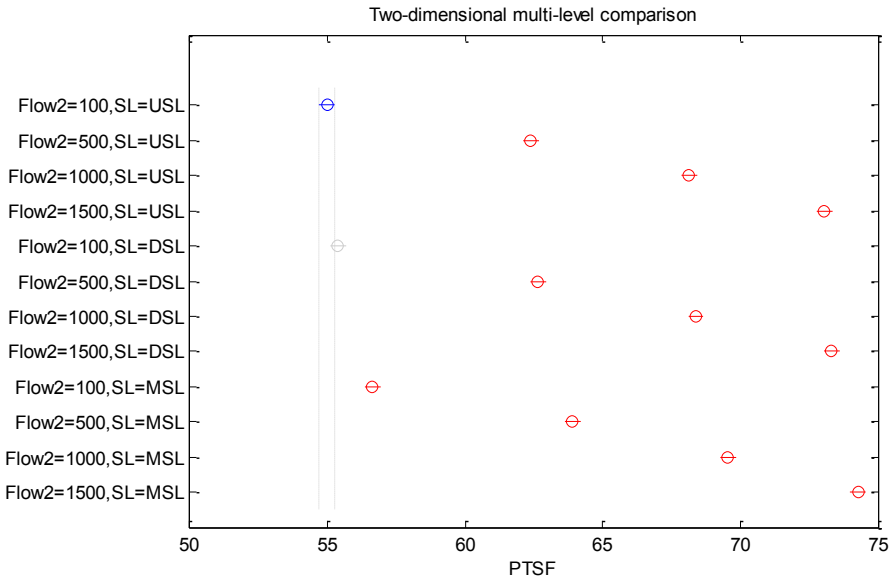

Figure C5- Flow2/SL versus PTSF

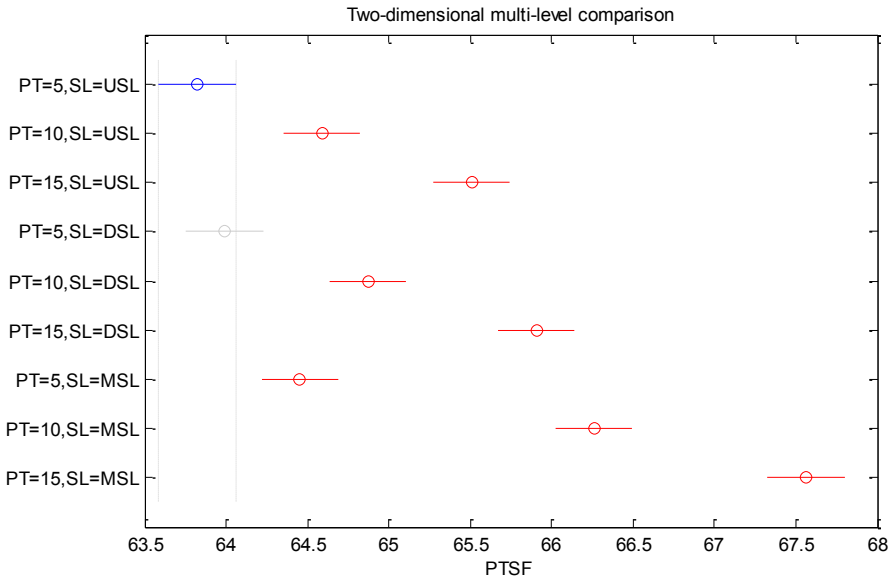

Figure C6- PT/SL versus PTSF

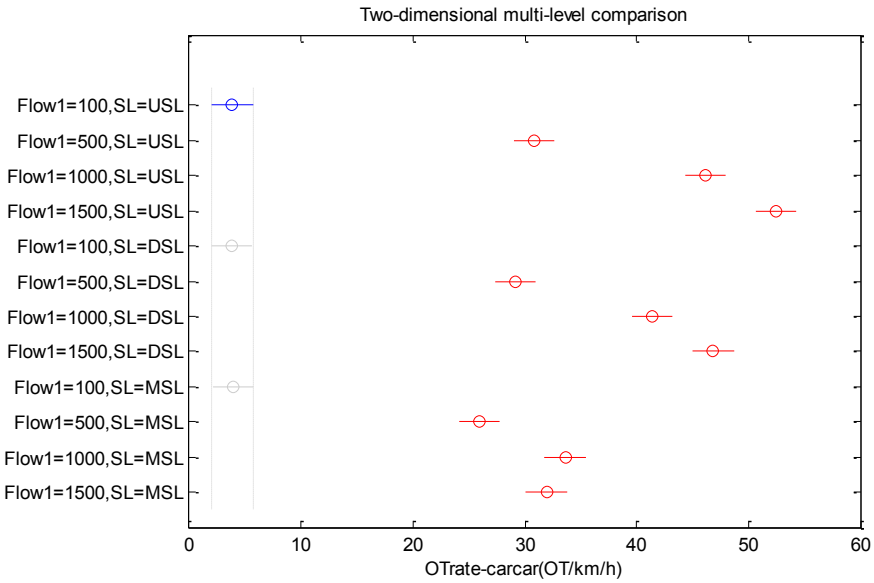

Figure C7- Flow1/SL versus OTrate-carcar

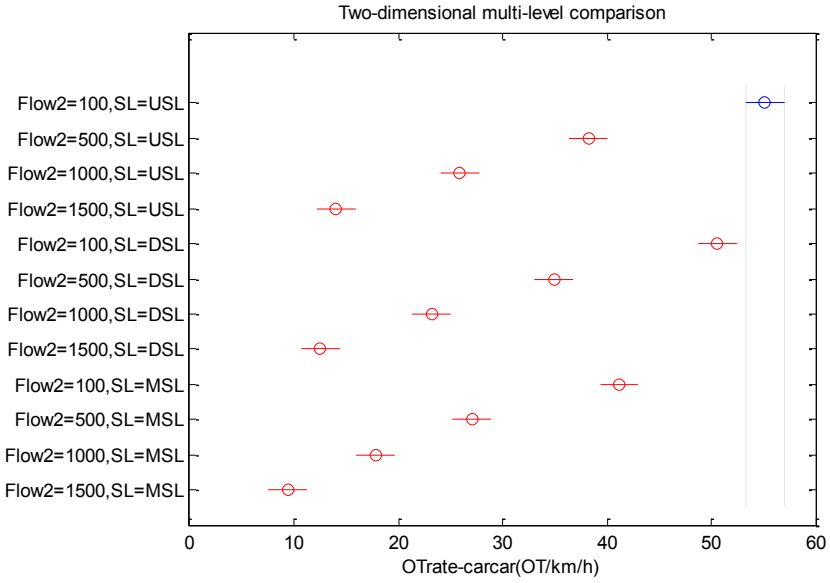

Figure C8- Flow2/SL versus OTrate-carcar

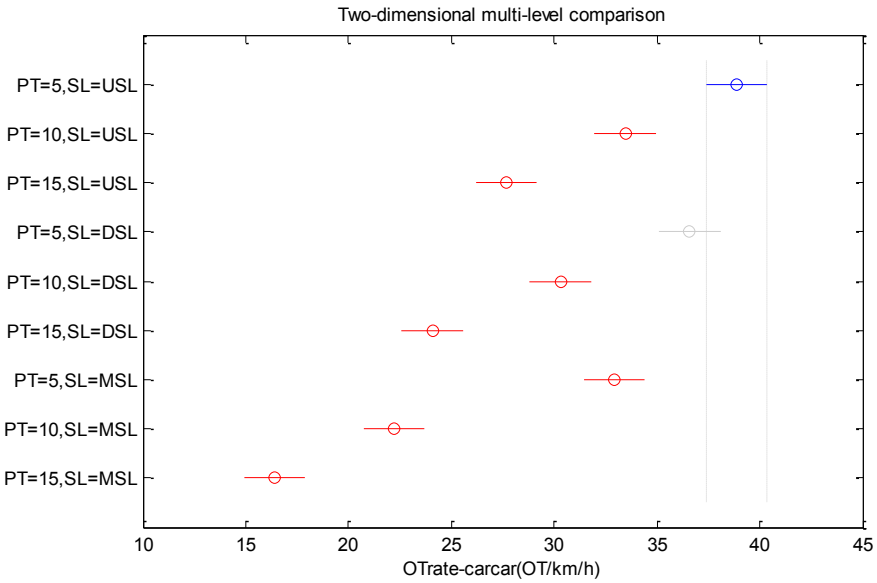

Figure C9- PT/SL versus OTrate-carcar

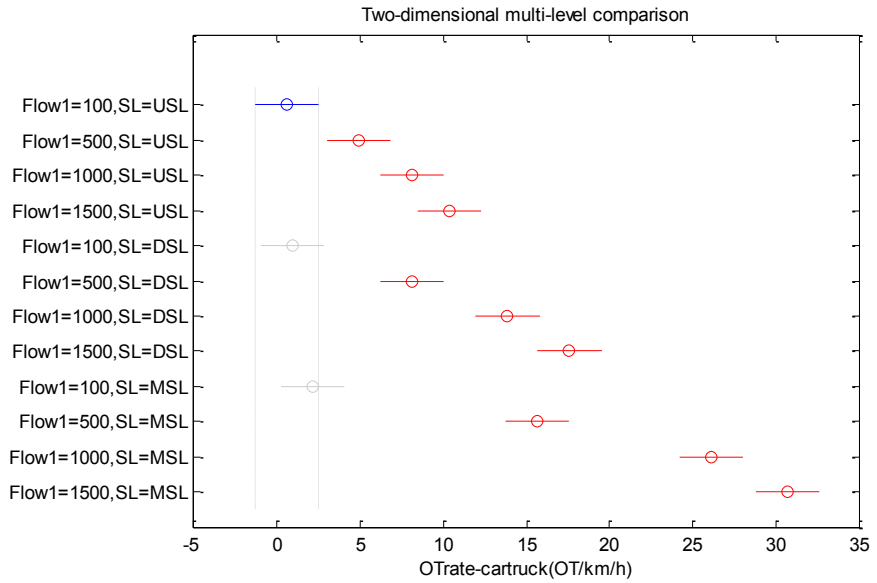

Figure C10- Flow1/SL versus OTrate-cartruck

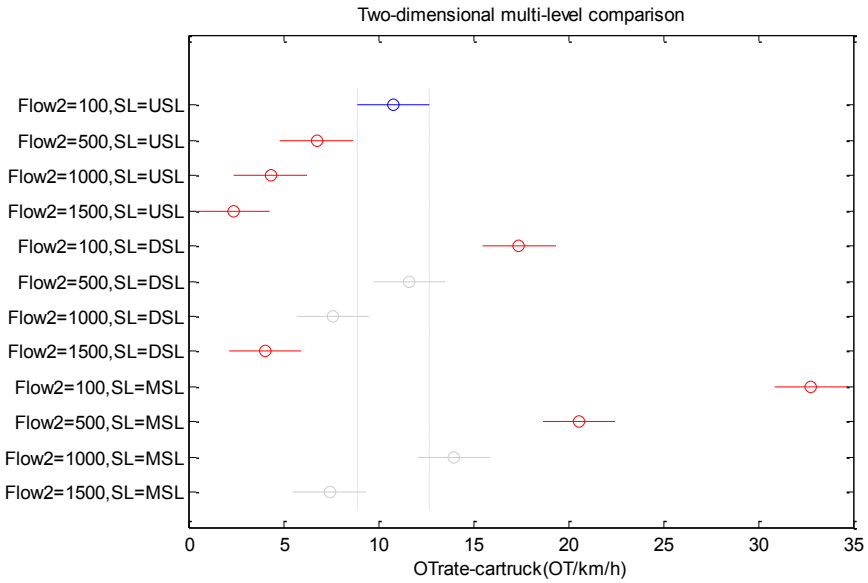

Figure C11- Flow2/SL versus OTrate-cartruck

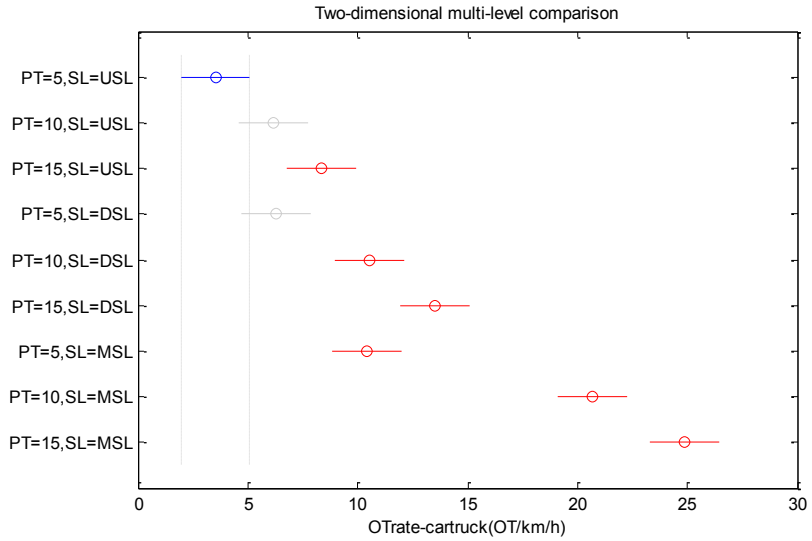

Figure C12- SL/SL versus OTrate-cartruck

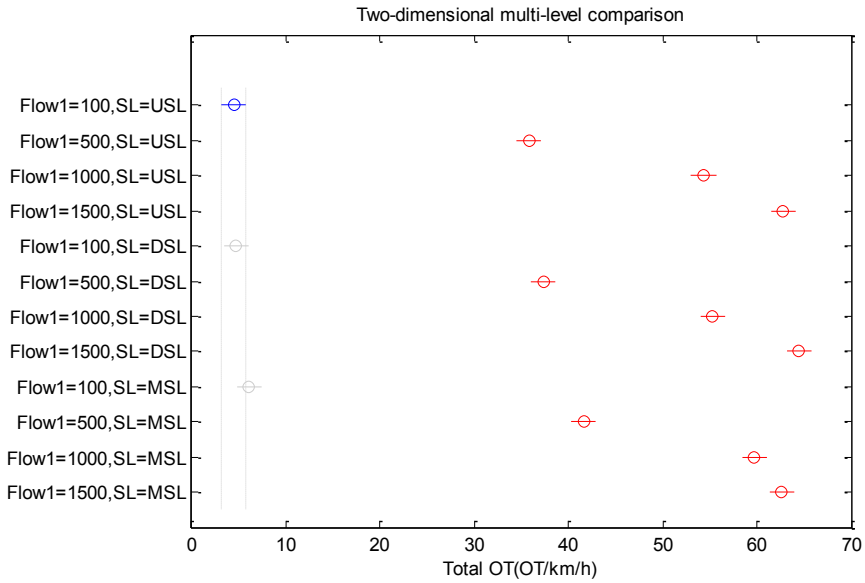

Figure C13- Flow1/SL versus Total OT

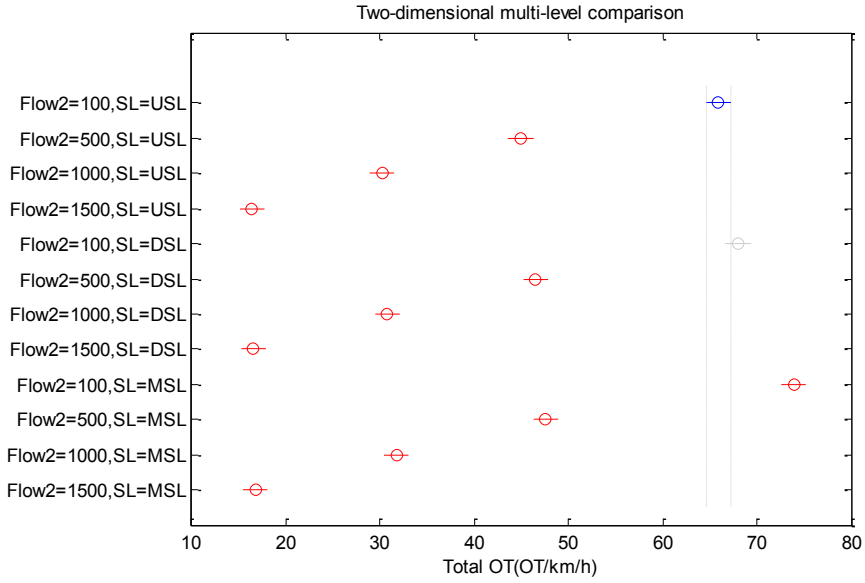

Figure C14- Flow2/SL versus Total OT

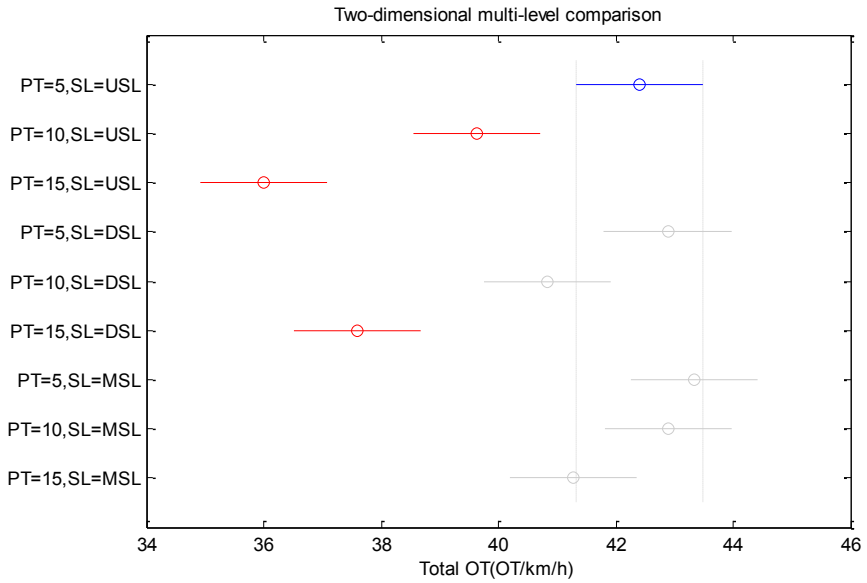

Figure C15- PT/SL versus Total OT

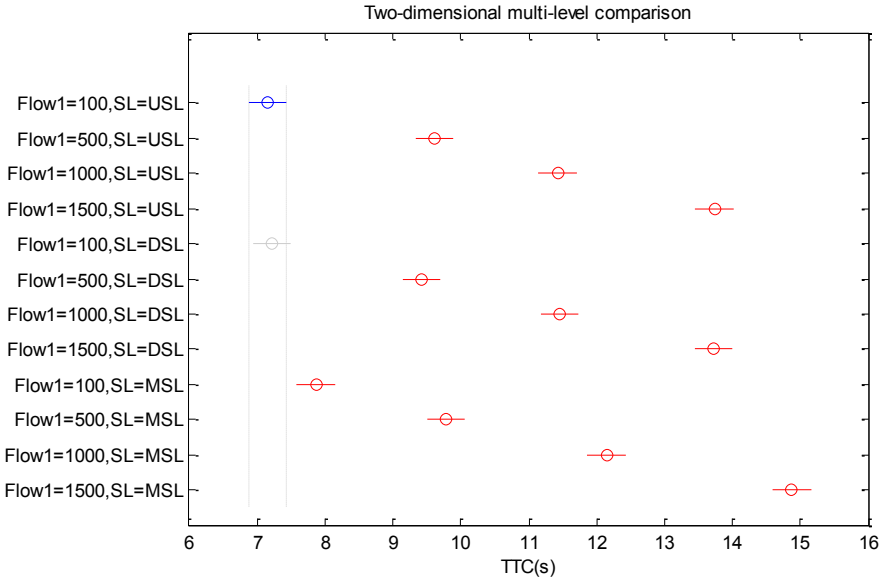

Figure C16- Flow1/SL versus TTC

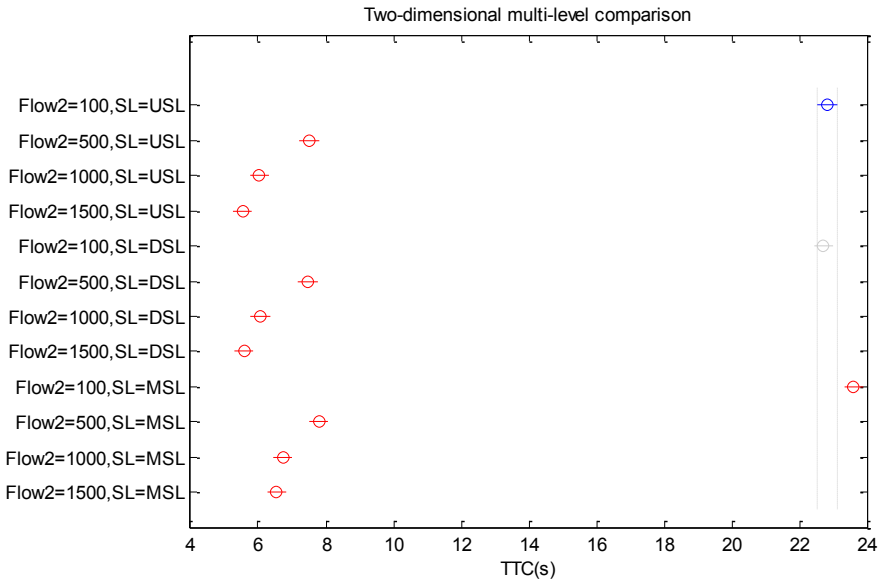

Figure C17- Flow2/SL versus TTC

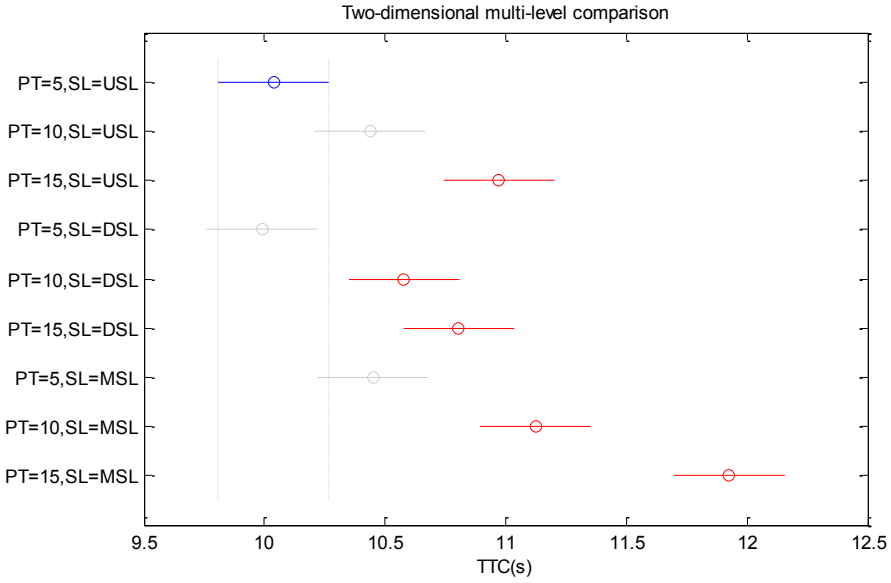

Figure C18- PT/SL versus TTC

References

AASHTO. 2004. *A policy on geometric design of highways and streets*. Fifth ed. Washinfton, D.C.: American Association of State Highway and Transportation Officials.

Ahman, K. I. 1972. Omkorningar av lastbilar. *Trafikstudier Statens Vag-Och Trafikinstitut* Raport 6 .

Allen, R. W., D. Harwood, J. P. Chrstos, and W. D. Glauz. 2000. *The capability and enhancement of VDANL and TWOPAS for analyzing vehicle performance on upgrades and downgrades within IHSDM.* Washington DC: Federal Highway Administration, FHWA-RD-00-078.

Bose, A., and P. Ioannou. 2001. *Analysis of traffic flow with mixed manual and intelligent cruise control vehicles: Theory and experiments.* Los Angeles, CA: University of Southern California, UCB-ITS-PRR-2001-13.

Brooks, R. M. 2012. Acceleration charachteristics of vehicles in rural pennsylvania. *International Journal of Research and Reviews in Applied Sciences* 12 (3): 449-453.

Carfolio. Car specification and technical database. [cited 05 2013]. Available from http://www.carfolio.com.

Carlson, P. J., J. D. Miles, and P. K. Johnson. 2006. Daytime high-speed passing maneuvers observed on rural two-lane, two-way highway findings and implications. Paper presented at Geometric Design and the Effects on Traffic Operations, .

Courage, K. G., S. Washburn, L. Elefteriadou, and D. Nam. 2010. *Use of alternative traffic analysis tools in highway capacity manual analysis*. University of Florida, Gainesville: National Cooperative Highway Research Progran, Project 3-85 Final Report.

Daganzo, C. F. 1981. Estimation of gap acceptance parameters within and across the population from direct roadside observation. *Transportation Research Part B: Methodological* 15 (1): 1-15.

Darzentas, J., D. F. Cooper, P. A. Storr, and M. R. C. McDowell. 1980. Simulation of road traffic conflicts at T-junctions. *Simulation* 34 (5): 155-64.

Elvik, R. 2005. Speed and road safety: Synthesis of evidence from evaluation studies. *Transportation Research Record: Journal of the Transportation Research Board* 1908 : 59-69.

Evans, L. 1991. *Traffic safety and the driver.* NewYork: Van Nostrand Reinhold Company.

Fancher, P., R. Ervin, J. Sayer, M. Hagan, S. Bogard, Z. Bareket, M. Mefford, and J. Haugen. 1997. *Intelligent cruise control field operation test.* Washington, DC: National Highway Traffic Safety Administration, HS-808 622, UMTRI-97-11,.

Farah, H., S. Bekhor, and A. Polus. 2009a. Risk evaluation by modeling of passing behavior on two-lane rural highways. *Accident Analysis & Prevention* 41 (4): 887-94.

Farah, H., S. Bekhor, A. Polus, and T. Toledo. 2009b. A passing gap acceptance model for two-lane rural highways. *Transportmetrica* 5 (3): 159-72.

FHWA. 2008. *Highway statistics.* Wahington, DC, U.S. Department of Transportation: Federal Highway Administration, .

———. 1994. *The magnitude and severity of passing accidents on two-lane rural roads (HSIS summary report).* Federal Highway Administration, FHWA-RD-94-068.

Fitzpatrick, K., P. Carlson, M. A. Brewer, M. D. Wooldrifge, and S. P. Miaou. 2003. *Design speed, operating speed, and posted speed practices.* NCHRP, 504.

FMCSA. 2008. *Large truck crash overview* Washingon D.C.: Federal Motor Carrier Safety Administration, .

Garber, N. J., J. S. Miller, B. Yuan, and X. Sun. 2003. The safety impacts of differential speed limits on rural interstate highways. Paper presented at 82nd annual meeting of the Transportation Research Board, Washington DC.

Gettman, D., and L. Head. 2003. *Surrogate safety measures from traffic simulation models, final report.* Federal Highway Administration, FHWA-RD-03-050.

Ghods, A. H., and F. F. Saccomanno. 2013a. Microscopic overtaking gap acceptance for two-lane highways. Paper presented at 93rd Annual Meeting of the *Transportation Research Board*, Washington D.C.

———. 2013b. Safety implications of truck and car speed limits for two-lane highway operations. Paper presented at 92nd Annual Meeting of the *Transportation Research Board*, Washington D.C.

———. 2012. Effect of Car/Truck differential speed limits on two-lane highways safety operation using microscopic simulation. Paper presented at SIIV, 5th International Congress on Sustainability of Road Infrastructures, Rome, Italy.

GHSA. State speed limit laws. in Governors Highway Safety Association [database online]. [cited July 2012]. Available from http://www.ghsa.org/html/stateinfo/laws/speedlimit_laws.html.

Gipps, P. G. 1981. A behavioural car-following model for computer simulation *Transportation Research Part B* 15 (2): 105-11.

Glennon, John C. 1988. New and improved model of passing sight distance on two-lane highways. *Transportation Research Record*(1195): 132-7.

Guido, G. P., A. Vitale, F. Saccomanno, V. Astarita, and V. P. Giofrè. 2013. Evaluating accuracy of new algorithm for extracting vehicle tracking data from videotaping. Paper presented at 92nd Annual Meeting of the *Transportation Research Board*, Washington D.C, Washington D.C.

Halati, A., H. Lieu, and S. Walker. 1997. CORSIM-corridor traffic simulation model. Paper presented at Proceedings of the Traffic Congestion and Traffic Safety in the 21st Century Conference, New York.

Hanowski, R. J., G. Bergoffen, J. S. Hickman, F. Guo, D. Murray, R. Bishop, S. Johnson, and M. Camden. 2012. *Research on the safety impacts of speed limiter device installations on commercial motor vehicles: Phase II.* Federal Motor Carrier Safety Administration (FMCSA), FMCSA-RRR-12-006.

Harwood, D. W., D. K. Gilmore, K. R. Richard, J. M. Dunn, and C. Sun. 2008. *Passing sight distance criteria.* Washington, D.C.: Transportation Research Board National Research Council, NCHRP REPORT 605.

Harwood, D. W., A. D. May, I. B. Anderson, L. Leiman, and A. R. Archilla. 1999. *Capacity and quality of service of two-lane highways* Transportation Research Board, NCHRP 3-55(3).

Harwood, D. W., I. B. Potts, K. M. Bauer, J. A. Bonneson, and L. Elefteriadou. 2003. *Two-lane road analysis methodology in the highway capacity manual.* Transportation Research Board National Research Council, NCHRP Project 20-7 (160) : MAl Project 110252.

Hauer, E. 1971. Accidents, overtaking and speed control. *Accident Analysis and Prevention* 3 : 1-13.

Hegeman, G. 2008. Assisted overtaking: An assessment of overtaking on two-lane rural roads. PhD., Delft University of Technology, TRAIL Thesis Series(T2008/4).

———. 2004. Overtaking frequency and advanced driver assistance systems. Paper presented at IEEE Intelligent Vehicles Symposium, .

Hegeman, G., A. Tapani, and S. Hoogendoorn. 2009. Overtaking assistant assessment using traffic simulation. *Transportation Research Part C: Emerging Technologies* 17 (6) (12): 617-30.

Hoban, C. J., R. J. Shepherd, G. J. Fawcett, and G. K. Robinson. 1991. A model for simulating traffic on two-lane rural roads: User guide and manual for TRARR version 3.2 Paper presented at Australian Road Research Board, .

HSIS. California accident data. in Highway Safety Information System [database online]. 2012 [cited 11/15 2012]. Available from www.hsisinfo.org.

Ioannou, P. A., and C. C. Chien. 1993. Autonomous intelligent cruise control. *Vehicular Technology, IEEE Transactions on* 42 (4): 657-72.

Johnson, S., and N. Pawar. 2005. *Cost-benefit evaluation of large truck-automobile speed limit differentials on rural interstate highways.* Mack-Blackwell National Rural Transportation Study Center, University of Arkansas, MBTC 2048.

Johnson, S., and N. Pawar. 2007. Analysis of heavy-truck and automobile speed distributions for uniform and differential speed limit configurations on rural interstate highways. Paper presented at 86th Annual Meeting of the *Transportation Research Board*, Washington D.C.

Kim, J., and L. Elefteriadou. 2010. Estimation of capacity of two-lane two-way highways using simulation model. *Journal of Transportation Engineering* 136 : 61.

Koorey, G. 2007. Passing opportunities at slow-vehicle bays. *Journal of Transportation Engineering* 133 (2): 129-37.

———. 2002. Assessment of rural road simulation modelling tools. Paper presented at IPENZ Transportation Group Technical Conference, New Zealand, .

Lamm, R., A. Beck, T. Ruscher, T. Mailaender, S. Cafiso, G. La Cava, and W. Matthews. 2006. *How to make two-lane rural roads safer*. Southampton, Boston: WIT Press.

Leiman, L., R. Archilla, and A. D. May. 1998. *TWOPAS model improvements.* Kansas City, MO: Institute of Transportation Studies, University of California, Berkeley, NCHRP - 3 - 55 (3).

Li, J., and S. S. Washburn. 2011. Implementing two-lane highway simulation modeling into CORSIM. Paper presented at 6th International Symposium on Highway Capacity and Quality of Service, Stockholm, Sweden.

Liang, C. Y., and H. Peng. 1999. Optimal adaptive cruise control with guaranteed string stability. *Vehicle System Dynamics* 32 (4-5): 313-30.

Lovell, D. J., SI LAU, and A. D. May. 1993. *Using the TRARR model to investigate alignment alternatives and passing lane configurations on the buckhorn grade.* California: Institute of Transportation Studies, UCB-ITS-RR-93-DRAFT.

Mahmassani, H., and Y. Sheffi. 1981. Using gap sequences to estimate gap acceptance functions. *Transportation Research Part B: Methodological* 15 (3): 143-8.

Marsden, G., M. McDonald, and M. Brackstone. 2001. Towards an understanding of adaptive cruise control. *Transportation Research Part C: Emerging Technologies* 9 (1): 33-51.

McLean, J. R. 1989. *Two-lane highway traffic operations: Theory and practice*. Transportation studies volume 11.Gordon and Breach.

Miller, A. J. 1967. Queueing in rural traffic. in vehicular traffic science. Paper presented at Proceedings of the Third International Symposium on the Theory of Traffic Flow, .

Morrall, J. F., and A. Werner. 1990. Measuring level of service of two-lane highways by overtakings. *Transportation Research Board* 1287 : 62-69.

MUTCD. 2006. *Manual on uniform traffic control devices*. Austin, Texas: Texas Department of Transportation.

Neeley, G. W., and L. E. Richardson Jr. 2009. The effect of state regulations on truck-crash fatalities. *Journal Information* 99 (3).

Neuman, T., R. Pfefer, K. Slack, K. Hardy, H. McGee, L. Prothe, K. Eccles, and F. Council. 2003. *A guide for addressing head-on collisions.* Washonfton D.C.: Transportation Research Board of the National Academies, NCHRP Report 500.

Paniati, J. F., and J. True. 1996. Interactive highway safety design model (IHSDM): Designing highways with safety in mind. Paper presented at Roadside Safety Issues Revisited, Irvine, California.

Panwai, S., and H. Dia. 2005. Comparative evaluation of microscopic car-following behavior *IEEE Transactions on Intelligent Transportation Systems* 6 (3): 314-25.

Persaud, B. N., R. A. Retting, and C. A. Lyon. 2004. Crash reduction following installation of centerline rumble strips on rural two-lane roads. *Accident; Analysis and Prevention* 36 (6) (Nov): 1073-9.

Reichart, G., R. Haller, and K. Naab. 1996. Driver assistance: BMW solutions for the future of individual mobility. Paper presented at Third World Congress on Intelligent Transport Systems, Orlando, Florida.

Saccomanno, F. F., D. Duong, F. Cunto, B. Hellinga, C. Philp, and P. Thiffault. 2009. Safety implications of mandated truck speed limiters on freeways. *Transportation Research Record: Journal of the Transportation Research Board* 2096 : 65-75.

Schurr, Karen S., Patrick T. McCoy, Geza Pesti, and Ryan Huff. 2002. Relationship of design, operating, and posted speeds on horizontal curves of rural two-lane highways in nebraska. *Transportation Research Record: Journal of the Transportation Research Board* 1796 (1): 60-71.

Shepherd, R. 1994. TRARR 4 user manual. *Australian Road Research Board Ltd*.

Solomon, D. H. 1964. *Accidents on main rural highways related to speed, driver, and vehicle*. Washington D.C.: US Government Printing Office.

St John, A. D., and D. W. Harwood. 1986. *TWOPAS User's guide.* Federal Highway Administration, .

St John, A. D., and D. R. Kobett. 1978. *Grade effects on traffic flow stability and capacity.* US Transportation Research Board. National Cooperative Highway Research Program, NCHRP 185.

TAC. 1990. *Canada' s roadway infrastructure: Selected facts and figures.* Ottawa, Ontario: Transportation Association of Canada, .

Tapani, A. 2005. Microscopic traffic simulation models: Calibration, validation, and computation: Versatile model for simulation of rural road traffic. *Transportation Research Record: Journal of the Transportation Research Board* 1934 : 167-78.

Touran, A., M. A. Brackstone, and M. McDonald. 1998. A computer model for assessing the safety impacts of autonomous intelligent cruise control. Paper presented at ASCE 98th annual convention, Boston, USA.

Transport Canada. 2006. *Canadian motor vehicle traffic collisions statistics.* Ottawa, Ontario, Canada: TP 3322.

TRB. 2010. *Highway capacity manual* . Washington D.C.: Transportation Research Board.

———. 2000. *Highway capacity manual*. Washington D.C.: Transporation Research Board.

Troutbeck, R. J. 1981. *Overtaking behaviour on australian two-lane rural highways.* Australian Road Research Board, Special Report SR20.

Vaziri, S. H., C. T. Haas, L. Rothenburg, and R. C. Haas. 2013. Investigation of the effects of air temperature and speed of vehicle factors on performance of piezoelectric weigh-in-motion systems in a central canadian climate. *Journal of the Canadian Society for Civil Engineering. (CSCE)* Accepted .

Wardrop, J. G. 1953. Some theoretical aspects of road traffic research. Paper presented at Proceedings of the Institution of Civil Engineers, .

Watanabe, T., N. Kishimoto, K. Hayafune, K. Yamada, and N. Maede. 1995. Development of an intelligent cruise control system. Paper presented at Steps Forward. Intelligent Transport Systems World Congress, .

Woll, J. 1997. Radar based adaptive cruise control for truck applications. *Society of Automotive Engineers Transaction*.

Zegeer, J. D., M. Blogg, K. Nguyen, and M. Vandehey. 2008. Default values for highway capacity and level-of-service analyses. *Transportation Research Record: Journal of the Transportation Research Board* 2071 : 35-43.